2021-08-01

Evaluation Of Electrodialysis Desalination Performance Of Novel And Conventional Ion Exchange Membranes

AHM Golam Hyder
University of Texas at El Paso

EVALUATION OF ELECTRODIALYSIS DESALINATION PERFORMANCE OF NOVEL AND CONVENTIONAL ION EXCHANGE MEMBRANES

A. H. M. GOLAM HYDER

Doctoral Program in Environmental Science and Engineering

APPROVED:

W. Shane Walker, Ph.D., Chair

Malynda A. Cappelle, Ph.D.

Anthony J. Tarquin, Ph.D.

Susan B. Rempe, Ph.D.

Stephen L. Crites, Jr., Ph.D.
Dean of the Graduate School

Dedication

This dissertation is dedicated for the betterment of billions of people globally who are suffering from freshwater scarcity. I would also like to dedicate this tremendous achievement to my parents, specially to my Dad Md. Golap Ali Pramanic who has passed away on January 1st, 2021, who have guided me to be a reasonable person and encouraged me to pursue my dreams, and to rest of my family members for their supports and love.

EVALUATION OF ELECTRODIALYSIS DESALINATION PERFORMANCE OF NOVEL AND CONVENTIONAL ION EXCHANGE MEMBRANES

by

A. H. M. Golam Hyder, M.Sc.

DISSERTATION

Presented to the Faculty of the Graduate School of

The University of Texas at El Paso

in Partial Fulfillment

of the Requirements

for the Degree of

DOCTOR OF PHILOSOPHY

Environmental Science and Engineering Program

THE UNIVERSITY OF TEXAS AT EL PASO

August 2021

Acknowledgements

This report is accomplished for the dissertation of the Doctor of Philosophy program in Environmental Science and Engineering (ESE) at The University of Texas at El Paso (UTEP), Texas, USA.

First of all, I would like to acknowledge the deepest and intense gratefulness to my Ph.D. advisor Dr. William Shane Walker, Associate Professor in the department of Civil Engineering, The University of Texas at El Paso, Texas, USA for giving me the opportunity to work in this challenging, and interesting project; for his brilliant supervision and mentorship, and delightful motivations and caring throughout my Ph.D. study, and financial, technical, mental supports and friendship while working in his Environmental Engineering Lab at UTEP.

I am grateful to my Ph.D. co-advisor Dr. Malynda A. Cappelle, Associate Director, the Center for Inland Desalination Systems at UTEP for her continuous efforts to provide valuable suggestions, encouragement, and cooperation throughout this study.

I would also like to extend my sincere gratitude to Dr. Anthony J. Tarquin, Professor in the department of Civil Engineering, UTEP and Dr. Susan B. Rempe, distinguish member of the technical staff in the Center for Integrated Nanotechnologies, Sandia National Labs, Albuquerque, New Mexico, USA for being the honorable committee members for my dissertation.

I appreciate Dr. Craig E. Tweedie, Director, Environmental Science and Engineering Program and Ms. Lina K. Hamdan, Coordinator, Environmental Science and Engineering Program for all the support they provided toward completing my Ph.D. graduation

I am honestly grateful to Sandia national Laboratory and NSF Center for Nanotechnology Enabled Water Treatment for funding my dissertation research work.

I would like to respectfully recognize Dr Carlos Ferregut, Department Chair for Civil Engineering at UTEP for providing me the opportunity to teach undergraduate Civil Engineering courses as an Instructor.

I am thankful to the Journal *Membranes* for accepting and publishing my first article from my PhD research works. Chapter 2 of this dissertation is copied from my open access article published in the Journal *Membranes*[1].

I especially acknowledge the wonderful mentorship and encouragement of the late Dr. Tom Davis for collaborating research on the topic of ion exchange membranes and electrodialysis.

I am lucky to have friendly lab mates Oluwaseye Owoseni, Shahrouz Ghadimi, Li Chen, Eva Deemer, and many more.

Finally, I would like to thank my parents (Hazera Khatun and late Md. Golap Ali Pramanic), sister (Dr. Shamim A. Begum and Dr. Khaledun Nessa), wife (Tanzida Sultana), daughter (Zeifa Hyder Aleena), son (Zaif Hyder Eiham), and other family members for their continuous inspiration, moral and prayerful supports, unconditional love, and sacrifices throughout my life.

[1] Hyder, A.G.; Morales, B.A.; Cappelle, M.A.; Percival, S.J.; Small, L.J.; Spoerke, E.D.; Rempe, S.B.; Walker, W.S. Evaluation of Electrodialysis Desalination Performance of Novel Bioinspired and Conventional Ion Exchange Membranes with Sodium Chloride Feed Solutions. *Membranes* **2021**, *11*, 217. https://doi.org/10.3390/membranes11030217

General Abstract

It was revealed from relevant recent literature that the electrodialysis (ED) desalination performance of commercial and laboratory-made ion exchange membranes (IEMs) had been studied previously but not in a systematic way so that the planners, designers, and engineers can evaluate a trade-off in selecting the suitable IEMs and optimum ED experimental conditions for their desired outcomes such as high ion-selectivity, high salinity removal, high water recovery, low energy consumption, or low water transport. Furthermore, the existing conventional and laboratory-made IEMs reported previously showed various technical and economical limitations with respect to permeability, permselectivity, ion-selectivity, electrical resistance, stability (mechanical, chemical, and thermal), and production costs. Thus, this research was mainly focused on the systematic comparison of ED desalination performances of five well-known commercial IEMs and two newly developed IEMs (*i.e.*, bio-inspired and polyethersulfone polymeric) under a set of well-controlled experimental conditions. The desalination performance of IEMs was evaluated by determining the key ED operational parameters such as the limiting current density (LCD), current efficiency (CE), salinity reduction (SR), normalized specific energy consumption (nSEC), osmotic water flux (oWF), individual ion concentration reduction rate, and relative ion transport ratio (divalent versus monovalent) as a function of feed solution concentration and composition, applied stack voltage, and velocity of feed solution. A laboratory-scale single stage ED stack was used with five cell-pairs of cationic and anionic membranes with an active cross-sectional area of 7.84 (2.8 x 2.8) cm^2. A programmable power supply, pH/conductivity meter, mass balance, pressure gauges, and magnetic stirrers were used for the ED experimental setup. A supervisory control and data acquisition (SCADA) system was developed by VIEW 2017 for automatic recording of experimental data at five seconds intervals for diluate reservoir mass

change, applied voltage and current, pH, temperature, and conductivity. Periodic samples were also collected from process streams (diluate and concentrate reservoirs) for post analysis using Ion Chromatography. The entire research work was divided into three projects. In first project, ED desalination performance difference between five commercial IEMs and a novel bioinspired cation exchange membrane (CEM) developed recently at Sandia National Laboratory was compared for synthetic sodium chloride (NaCl) feed solutions concentration of 1, 3, 10, 35, and 100 g/L, voltage application to ED stack of 0.4, 0.8, and 1.2 volts per cell pair, and superficial feed velocity of feed solution of 2, 4, and 8 cm/s. Sandia's bioinspired CEM performed relatively well compared to the commercial membranes. The second project investigated the effects of key ED operational parameters on the desalination performance of five pairs of commercial IEMs used in the first project for brackish groundwater feed solutions (2.79 and 5.26 g/L TDS), 0.4 and 0.8 volts per cell pair stack voltage application, and 4 cm/s superficial feed velocity of feed solution. The membranes were ranked according to performance with respect to several figures of merit. The results of this work will be helpful for ED process optimization and performance analysis for the specific application and expected outcomes. In the third project, a set of novel nanocomposites polymeric CEMs was developed from a highly durable and relatively inexpensive material polyethersulfone (PES) and the influence of CEM's microstructure, fabrication method, physiochemical properties of polymeric substances, nanofillers, and crosslinkers on ED desalination performance were evaluated. The results showed the potential of using sulfonated PES with graphene oxide (GO) nanofillers and polyvinylpyrrolidone (PVP) crosslinkers for fabricating CEMs using phase inversion methods.

Keywords: Electrodialysis, desalination, bioinspired, nanocomposite, polyethersulfone, graphene oxide, ion exchange membrane, NaCl feed, brackish groundwater.

Table of Contents

Dedication iii

Acknowledgements v

General Abstract vii

Table of Contents ix

List of Tables xiii

List of Figures xiv

Chapter 1: General Introduction 1

1.1. Background 1

1.2. Overview of Electrodialysis Process 3

1.2.1. Electrodialysis stack 3

1.2.2. Ion exchange membranes used in electrodialysis 5

1.2.3. Electrical aspects involved in electrodialysis 6

1.2.4. Hydraulic aspects involved in electrodialysis 7

1.2.5. Chemical aspects involved in electrodialysis 8

1.2.6. Concentration polarization and limiting current density 8

1.3. Problem Statement 10

1.4. Goals and Objectives of Research 11

1.5. References 13

Chapter 2: Evaluation of Electrodialysis Desalination Performance of Novel Bioinspired and Conventional Ion Exchange Membranes with Sodium Chloride Feed Solutions 16

Abstract 16

2.1. Introduction 17

2.1.1. Background 17

2.1.2. Objectives 17

2.2. Materials and Methods 18

2.2.1. Experimental plan and variables 18

2.2.2. Experimental system and chemicals 19

2.2.3. Experimental Electrodialysis (ED) stack or Electrodialyzer 21

2.2.4. Experimental Ion exchange membranes (IEMs) 22
2.2.5. Experimental procedure 24
2.2.6. Data acquisition and control hardware 26
2.2.7. Data analysis 27
2.2.8. Calculation methods 27
2.2.8.1. Electrode voltage loss 27
2.2.8.2. Power and specific energy consumption (SEC) 27
2.2.8.3. Current density 29
2.2.8.4. Limiting current density (LCD) and limiting polarization parameter (LPP) 29
2.2.8.5. Current efficiency 30
2.2.8.6. Salinity reduction 31
2.2.8.7. Water transport 31
2.3. Results 32
2.3.1. Evaluation of limiting current density and areal resistance 32
2.3.2. Evaluation of current density and current efficiency 34
2.3.3. Evaluation of salinity reduction and normalized specific energy consumption 36
2.3.4. Evaluation of water flux by osmosis 38
2.4. Conclusions and Recommendations 40
2.5. References 43

Chapter 3: Evaluation of electrodialysis desalination performance for five commercial ion exchange membrane sets with brackish water feed solutions 48

Abstract 48
3.1. Introduction 49
3.1.1. Background 49
3.1.2. Objectives 52
3.2. Materials and Methods 53
3.2.1. Experimental plan, variables, system, and chemicals 53
3.2.2. Experimental feed water solutions 55
3.2.3. Electrodialysis testing 55
3.2.4. Calculation methods 56
3.2.4.1 Relative transport number (RTN) of salt ions 57

3.3. Results 57
3.3.1. Evaluation of limiting current density, areal resistance, and polarization parameter 57
3.3.2. Evaluation of current density, and current efficiency 59
3.3.3. Evaluation of conductivity reduction and specific energy consumption 60
3.3.4. Evaluation of concentration reduction of predominant monovalent and divalent ions 62
3.3.5. Evaluation of relative transport ratio between divalent and monovalent ions 65
3.4. Conclusions and Recommendations 66
3.5. References 69

Chapter 4: Preliminary development of polyethersulfone cation exchange membranes for electrodialysis desalination 73

Abstract 73
4.1. Introduction 74
4.1.1 Background 74
4.1.2. Objective 76
4.2 Materials and Methods 76
4.2.1. Chemicals 76
4.2.2. Sulfonated polyethersulfone (sPES) preparation 77
4.2.3. Membrane fabrication 78
4.2.4. Membrane characterization 79
4.2.4.1. Degree of sulfonation (DS) measurement 79
4.2.4.2. Water content measurement 79
4.2.4.3. Ion-exchange capacity (IEC) measurement 80
4.2.5. Electrodialysis testing 80
4.3 Results 82
4.3.1. Evaluation of limiting current density, areal resistance, and polarization parameter 82
4.3.2. Evaluation of current density and current efficiency 85
4.3.3. Evaluation of diluate salinity reduction and specific energy consumption 86
4.3.4. Evaluation of membrane structure-property relationships 87
4.4 Conclusions and Future work 91

4.5 References 93

Chapter 5: General Conclusions 97

Vita 99

List of Tables

Table 2.1: Experimental variables, value ranges, and combinations 19

Table 2.2: Standard properties of IEMs used in this study 23

Table 2.3: Membrane performance comparison. 42

Table 3.1: Salt ions compositions and concentrations in brackish groundwaters 53

Table 3.2: Experimental variables, value ranges, and combinations 54

Table 3.3: Performance trends for five commercial membrane sets 62

Table 3.4: Key performance parameters comparison for membranes. 68

Table 4.1: Experimental variables, value ranges, and combinations 81

Table 4.2: Performance trends for five membrane sets (each with AMX anion membranes) 84

Table 4.3: Physiochemical properties and ED performances of fabricated membranes 89

List of Figures

Figure 1.1: Schematic diagram of the principle of electrodialysis process 4

Figure 1.2: Inter-membrane velocity and concentration profiles..... 9

Figure 2.1: A schematic diagram for the batch-recycle electrodialysis process..... 20

Figure 2.2: Experimental setup..... 21

Figure 2.3: LCD determination using (a) Shoulder plot and (b) Cowan-Brown plot..... 30

Figure 2.4: Limiting current density (a,c), areal resistance per cell-pair of the membrane (b,d), and limiting polarization parameter (e,f) 33

Figure 2.5: Average current density (a-c) and average charge efficiency (d-f) for 60 minutes of experiment against applied stack voltage per cell-pair of the membrane. 35

Figure 2.6: Salinity reduction (a-c) and normalized specific energy consumption (nSEC) (d-f) of diluate stream after 60 minutes of treatment..... 38

Figure 2.7: Water flux by osmosis versus concentration differences (a) and osmotic permeance versus osmotic pressure difference (b). 39

Figure 3.1: Limiting current density (a) and areal resistance per cell-pair of membranes at LCD (b) against ED stack voltage per cell-pair of membranes. 59

Figure 3.2: Effect of stack voltage and feed solution composition on current density (a,b) and current efficiency (c,d) for KBH (a,c) and BGNDRF (b,d) feed solutions. 60

Figure 3.3: Effect of stack voltage and feed solution composition on conductivity reduction (c,d), and specific energy consumption (SEC) (e,f) for two different brackish water feed solutions: KBH (a,c,e) and BGNDRF (b,d,f). 61

Figure 3.4: Effect of stack voltage and feed solution composition on removal performance of predominant monovalent and divalent ions from KBH (a,c,e,g) and BGNDRF (b,d,f,h) brackish water feed solutions. 64

Figure 3.5: Effect of stack voltage and feed solution composition on relative transport of divalent ions against monovalent ions: Ca^{2+} vs Na^{+} (a,b) and SO_4^{2-} vs Cl^{-} (c,d) from KBH (a,c) and BGNDRF (b,d) brackish water feed solutions. 66

Figure 4.1: Chemical structure of PES, sPES, PVP, GO and diagram of sulfonation methods. .. 78

Figure 4.2: (a) Limiting current density, (b) areal resistance per cell-pair of membranes at LCD, and (c) limiting polarization parameter versus ED stack voltage per cell-pair..... 84

Figure 4.3: Effect of membranes and feed solution concentrations on (a) current density and (b) current efficiency for five membrane sets. 86

Figure 4.4: Effect of membranes and feed solution concentrations on (a) salinity reduction, and (b) normalized specific energy consumption (nSEC) for five membrane sets. 87

Figure 4.5. Scanning Electron Micrographs (SEM) of fabricated membranes (top) and diagram showing constituents in membranes (bottom). 91

Chapter 1: General Introduction

1.1. Background

Fresh water is a limited natural resource. Unfortunately, this limited freshwater resource is becoming depleted due to overuse. Approximately 748 million people currently live without access to fresh water, and over 2.5 billion people have access to meager water supply [1]. According to the United Nations, water usage is increasing twice as fast as population growth [1]. As the global population is expected to reach nearly 10 billion by 2050, the scarcity of drinking water is expected to worsen. Water scarcity, which is caused by natural and anthropogenic activities (e.g., climate change, drought, global warming, industrialization, agriculture, and fast population growth), will increasingly exacerbate international conflict in years to come.

Three-fourths of the earth's surface is covered by water. However, 97.5% of this total water is seawater, and the remaining portion i.e., 2.5% is fresh water. Only 0.3% of this fresh water is found as surface water (e.g., river, lake, pond, etc.), 30% of the fresh water is available as groundwater (out of which 40% is pure and impure groundwater and 60% is brackish groundwater), and the rest of the fresh water is in the unusable forms of icecaps and glaciers [2]. Since seawater and brackish water are abundant sources of natural water resources, treatment and use of this water will be one of the solutions to the freshwater scarcity problem. In order to utilize this huge amount of seawater and brackish groundwater resources existing globally, alternative technologies and treatment options must be explored [3]. One of the most promising options is desalination, which produces potable water from non-traditional sources such as seawater and brackish groundwater.

Around the world, desalination is considered as one of the preferable techniques for treating seawater and brackish water. The future of desalination in solving the water scarcity

problem looks promising. There are more than 18,000 desalination plants in operation globally [4]. The United States and the Middle Eastern countries are the leaders in developing desalination technologies in the last couple of decades, and the application of desalination technology is expected to grow continuously [5]. Global online desalination capacity increased from 20 million m^3/day in 1995 to 92.5 million m^3/day in 2017 [6]. The global average freshwater consumption is around 10 billion tons or 1013 m^3 per day [6].

The most common methods of modern desalination are thermal processes and membrane desalination. Thermal processes, such as multi-stage flash, multi-effect distillation, vapor compression, and humidification-dehumidification, usually follow the concept of evaporation and condensation of water. Membrane desalination technologies, such as reverse osmosis (RO), forward osmosis (FO), electrodialysis (ED), and nanotechnology-based processes use membranes as salt rejection barriers to desalinate water. Membrane technologies are advantageous as compared to thermal processes because of their substantially lower energy usage [7].

Reverse osmosis (RO) is the prominent membrane-based desalination process, but it has some critical challenges. A significant problem is the limited water recovery ratio (the portion of feed water that becomes product water). Water recovery ratio is rarely greater than 75% in brackish water reverse osmosis (BWRO) systems without antiscalants, and recovery is rarely greater than 90% even with antiscalants [8], which means that generation and disposal of waste brine are common in RO desalination. For most inland brackish groundwater reverse osmosis (BWRO) systems, the concentrate disposal requires the highest cost which is sometimes greater than 50% of the entire desalination project capital cost [9]. Electrodialysis (ED) is a technology that may overcome the limitations of RO desalination.

1.2. Overview of Electrodialysis Process

Electrodialysis is an electro-membrane process in which ions are transported through ion exchange membranes from one solution compartment to another under the application of electrical potential (i.e., voltage). ED has several advantages compared to RO: (i) ED can achieve greater product recovery than RO, thus decreasing total brine disposal; (ii) ED is more robust than RO with respect to feed turbidity, feed silica concentration, and biological growth (i.e., ion exchange membranes can tolerate a mild chlorine dose); and (iii) ED can be used to recover mineral resources from RO brine [10]. The main components in ED desalination include (i) the ED stack or electrodialyzer, and (ii) the ion exchange membranes.

1.2.1. Electrodialysis stack

An ED stack (Electrodialyzer) is built of alternating cation exchange membranes (CEM) and anion exchange membranes (AEM) which are separated by flow spacers, and these membranes and spacers are placed in between an anode (positively charged electrode) and a cathode (negatively charged electrode) as shown in Figure 1.1. A cell-pair is composed of a cation- and an anion-exchange membrane including two spacers in between these two adjacent ion exchange membranes. The complete collection of membranes and spacers is referred to as a stack. The feed solution (*e.g.,* brackish water) enters into each cell, and the electrode rinse solution enters into the electrode rinse compartment of the ED stack (usually from the bottom). When a direct-current (DC) electrical potential is applied on both electrodes, negatively charged anions move towards the positively charged anode through the positively charged anion exchange membrane, whereas positively charged cations move towards the negatively charged cathode through the negatively charged cation exchange membrane. Cations are passed through the cation exchange membrane (moving towards the right-hand direction in Figure 1.1) but retained by the anion exchange

membrane. Similarly, anions are passed through the anion exchange membrane (moving towards the left-hand direction in Figure 1.1) but retained by the cation exchange membrane. This leads to changes in the salt concentration in alternating streams; one resulting in a diluted stream (called diluate) where the salt content is less than the feed solution, and another resulting in a concentrated stream (called concentrate) where salt content is greater than the feed solution. At the anode, oxygen (from water) is oxidized to produce oxygen gas, protons, and electrons; whereas, at the cathode, hydrogen (from water) is reduced to produce hydrogen gas and hydroxide ions. Water travels through the spacers (*e.g.*, from bottom to upward direction) parallel to the membrane, and salt ions pass orthogonally through the membranes.

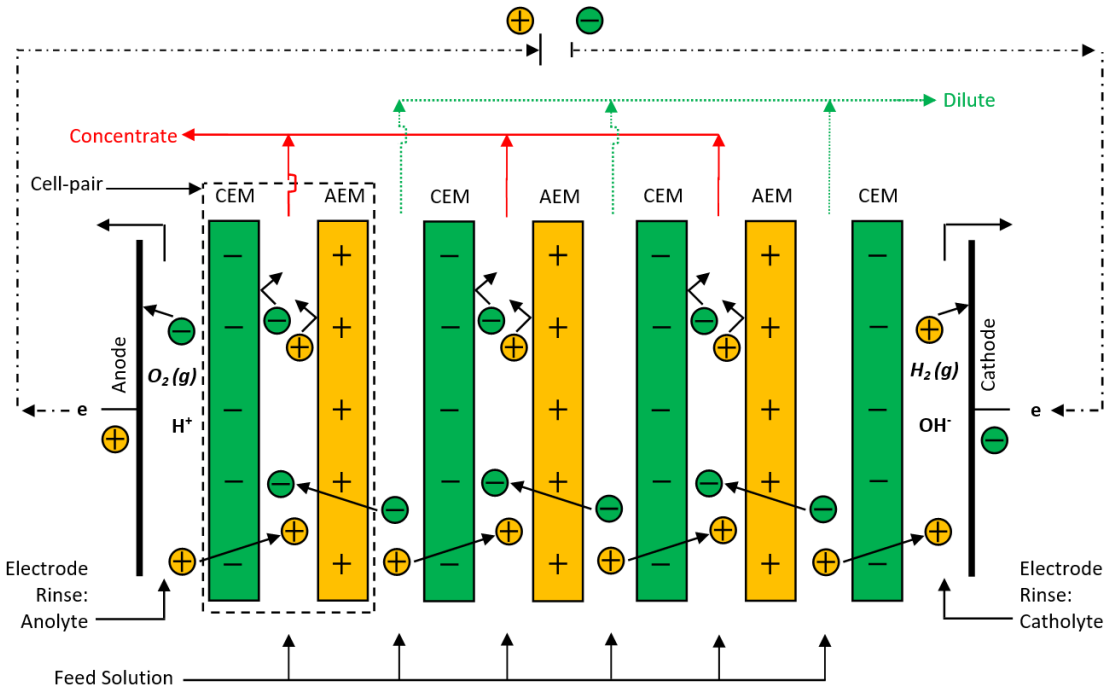

Source: Adapted from [11]

Figure 1.1: Schematic diagram of the principle of electrodialysis process

[CEM: cation exchange membrane, AEM: anion exchange membrane, e = electron]

1.2.2. Ion exchange membranes used in electrodialysis

Ion exchange membranes used in ED are either (i) cation exchange membranes (CEM) or (ii) anion exchange membranes (AEM) [12]. CEMs are preferentially permeable to cations, and they have negatively charged fixed groups. Most commercial CEMs carry sulfonate ($-SO_3^-$) (as strong acid) and carboxyl (-COO-) (as weak acid) as fixed charged groups [12,13]. AEMs are preferentially permeable to anions, and they contain positively charged fixed groups. Most commercial AEMs have quaternary ammonium ($-NR_3^+$) (as strong base) and tertiary ammonium (as weak base) as fixed charged groups [12, 13].

According to the structure, ion exchange membranes are also classified as (i) homogeneous and (ii) heterogeneous membranes [12]. The homogeneous membranes are composed of a homogeneous mixture of structural and ion exchange materials, whereas, heterogeneous membranes have a structural component (*e.g.,* mesh sheet) with ion exchange material packed around it. Heterogeneous ion exchange membranes have generally a higher electrical resistance compared to homogeneous membranes because mobile ions need to travel a longer pathway in the heterogeneous structure [14]. Permselectivity of heterogeneous membranes is also lower than homogeneous membranes because of a leakage of co-ions through water-filled gaps in the membrane matrix [12]. During the formation process of ion exchange membranes, different parameters are important to consider such as density of the polymer network, hydrophobic or hydrophilic character of the polymer matrix, type, and concentration of the fixed charges in the polymer, and morphology of the membrane [12]. The most desired properties of ion exchange membranes include high permselectivity, high ion permeability, low electrical resistance, cheap, high mechanical, chemical, and thermal stability [12]. Several existing ion exchange membranes have most of these desired properties, but large differences in the properties exist [14]. The detailed description of the development, prospects, applications, and physio-chemical properties of different types of ion exchange membranes such as homogeneous, heterogeneous, organic,

inorganic, bipolar, amphoteric, mosaic, profiled membranes have been articulated in literature and the company's websites [15,16,17,18].

1.2.3. Electrical aspects involved in electrodialysis

Electrical voltage loss at the electrodes is the summation of voltage drop from gas equilibrium, electrode over potential loss corresponding to the kinetics of gas production, and electrical resistance of the electrode rinse solutions. The amount of electrical voltage loss at the electrodes is usually significant compared to the amount of voltage loss across the ED stack in laboratory-scale ED. The opposite is true for full-scale ED. On the other hand, the ED stack voltage loss is calculated by subtracting electrical voltage loss at the electrodes from the total voltage applied in the ED process. Electrical voltage loss across the ED stack essentially drives the separation of salt ions from the diluate to the concentrate stream [12].

Electrical current density (CD) is an important electrical aspect, which is the amount of electrical current (or charge flux ~ coulombs per second per square meter) passing through a square meter of the membrane active area inside the ED stack. Current density increases with the increase in feed solution's concentration [19] and with the increase in process stream solution's velocities [20]. Current density declines with the decrease in process stream solution's temperature as the effective cell resistance increases [21]. Theoretically, in an ideal ED system, the ions separation rate is proportional to the electrical current density through the electrodialyzer.

Current utilization capacity is also known as current efficiency, charge efficiency, or coulombic efficiency (ξ), which is the ratio of the amount of the current used in the electrodialyzer to effectively separate salt ions (from the diluate to the concentrate stream) to the amount of the total current applied to the electrodialyzer. Typically, current utilization is greater than 90% in the ED desalination process [10].

A fraction of the effective current that anion carries is called the transport number, which is another important aspect in ED. The summation of transport numbers equals to one for both

solution phase and membrane phase. For instance, transport numbers of Na^+ and Cl^- are approximately 0.4 and 0.6, respectively in a well-mixed NaCl solution.

Electrical power consumption by the electrodialyzer is calculated by the multiplication of the applied voltage to the electrodialyzer, and the electrical current passing through the electrodialyzer. Energy consumption by the electrodialyzer is determined by multiplying the consumed electrical power with the experimental period. Energy consumption by the hydraulic pumps is calculated from the flow rate and pressure drop. Moreover, specific energy consumption (SEC) (expressed as kWh/m^3) is the amount of energy consumed by the desalination process to produce a given volume of product water.

1.2.4. Hydraulic aspects involved in electrodialysis

Hydraulic efficiency or recovery ratio is an important hydraulic aspect, which is the ratio of the volumetric flow rate of the diluate to the volumetric flow rate of the feed. The typical recovery ratio of single-stage ED is around 80-85% [22].

The hydraulic flow rate, which is related to the inter-membrane velocity of the solution flowing through either the concentrate cell or diluate cell, is another significant hydraulic parameter. The hydraulic flow rate influences the performance of the ED system. An increase in flow rate through a diluate cell increases the mixing or turbulence of the solution inside the dilute cell [23,24]. Higher solution turbulence corresponds to an increase of mass transport through the diluate diffusion boundary layer by decreasing the thickness of the diffusion boundary layer (Figure 1.2). A decrease in the diluate diffusion boundary layer thickness results in a decrease in the electrical resistance of the stack. A decrease in the inter-membrane flow rate or velocity reduces the flow distance inside the cell for the same mean hydraulic residence time.

However, with higher flow, a decrease in the concentrate diffusion boundary layer thickness by increasing solution turbulence in the concentrate cell corresponds to a lower salts

concentration at the membrane surfaces. A higher flow rate allows the ED system to operate at a greater current density and to prevent the precipitation and crystallization of salt ions [25].

1.2.5. Chemical aspects involved in electrodialysis

The chemical efficiency or removal ratio is an important chemical aspect in the ED process, which is the ratio of the amount of salt concentration reduction in the dilute stream after a certain period of experimental time to the initial salt concentration of a feed stream. The typical removal ratio of a single-stage ED varies between 50% and 99% depending on source water quality (100-12,000 mg/L TDS), finished water quality (10-1,000 mg/L), and system design [10].

Chemical flux or transport of a particular ion through the concentrate and diluate cells is another chemical aspect in an ED system, which depends on the gradient of that particular ion in electrochemical potential [13,22]. The ion transport within the electrodialyzer is determined by the summation of three different types of migration such as diffusion and dispersion, electromigration, and advection [13].

Super-saturation of ions in the concentrate cells causes scaling and fouling problems of the membranes (facing towards concentrate cells), which hampers ED operational performance by creating precipitation of different salts. The addition of acid (*e.g.,* HCl or $CO_{2(g)}$) effectively prevents CO_3^{2-} and OH^- salt precipitation by reducing the pH of the concentrate process stream. In order to delay the precipitation of several salts (*e.g.,* $CaSO_4$ and $BaSO_4$), different antiscalants such as condensed sodium phosphate, carboxyl methyl cellulose, or poly-acrylic acid are added to the concentrate stream in traditional ED systems [25,26].

1.2.6. Concentration polarization and limiting current density

Concentration polarization (CP) and limiting current density (LCD) are the two important challenges that affect the ED process performance. Concentration polarization is the difference in salt ions concentrations at both the surfaces of a membrane inside the dilute and concentrate cells

of the ED stack [13,26]. In the ED process, the salt ions concentration decreases at the membrane surface compared to the bulk solution inside the dilute cell by removing salt ions from this cell through the membrane (Figure 1.2). On the other hand, the salt ions concentration increases at the membrane surface compared to the bulk solution inside the concentrate cell by supplying salt ions into this cell through the membrane (Figure 1.2). This difference in salt ions concentrations at both surfaces of each membrane creates concentration polarization, which is responsible for scaling and fouling problems at the membrane surface [13,26]. The concentration gradient within the laminar/diffusion boundary layer is approximately proportional to the electrical current density flowing through the electrodialyzer. This high salt concentration in the laminar/diffusion boundary layer at one side of a membrane surface facing the concentrate cell is problematic because the backward diffusive flow of concentrated flux from concentrate cell towards dilute cell may take place.

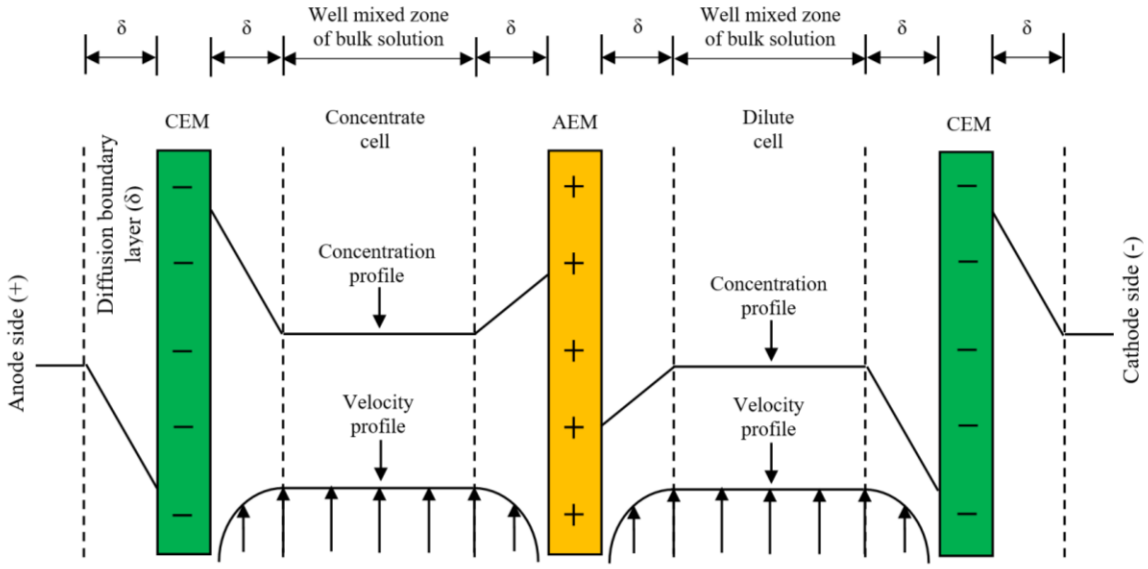

Source Adapted from [22]

Figure 1.2: Inter-membrane velocity and concentration profiles

Limiting current density (LCD) is the maximum allowable current density at which salt ion concentration at the membrane surface becomes zero inside the dilute cell of the ED stack. Current density increases across the electrodialyzer with the increase of the applied voltage at the

electrodes. If current density increases beyond the LCD, the linear concentration gradient in the diluate diffusion boundary layer becomes steeper (or diluate diffusion boundary layer becomes thinner) and the salt ion concentration within the diluate diffusion boundary layer approaches zero at the membrane surface (Figure 1.2) [22]. Identification of the LCD helps to determine how much voltage application is needed for an efficient ED operation. ED systems should run below the LCD in order to prevent water splitting, wastage of power, and damage to ED equipment. LCD is affected by ED operating conditions such as feed concentration, velocity, and temperature of process streams [19, 21, 27]. LCD increases with the increase in the feed solution's concentrations [19] and with the increase in the process stream solution's velocities [20]. LCD declines with the decrease in the process stream solution's temperatures as the effective cell resistance increases [21,28].

1.3. PROBLEM STATEMENT

The electrodialysis desalination performance of different types of ion exchange membranes has been studied by several researchers, but they used their own sets of experimental conditions such as feed solution compositions and concentrations, superficial velocities (Reynolds number) of the process streams (dilute, concentrate, and electrode rinse), and electrical potential application. Because of this problem, it is difficult to compare and recommend which ion exchange membranes are suitable for ED in order to achieve a specific desirable outcome (*e.g.,* high ion-selectivity, high recovery, low energy consumption).

In addition, the conventional ion exchange membranes used in ED still have various technical and economical limitations with respect to permeability, permselectivity, ion-selectivity, electrical resistance, stability (mechanical, chemical, and thermal), and production costs [12,13]. In order to overcome the limitations of conventional ion exchange membranes, it is necessary to develop novel ion exchange membranes (*e.g.,* bioinspired and nanocomposite polymeric membranes) and apply them in ED desalination. Moreover, the use of bioinspired ion exchange

membrane in ED has not been reported yet. Therefore, the development and use of novel laboratory-scale ion exchange membranes (*e.g.,* bioinspired and nanocomposite polymeric membranes) could represent a technological breakthrough by making ED more energy-efficient, environmentally friendly, and/or and cost-effective. It can be hypothesized that the bioinspired and nanocomposite polymeric ion exchange membranes might be compatible because of the advantages they have over conventional membranes, including high ion permeability, specific ion selectivity, dense and narrow pores, ultra-thinness, and material robustness [4].

1.4. Goals and Objectives of Research

In order to compare the ED performance and overcome the drawbacks of conventional ion exchange membranes, the overall goal of this research is (i) to develop novel ion exchange membranes (*e.g.,* nanocomposite polymeric membranes) and (ii) to quantify the ED desalination performance differences between commercial ion exchange membranes and novel laboratory-scale ion exchange membranes (*e.g.,* bioinspired and nanocomposite polymeric membranes) with a similar set of experimental conditions (*e.g.,* superficial velocity of the feed solution, solution composition and concentration, and applied electrical potential) to evaluate outcomes such as ion permeability, ion selectivity, current density, current efficiency, energy consumption, water transport, salt rejection, and water recovery. The specific objectives of this research are as follows:

1. Evaluate the electrodialysis desalination performance differences between bioinspired ion exchange membranes and conventional ion exchange membranes with sodium chloride (NaCl) feed solutions (Chapter 2 of this dissertation).
2. Evaluate the permselectivity differences of conventional ion exchange membranes in an electrodialysis system with brackish groundwater feed solutions (Chapter 3 of this dissertation).

3. Preliminary development of polyethersulfone cation exchange membranes for electrodialysis desalination (Chapter 4 of this dissertation).

1.5. REFERENCES

1. WHO/UNICEF, 2014. Progress on Drinking-water and Sanitation 2014 Update. World Health Organization, 1, 1.
2. U.S. Geological Survey, The World's Water. 2016. Available from: https://water.usgs.gov/edu/earthwherewater.html, Accessed on 2017 February 04.
3. Hoffbuhr, J., Archuleta, E., Crook, J., Gritzuk, M., Lynch, G., Richardson, A., and Towry, J. V. (2004). "What's driving water reuse?" Journal AWWA, 96(4), 58-62.
4. Giwa, S.W. Hasan, A. Yousuf, S. Chakraborty, D.J. Johnson, N. Hilal, Biomimetic membranes: A critical review of recent progress, Desalination 420 (2017) 403–424.
5. Fritzmann, C., Lowenberg, J., Wintgens, T., and Melin, T. (2007). "State-of-the-art of reverse osmosis desalination." *Desalination*, 216(1-3), 1-76
6. GWI IDA Yearbook 2017-2018, Desal Data, https://www.desaldata.com, Accessed: 2018 February 12.
7. U.K. Kesieme, N. Milne, H. Aral, C.Y. Cheng, M. Duke, Economic analysis of desalination technologies in the context of carbon pricing, and opportunities for membrane distillation, Desalination 323 (2013) 66 –74.
8. Bonné, P. A. C., Hofman, J. A. M. H., and van der Hoek, J. P. (2000). "Scaling control of RO membranes and direct treatment of surface water." *Desalination*, 132(1-3), 109-119.
9. Reedy, K. A., and Tadanier, C. J. (2008). "Controlling groundwater desalination costs: Facility and process planning (poster)." AWWA Annual Conference and Exposition (ACE), AWWA, Atlanta, GA.
10. AWWA, (1995). "M38 - electrodialysis and electrodialysis reversal." Manual of water supply practices, P. Murray, ed., American Water Works Association, Denver, CO.
11. Cappelle, M., A., High recovery inland desalination: a technical and economic performance evaluation of zero discharge desalination, doctoral thesis report, civil engineering dept, The University of Texas at El Paso, 2018. Available from:

https://scholarworks.utep.edu/cgi/viewcontent.cgi?article=2405&context=open_etd, Accessed on 2018 April 14.

12. Strathmann, H. (2010). Electrodialysis, a mature technology with a multitude of new applications. Desalination, 264(3), 268-288.
13. Strathmann, H. (2004). *Ion-exchange membrane separation processes*, Membrane science and technology series, Elsevier, Boston.
14. T.W. Xu, Ion-exchange membranes: state of their development and perspective, J. Membr. Sci. 263 (2005) 1 –29.
15. A.J.B. Kemperman, Membrane and equipment manufacturers, in: A.J.B., Kemperman (Ed.), Handbook on Bipolar Membrane Technology, Twente University Press, Enschede, 2000, pp. 9–16.
16. http://www.astom-corp.jp/en/index.html; http://www.ameridia.com/html/mbt.html; http://www.pca-gmbh.com; http://www.fuma-tech.de; http://www.tw-membrane.com; http://www.ionics.com; http://www.solvay.com; http://www.ionexchange.com.
17. Goh, P. S., Ismail, A. F., & Matsuura, T. (2018). Perspective and roadmap of energy-efficient desalination integrated with nanomaterials. Separation & Purification Reviews, 47(2), 124-141.
18. Firdaous, L., Malériat, J. P., Schlumpf, J. P., & Quéméneur, F. (2007). Transfer of monovalent and divalent cations in salt solutions by electrodialysis. *Separation Science and Technology*, *42*(5), 931-948.
19. Krol, J. J., Wessling, M., & Strathmann, H. (1999). Concentration polarization with monopolar ion exchange membranes: current–voltage curves and water dissociation. *Journal of Membrane Science*, *162*(1-2), 145-154.
20. Káňavová, N., Machuča, L., & Tvrzník, D. (2014). Determination of limiting current density for different electrodialysis modules. *Chemical Papers*, *68*(3), 324-329.
21. F. Leitz, "High temperature electrodialysis: Phase V," 1974.

22. Walker, W. S., Kim, Y., & Lawler, D. F. (2014). Treatment of model inland brackish groundwater reverse osmosis concentrate with electrodialysis—Part I: sensitivity to superficial velocity. *Desalination*, *344*, 152-162.
23. Grossman, G., and Sonin, A. A. (1972). "Experimental study of the effects of hydrodynamics and membrane fouling in electrodialysis." *Desalination*, 10(2), 157-180.
24. Grossman, G., and Sonin, A. A. (1973). "Membrane fouling in electrodialysis: A model and experiments." *Desalination*, 12(1), 107-125.
25. Berger, C., and Lurie, R. M. (1962). "Supersaturation of sulfates in electrodialysis. "*Industrial & Engineering Chemistry Process Design and Development*, 1(3), 229- 236.
26. Tanaka, Y. (2007). *Ion exchange membranes: Fundamentals and applications*, Membrane science and technology series, Elsevier, Boston.
27. R. Bond, T. A. Davis, J. DeCarolis, and M. Dummer, “Demonstration of a new electrodialysis technology to reduce energy required for salinity managment: Treatment of RO concentrate with EDM,” 2015.
28. Lee, H., Strathmann, H., Moon, S., Determination of the limiting current density in electrodialysis desalination as an empirical function of linear velocity, Desalination, 190 (2006) 43-50.

Chapter 2: Evaluation of Electrodialysis Desalination Performance of Novel Bioinspired and Conventional Ion Exchange Membranes with Sodium Chloride Feed Solutions[2]

Abstract

Electrodialysis (ED) desalination performance of different conventional and laboratory-scale ion exchange membranes (IEMs) has been evaluated by many researchers, but most of these studies used their own sets of experimental parameters such as feed solution compositions and concentrations, superficial velocities of the process streams (diluate, concentrate, and electrode rinse), applied electrical voltages, and types of IEMs. Thus, direct comparison of ED desalination performance of different IEMs is virtually impossible. While the use of different conventional IEMs in ED has been reported, the use of bioinspired ion exchange membranes has not been reported yet. The goal of this study was to evaluate the ED desalination performance differences between novel laboratory-scale bioinspired IEM and conventional IEMs by determining (i) limiting current density, (ii) current density, (iii) current efficiency, (iv) salinity reduction in diluate stream, (v) normalized specific energy consumption, and (vi) water flux by osmosis as a function of (a) initial concentration of NaCl feed solution (diluate and concentrate streams), (b) superficial velocity of the feed solution, and (c) applied stack voltage per cell-pair of membranes. A laboratory-scale single-stage batch-recycle electrodialysis experimental apparatus was assembled with five cell-pairs of IEMs with an active cross-sectional area of 7.84 cm^2. In this study, seven combinations of IEMs (commercial and laboratory-made) were compared: (i) Neosepta AMX/CMX, (ii) PCA PCSA/PCSK, (iii) Fujifilm Type 1 AEM/CEM, (iv) SUEZ AR204SZRA/CR67HMR, (v) Ralex AMH-PES/CMH-PES, (vi) Neosepta AMX/Bare Polycarbonate cation exchange membrane (Polycarb), and (vii) Neosepta AMX/Sandia novel bioinspired cation exchange membrane (SandiaCEM). ED desalination performance with the

[2] Chapter 2 of this dissertation has been published (open access):
Hyder, A.G.; Morales, B.A.; Cappelle, M.A.; Percival, S.J.; Small, L.J.; Spoerke, E.D.; Rempe, S.B.; Walker, W.S. Evaluation of Electrodialysis Desalination Performance of Novel Bioinspired and Conventional Ion Exchange Membranes with Sodium Chloride Feed Solutions. *Membranes* **2021**, *11*, 217. https://doi.org/10.3390/membranes11030217

Sandia novel bioinspired cation exchange membrane (SandiaCEM) was found to be competitive with commercial Neosepta CMX cation exchange membrane.

Keywords: Electrodialysis, desalination, bioinspired, ion-exchange membrane, NaCl feed.

2.1. INTRODUCTION

2.1.1. Background

Many studies of electrodialysis (ED) have evaluated the desalination performance of commercial and laboratory-scale ion exchange membranes (IEMs), but most of these studies used independent sets of experimental parameters or conditions such as feed solution compositions and concentrations, superficial velocities of the process streams (diluate, concentrate, and electrode rinse), and applied electrical voltages [1-12]. IEMs work by allowing mainly ions to pass through them while rejecting the transport of water molecules (*i.e.*, opposite of reverse osmosis or forward osmosis membranes). Most studies use only one type of anion exchange membrane (AEM) and cation exchange membrane (CEM) [1-7,10], and only a few compare two different types of AEM and CEM membranes [9,11-12]. Therefore, it is difficult to assess the desalination performance of different commercially available and well-known IEMs and to recommend suitable IEMs for ED to achieve a desirable outcome (*i.e.,* high ion-selectivity, high salinity removal, high water recovery, low energy consumption, or low osmotic water flux). Moreover, the bioinspired IEM developed recently [13,14] has not been reported yet for use in ED.

2.1.2. Objectives

The goal of the study was to evaluate the ED desalination performance differences between novel laboratory-scale bioinspired IEM and conventional IEMs, using a similar set of experimental parameters. The ED desalination performance of the IEMs was evaluated by determining (i) limiting current density, (ii) current density, (iii) current efficiency, (iv) salinity reduction in diluate stream, (v) normalized specific energy consumption, and (vi) water flux by osmosis as a

function of (a) initial concentration of NaCl feed solution (diluate and concentrate streams), (b) superficial velocity of the feed solution, and (c) applied stack voltage per cell-pair of membranes.

2.2. MATERIALS AND METHODS

2.2.1. Experimental plan and variables

The laboratory-scale batch-recycle experimentation was planned to examine the pseudo-steady-state operation of the electrodialysis system as a function of time, which is equivalent to a full-scale single pass operation as a function of distance along the flow path, from inlet to outlet. The experimentation was designed, following another study [10], by maintaining dynamic similitude between full-scale and batch-recycle operation for (i) the velocity of the feed solution flow between AEMs and CEMs, and (ii) the electric potential drop per cell-pair of membranes (consequently, the current density and current efficiency).

Discrete values and ranges of experimental variables are shown in Table 2.1. The feed water concentrations were representative of freshwater (1 g/L), brackish water (3-10 g/L), seawater (35 g/L), and produced water (100 g/L). The electrode rinse solution was prepared with a fixed concentration of 0.1 molar (14.2 g/L) sodium sulfate (Na_2SO_4). The range of electrical and hydraulic conditions simulated full-scale ED systems. The membranes used in this study were commercially available general desalination IEMs, commercial bare polycarbonate CEM (Polycarb), and laboratory-made Sandia novel bioinspired CEM (SandiaCEM). The ED desalination performances of seven membrane pairs were compared through various experimental conditions (*e.g.,* superficial velocity, stack voltage, and feed concentration) in terms of current density, current efficiency, salinity reduction in diluate stream, normalized specific energy consumption, and water flux.

Table 2.1: Experimental variables, value ranges, and combinations

Variables	Discrete Values/Combinations
NaCl feed water concentration	1, 3, 10, 35, 100 g/L
Superficial velocity of diluate stream	2, 4, 8 cm/s (corresponding flow: 15, 30, 60 mL/minute)
Stack voltage	0.4, 0.8, 1.2 V/cell-pair
Combination of membranes during stack assembly	i. Neosepta AMX & CMX ii. PCA PCSA & PCSK iii. Fujifilm Type 1 AEM & CEM iv. SUEZ AR204SZRA & CR67HMR v. Ralex AMH-PES & CMH-PES vi. Neosepta AMX & bare polycarbonate CEM (Polycarb) vii. Neosepta AMX & Sandia novel bioinspired CEM (SandiaCEM)

2.2.2. Experimental system and chemicals

A batch-recycle electrodialysis experimental system was assembled, and a schematic diagram of the process is shown in Figure 2.22.1. A laboratory-scale Master Flex peristaltic cartridge pump (Cole-Parmer, USA, Model: 7519-00) was used to circulate the solutions through each of the three process streams (*i.e.,* diluate, concentrate, and electrode rinses). The flow rates through each of the process streams were controlled manually and the flow rate was monitored manually at 30-minute intervals. The process stream reservoirs were one-liter plastic bottles that are stirred by non-heating magnetic stirrers (Fisher Scientific, USA, model: Fisher 14-955-150). The electrical conductivity, pH, and temperature of the process stream reservoirs were determined using a pH/conductivity meter (Thermo Scientific, USA, model: Orion Star A325). The mass of the diluate reservoir was measured continuously to the nearest 0.1 g using a digital mass balance

(Meller Toledo, USA, model: XS2002S) to gravimetrically quantify the net mass of water and salt transportation across the membranes. Analog pressure gauges (Grainger low-pressure gauge, model: 18C774) were used at the inlet of the diluate, concentrate, and electrode rinse streams to observe the head loss through each stream and the average transmembrane pressures. A programmable DC Power Supply (B&K Precision, USA, Model: 9123A) was used for monitoring and controlling voltage and current through the electrodialysis stack. A photo of the experimental setup is shown in Figure 2.22.2.

Laboratory-grade sodium chloride (NaCl, ACS reagent grade) and sodium sulfate (Na_2SO_4, ACS reagent grade) salts were purchased from Fisher Scientific (USA) to prepare the feed water and electrode rinse solutions, respectively. All reagent water was purified and deionized to a resistivity of 18.2 MΩ cm.

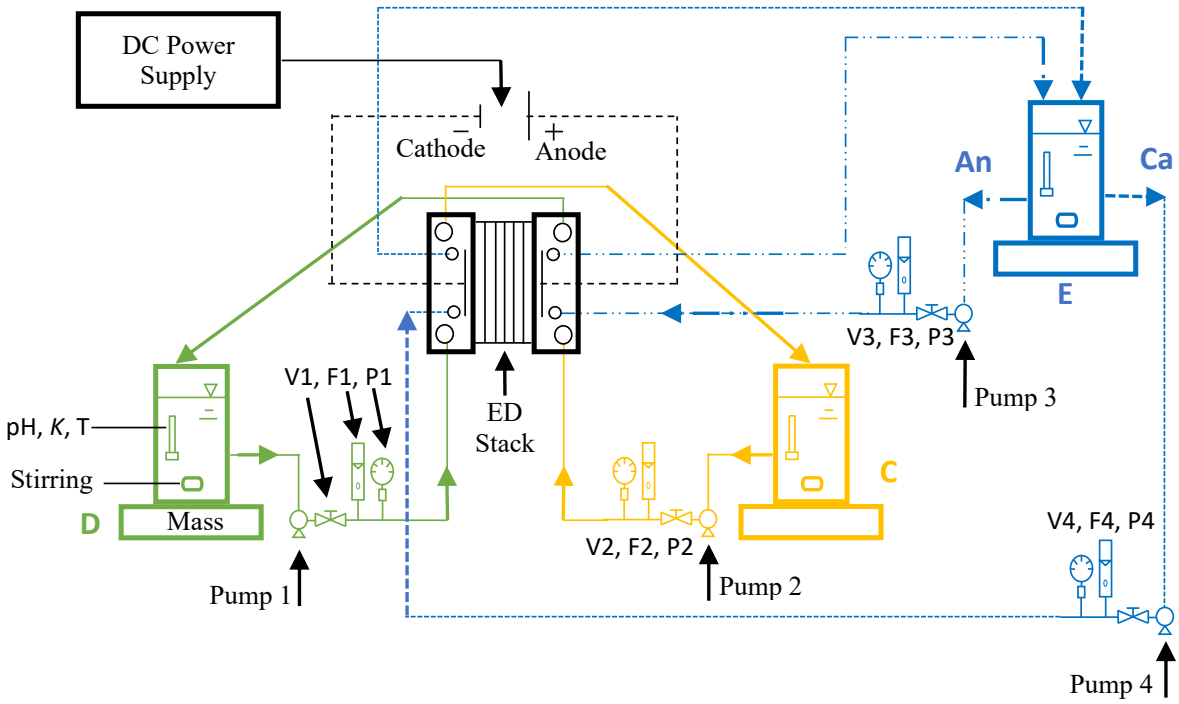

Source: Adapted from 10

K = Conductivity, T = Temperature; V = Valve, F = Flow Meter, P = Pressure gauge, D = Diluate Stream, C = Concentrate Stream, E = Electrode Rinse, An = Anolyte, Ca = Catholyte

Figure 2.1: A schematic diagram for the batch-recycle electrodialysis process

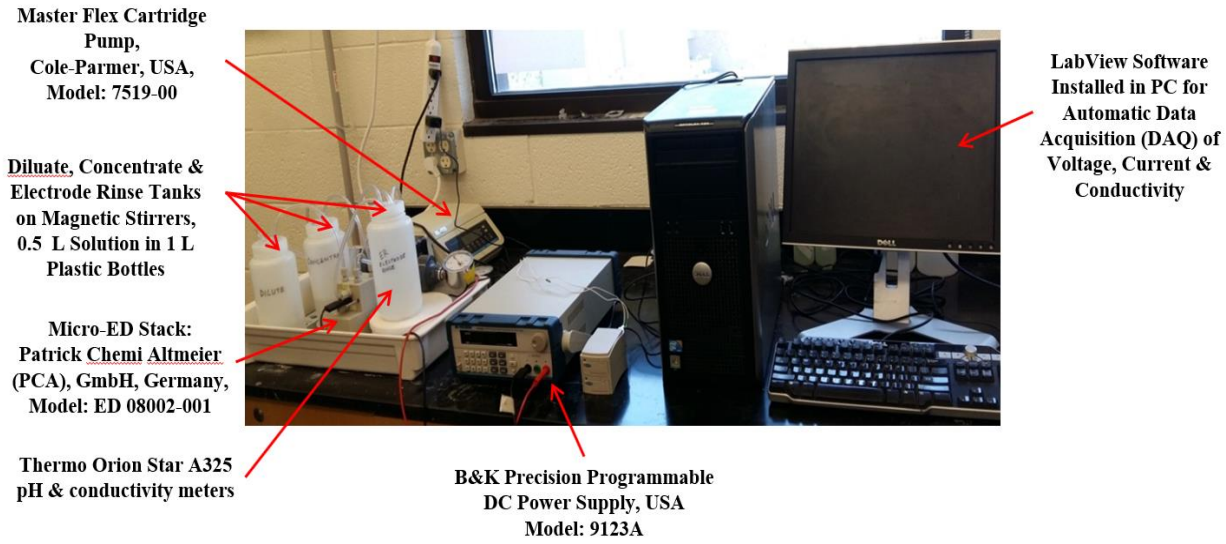

Figure 2.2: Experimental setup

2.2.3. Experimental Electrodialysis (ED) stack or Electrodialyzer

A laboratory-scale single-stage electrodialysis stack (model: 08002-001) was purchased from PCCell/PCA, GmbH (Germany). The anode was made of titanium metal with platinum/ iridium coating, and the cathode was stainless steel. The end-plates, surrounding the electrodes and compressing the stack, were made of polypropylene. The active cross-sectional area of the membrane subjected to the applied electric field was 7.84 cm^2 (2.80 cm x 2.80 cm). Polyester mesh spacer-gaskets of thickness 0.45 mm physically separated the AEMs and CEMs. In assembling the ED stack, the end-plates compressing the stack were tightened until a given flow rate yielded the same pressure drops (*i.e.*, 3 kPa) through the stack (*i.e.*, from inlet to outlet of diluate and concentrate streams) for each experiment. For a specific combination of membranes, consistency across the replicate tests was confirmed by measuring the distance between the end-plates with a digital calliper.

2.2.4. Experimental Ion exchange membranes (IEMs)

In this study, seven combinations of IEMs (commercial and laboratory-made) were used:

i. Neosepta AMX/CMX,

ii. PCA PCSA/PCSK,

iii. Fujifilm Type 1 AEM/CEM,

iv. SUEZ AR204SZRA/ CR67HMR,

v. Ralex AMH-PES/ CMH-PES,

vi. Neosepta AMX/Bare Polycarbonate membrane (Polycarb), and

vii. Neosepta AMX/Sandia novel bioinspired cation exchange membrane (SandiaCEM).

The Neosepta AMX/CMX membrane pair was considered as the control membrane to compare the performances of the other six membrane pairs with the AMX/CMX pair. Bare polycarbonate membrane (0.05 μm pore, 90 mm diameter, 6 μm thick) was purchased from Sterlitech Corporation (USA). The detailed description of the development, prospects, applications, and properties of these commercial IEMs have been articulated in literature and the company's websites [15-26]. However, a list of standard properties is summarized in Table 2.

Table 2.2: Standard properties of IEMs used in this study

Membrane	Type	Thickness (mm)	IEC (meq/g)	Areal Resistance (Ω cm^2)	Remarks	Ref.
Polycarbonate	-	0.006	-	- 10.3	Filtering air/water	[22]
Ralex AMH-PES*	AEM	0.55 Dry	1.8	< 8	ED, EDI	[15,20]
Ralex CMH-PES*	CEM	0.45 Dry	2.2	< 9	ED, EDI	[15,20]
PCA PCSA	AEM	0.232	1.69	-	Standard ED	[19]
PCA PCSK	CEM	0.098	1.25	-	Standard ED	[19]
Neosepta AMX	AEM	0.12-0.18	1.4-1.7	2.0-3.5	High strength	[15,17]
Neosepta CMX	CEM	0.14-0.20	1.5-1.8	2.0-3.5	High strength	[15,17]
Fujifilm Type 1 AEM	AEM	0.125	1.50	1.3	Water softening	[21]
Fujifilm Type 1 CEM	CEM	0.135	1.43	2.7	Water softening	[21]
SUEZ AR204SZRA	AEM	0.48-0.66	2.3-2.7	6.2-9.3	EDR	[15,20]
SUEZ CR67HMR	CEM	0.53-0.65	2.1-2.45	7.0-11.0	ED	[15,20]
Sandia CEM*	CEM	0.0072	-	-18.5	ED, EDR	[13]

*Note: *****Heterogeneous membranes (others are homogeneous), IEC: Ion-exchange Capacity, ED: Electrodialysis, EDR: Electrodialysis Reversal, and EDI: Electro-deionization.*

A bioinspired membrane is a type of membrane that is developed to incorporate structural features of biological cellular membranes, specifically, ion channel proteins [27]. Water permeable bioinspired desalination membranes using aquaporin (AQPs) water channels are reported for use in pressure-driven and osmotically-driven desalination [28-32].

However, the use of bioinspired IEM in ED has not been reported yet. To our knowledge, this is the first testing of a bioinspired IEM in electrodialysis. The Sandia novel bioinspired cation exchange membrane (SandiaCEM) used in this study was fabricated by Percival, et al. [13,14] using a layer by layer (LbL) dip coating assembly process of electrolytes (*e.g.,* polyacrylic acid (PAA) and polyethylimine (PEI)) with crosslinking reagents (*e.g.,* glutaraldehyde (GA) and N-dimethylaminopropyl-N_0-ethylcarbodimide hydrochloride (EDC)) over a bare polycarbonate (Polycarb) support membrane. The SandiaCEM demonstrated ionic selectivity which was

achieved with the use of LbL deposition of many nanostructured polyelectrolyte layers [13,14]. The cation transport selectivity was increased with the increasing number of polyelectrolyte layers when the polyelectrolyte or polymer layers were cross-linked with GA [13]. Ionic selectivity was independent of ionic conductivity and the ionic conductivity was decreased with the coatings but was found to regain a portion of it upon crosslinking the polyelectrolyte [13,14]. Cross-linking the membranes also increased the intermolecular integrity of the polyelectrolyte films and inhibited the slow surface diffusion and redissolution of the polyelectrolyte films [13]. The SandiaCEM is an example of how a controllable and inexpensive method can be tailored to create ion-selective and chemically robust bioinspired membranes on porous supports for a wide range of applications.

2.2.5. Experimental procedure

All membranes used in this study were soaked in 0.01 M NaCl solution for 24 hours prior to use. Soaked membranes were trimmed to 6.4 cm x 4.4 cm size, and three holes were punched at precise locations along each side. The electrodialysis stack was assembled with five cell-pairs of cation- and anion-exchange membranes by arranging them in an alternating pattern between two electrodes. Five cell-pairs were built with five anion exchange membranes, five cation exchange membranes, and one additional Neosepta CMB membrane was always placed adjacent to the end spacer on the cathode side. The Neosepta CMB membrane is a cation exchange membrane that has high mechanical strength (burst strength ≥ 0.40 MPa) and alkali resistance (electrical areal resistance = 4.5 Ω cm^2), and it can resist the effect of high pH occurring as a result of reduction of water on the cathode during the electrodialysis experiments [33].

Synthetic feed water solutions (diluate and concentrate) of 1, 3, 10, 35, and 100 g/L were prepared by adding NaCl salt in deionized water in the laboratory. The feed water concentrations were representative of freshwater (1 g/L), brackish water (3 and 10 g/L), seawater (35 g/L), and produced water (100 g/L). In the study, sodium chloride (NaCl) feed solution was used, but real brackish water, seawater, and produced water contains additional ions (*e.g.,* calcium, sulfate,

nitrate, and fluoride), depending on the sources water types and locations. Since the concentration of sodium and chloride ions is relatively abundant among brackish water, seawater, and produced water samples, a binary NaCl feed solutions was used in this study [34]. As with this study, many other studies also used NaCl feed solution with different concentration ranges such as 3-40 g/L [34-36], even for 3-150 g/L [37]. Synthetic electrode rinse solution was also prepared by mixing a fixed concentration of 0.1 molar sodium sulfate (14.2 g/L Na_2SO_4) with deionized water in the laboratory.

The diluate solution was circulated at a flow rate of 15, 30, and 60 mL/minute (corresponding to a superficial velocity of 2, 4, and 8 cm/s, respectively through the diluate cells inside electrodialysis stack), and the pressure of the diluate cell for the relevant flow rate was recorded. The solution flow rate through the concentrate cells and electrode rinse compartments was adjusted to maintain the same pressure as diluate cells. The transmembrane pressure difference between the diluate, concentrate, and electrode rinse compartments was kept lower than 1.4 kPa (0.2 lb/in^2), which was recommended by another study [25], to stabilize the electrodialysis system.

After stabilizing the flows and pressures, the voltage loss at the electrodes (including thermodynamic, overpotential, and ohmic contributions) was determined experimentally (see the calculation section of this article for more information). Afterward, the applied stack voltage (voltage requirement across the electrodialysis stack) was calculated by subtracting the voltage loss at the electrodes from the total applied voltage. Every 5s, the experimental LabVIEW supervisory control and data acquisition (SCADA) system automatically calculated the voltage loss at the electrodes and recalculated the corresponding total applied voltage to maintain a desired stack voltage (e.g., 0.4, 0.8, or 1.2 V per cell-pair).

The experimental data for hydraulic (e.g., diluate reservoir mass change), electrical (e.g., applied voltage and current), and chemical (e.g., pH, temperature, conductivity) parameters were recorded automatically in excel spreadsheets in the computer by the LabVIEW SCADA system. Finally, the acquired data were analyzed to evaluate ED desalination performance of the novel laboratory-scale bioinspired and conventional IEMs with respect to (i) current density, (ii) current

efficiency, (iii) salinity reduction in diluate stream, (iv) normalized specific energy consumption, and (v) water flux by osmosis as a function of (a) initial concentration of NaCl feed solution (diluate and concentrate streams), (b) superficial velocity of feed solution, and (c) applied stack voltage per cell-pair of membranes. Each of the experiments was conducted in triplicate to check the accuracy and consistency of data while maintaining a standard deviation lower than 5%.

The step-by-step general experimental procedures are summarized below:

1. Experimental and pre-rinse solutions (same as experimental concentration) were prepared for electrodialysis system equilibration.
2. Pre-rinse solutions from the three process streams were circulated, and the experimental DC voltage was applied at the electrodes to approach the equilibration of the membranes with the solution.
3. After evacuating the pre-rinse solution, the electrodialysis apparatus was loaded with the experimental solutions.
4. The experiment was performed with full data acquisition.
5. Acquired data were analyzed to determine ED desalination performance.

2.2.6. Data acquisition and control hardware

A custom supervisory control and data acquisition (SCADA) system was developed in LabVIEW 2017 software for controlling and monitoring hardware such as the programmable mass-balance, DC Power supply, and pH/conductivity meters at five-second intervals during each of the experiment. The experimental data were recorded for hydraulic (*e.g.,* flow rates and diluate reservoir mass change), electrical (*e.g.,* applied voltage and current), and chemical (*e.g.,* pH, temperature, conductivity) characterization.

2.2.7. Data analysis

Output files generated by the custom LabVIEW SCADA system were saved automatically as spreadsheets, which were subsequently analyzed to calculate limiting current density, current density, charge efficiency, salinity reduction, electrical power, hydraulic power, normalized specific energy consumption, and water flux by osmosis using the calculation methods described in the following section.

2.2.8. Calculation methods

2.2.8.1.Electrode voltage loss

The voltage loss at the electrodes (including thermodynamic, overpotential, and ohmic contributions) was determined experimentally by measuring the voltage and current density relationship of the electrodes and electrode rinse solution of the electrodialysis stack by following the experimental and calculation procedures reported by Walker *et al.* [10]. The electrodialysis stack was assembled using a single Neosepta CMB membrane with two end spacers and circulating only electrode rinse solution (concentrate and diluate cells were absent). The tests for determining the voltage loss at the electrodes were performed by applying the current density up to 3,000 A/m^2 (300 mA/cm^2). Each component of the total electrode voltage loss equation was identified from the model and those values were: voltage drop from gas equilibrium at the electrodes ($\Delta\phi_{equ}$) ≈1.23 V, the distance between the electrode and the first membrane of the stack (w) = 4.1 mm, conductivity of electrode rinse solution (κ_{rinse}) =15.85 mS/cm, the modified transfer coefficient (α) = 0.0458, and exchange current density (i_o) = 1.069 A/m^2. The values of w, α, and i_o were determined simultaneously by non-linear regression.

2.2.8.2.Power and specific energy consumption (SEC)

Electrical power consumption by the electrodialysis stack was calculated by the multiplication of the applied voltage to the electrodialysis stack and the electrical current passing

through the electrodialysis stack. Energy consumption by the electrodialysis stack was determined by multiplying the consumed electrical power with the experimental period. Energy consumption by the hydraulic pumps was calculated from the flow rate and pressure drop. Moreover, specific energy consumption (SEC) (expressed as kWh/m^3) was the amount of energy consumed by the desalination process to produce a given volume of product water. Normalized specific energy consumption (nSEC) [expressed as (kWh/m^3) / (mol/L removed) or (kWh/m^3) per (eq/L-removed)] was the amount of energy consumption (kWh) required for the production of one cubic meter (m^3) product water for per mol/L of salt removal.

The DC electrical power ($P_{electrical}$) consumed by the electrodialysis stack was calculated using the formula as below [10]:

$$P_{electrical} = \Delta V_{stack}\, I \tag{2.1}$$

where, ΔVstack is the voltage drop across the electrodialysis stack (V), and I is the electrical current measured through the electrodialysis stack (A).

The hydraulic power ($P_{hydraulic}$) for pumping the solution through the electrodialysis stack was calculated using the formula as below [10]:

$$P_{hydraulic} = \rho\, g\, Q\, \Delta H \tag{2.2}$$

where, ρ is the solution mass-density, g is the gravitational constant, Q is the volumetric flow rate, and ΔH is the hydraulic head loss through the stack.

The specific energy consumption (SEC) was calculated using the formula below [10]:

$$SEC = \frac{P_{\text{electrical}} + P_{\text{hydraulic}}}{Q_{\text{d}}} \tag{2.3}$$

where, P is the power (kW) and Q_{d} is the flow rate of the diluate stream (m^3/hr).

Normalized SEC was calculated using the formula below [10]:

$$SEC_{\text{normalized}} = \frac{SEC}{C_{\text{f}} - C_{\text{d}}} \tag{2.4}$$

where C_{f} is the concentration of feed solution at the beginning of the experiment (meq/L) and C_{d} is the concentration (meq/L) of diluate solution at any time (t) of the experiment.

2.2.8.3.Current density

Electrical current density is the amount of electrical current (or charge flux: Coulombs per second per square meter) passing through the per square meter of the membrane's active area inside the electrodialysis stack. Current density increases with the increase of concentrations in feed solution and the increase of solution velocity in the process streams whereas current density declines with the decrease of solution temperature in the process streams as the effective cell resistance increases [38,39] Theoretically, in an ideal electrodialysis system, the ion separation rate is proportional to the electrical current density through the electrodialysis stack. Current density (i) was calculated using the following formula [10]:

$$i = \frac{I}{\mathrm{A}} \tag{2.5}$$

where, I is the electric current (A) and A is the active transfer area of membrane (m^2).

2.2.8.4.Limiting current density (LCD) and limiting polarization parameter (LPP)

The limiting current density (LCD) is the maximum allowable current density at which the concentration of salt ions at the membrane surface becomes zero inside the diluate cell of electrodialysis stack. Electrodialysis systems should operate at a current density less than the LCD in order to prevent water splitting, wastage of power, and damage to electrodialysis equipment. LCD depends on the electrodialysis process parameters such as feed water concentration, and velocity and temperature of process streams [38,39]. LCD increases with the increase of concentration in feed solution and with the increase of solution velocity in the process streams [38,39]. LCD declines with the decrease of solution temperature in the process streams because the effective cell resistance increases [38-40].

LCD was determined using the voltage and current data that were recorded during the experiments. Theoretically, there are different approaches employed to determine and compare the LCD [41]; firstly, the "Shoulder" method was used which involves plotting stack voltage on the abscissa and current density (i) on the ordinate (Figure 2.3a), and secondly, the "Cowan-Brown" method was used which involves plotting inverse of stack's current density ($1/i$) on the abscissa

and stack's areal electrical resistance per cell-pair on the ordinate (Figure 2.3b) [39-41]. As shown in Figure 2.3a-b, the LCD was the point where two lines (blue and red) intersected in both methods [41].

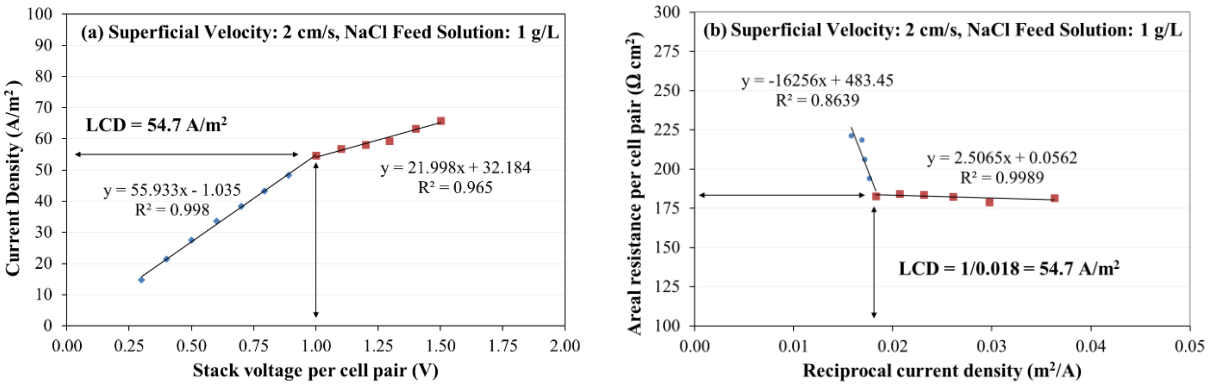

Figure 2.3: LCD determination using (a) Shoulder plot and (b) Cowan-Brown plot

The limiting polarization parameter (LPP) is the limiting current density divided by the normality of the feed solution [10]:

$$\text{LPP} = \frac{\text{LCD}}{C_{\text{f}}} \tag{2.6}$$

where, C_{f} is the concentration (meq/L) of the feed solution. A larger LPP value means that the LCD is greater for a given feed concentration. If the LCD is the "speed limit", then the the LPP is a "normalized speed limit" that is associated with the flow conditions in the diluate cells.

2.2.8.5.Current efficiency

Current utilization capacity, known as the current efficiency, Coulombic efficiency, or charge efficiency (ξ), is the ratio between the amount of the current used in the electrodialysis stack to effectively separate salt ions (from the diluate to the concentrate stream) and the amount of the total current applied to the electrodialysis stack. Typically, current utilization is greater than 90% in electrodialysis desalination processes [42]. Charge efficiency (ξ) was calculated using the formula below [8,25,36]:

$$\xi = \frac{(C_f - C_d)\ \mathrm{Q}\ \mathrm{F}}{\mathrm{I}\ N_{cp}} \quad (2.7)$$

where, C_f and C_d are the concentrations (mol/L) of feed solution and diluate solution, respectively, Q is solution flow rate in diluate and concentrate streams (L/s), F is the Faraday constant (96485.3 Coulombs/eq or Amp-s/eq), I is the measured electrodialysis stack current (Amp), and N_{cp} is number of cell-pair in electrodialysis stack.

2.2.8.6.Salinity reduction

Salinity reduction is the ratio of the amount of salt concentration reduction from the initial salt concentration in the diluate stream as a function of experimental time. Typical, salinity reduction of a single-stage electrodialysis system varies between 50% and 60% depending on source water quality (100-12,000 mg/L TDS), finished water quality (10-1,000 mg/L), and system design [42].

Salinity reduction (R) was calculated using the formula below [10]:

$$\mathrm{R} = \frac{(C_f - C_d)}{C_f} \quad (2.8)$$

where, C_f is the concentration (g/L) of feed solution at the beginning of the experiment and C_d is the concentration (g/L) of diluate solution at any time (t = 60 minutes in this study) of the experiment. The concentration of sodium chloride was calculated from measured electrical conductivity by the following equation:

$$C = 1.224 \times 10^{-9}\,\kappa^4 - 3.243 \times 10^{-7}\,\kappa^3 + 5.135 \times 10^{-5}\,\kappa^2 + 8.869 \times 10^{-5}\,\kappa \quad (2.9)$$

where κ is electrical conductivity in units of mS/cm. This equation is an empirical fit of CRC [43] and Landolt-Börnstein [44] data with relative error less than 1% from 0.1 mol/L to 2 mol/L (10.6 mS/cm to 149 mS/cm), relative error less than 5% from 0.02 mol/L to 0.1 mol/L (2.3 mS/cm to 10.6 mS/cm), and relative error less than 10% from 0.0005 mol/L to 0.02 mol/L (0.062 mS/cm to 2.3 mS/cm).

2.2.8.7.Water transport

Water transport through IEMs decreases the efficiency of the ED separation process [3]. Water transport can occur in two different ways such as (i) osmosis water transport (free water or water molecules only) and (ii) electro-osmosis water transport (water bound to ions). Osmosis water transport or flux occurs when only water molecules pass through the membrane due to the

larger osmotic pressure differences caused by the difference in concentration of the dilute and concentrate channels. Electro-osmosis water transport occurs when water molecules bound to the primary hydration sphere of the ions pass through the membrane at the same time when ions pass through the membrane [3].

Average water flux by osmosis was calculated using the formula [3,8] below:

$$J_w = \frac{\Delta m_{\mathrm{w}}}{(2\, N_{\mathrm{CP}}\, A_{\mathrm{mem}})\, \Delta t_{expt}} \tag{2.10}$$

where, Δm_{w} is change of mass of water (kg), N_{cp} is number of cell-pair in the ED stack (each cell-pair contains two membranes), A_{mem} is the active area of each membrane (m^2), and Δt_{expt} is the experiment duration (hr).

2.3. RESULTS

2.3.1. Evaluation of limiting current density and areal resistance

The limiting current density (LCD), the areal resistance per cell-pair of the membrane, and the limiting polarization parameter were identified for feed solution's superficial velocity of 2, 4, and 8 cm/s at 1, 3, and 10 g/L concentration of NaCl feed solution using the Neosepta AMX-CMX ion exchange membrane pair (a well-known commercial membrane) as they were considered as the control membranes in this study (Figure 2.4). LCD and areal resistance results were not achieved for feed solution concentrations of 35 and 100 g/L because the maximum working capacity of the power supply (30 V, 5 A) was reached before observing LCD (thus, results are not shown for 35 and 100 g/L feed solutions in Figure 2.4). The LCD ranged from 50 to 600 A/m^2, increasing with salinity and increasing with superficial velocity (Figure 2.4a and 2.4c), which is consistent with other studies [39-41]. The voltage application required to achieve LCD ranged from 0.9 to 1.4 Volts per cell pair, the corresponding areal resistance per cell pair at LCD ranged from 22 to 183 $\Omega\ cm^2$ (Figure 2.4b and 2.4d) and limiting polarization parameter ranged from 0.66 to 5.28 A/m^2 per meq/L (Figure 2.4e). The ranges of the limiting polarization parameter are shown in a quartile box and whisker plot (Figure 2.4f) for feed solution velocities of 2, 4, and 8 cm/s. Subsequent experiments were performed with a voltage application less than that observed at LCD.

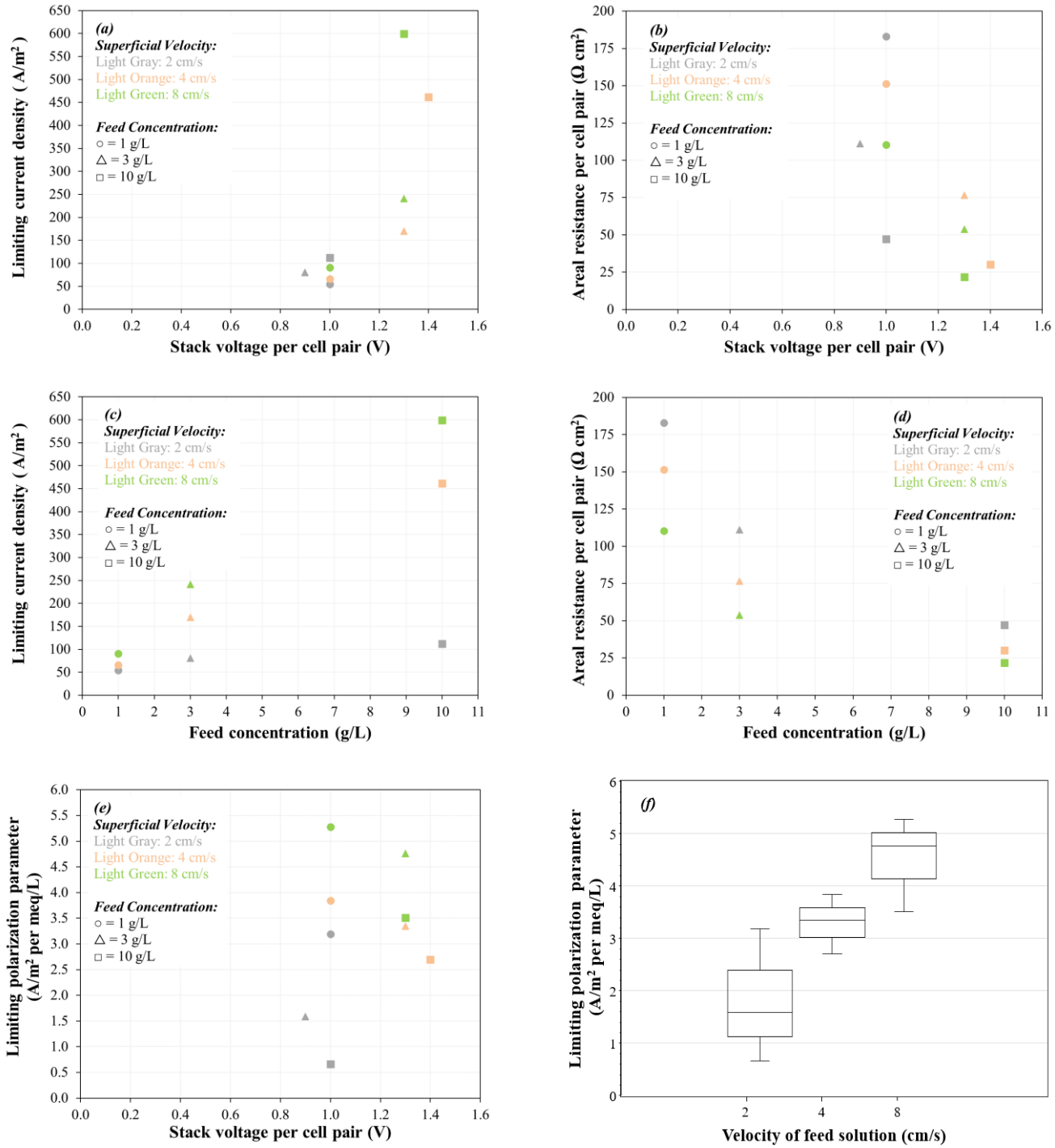

Experimental conditions: 5 Cell-pairs AMX/CMX stack; 2-8 cm/s superficial velocity; constant stack voltage application; 0.1 M (14.2 g/L) Na_2SO_4 electrode rinse solution; and 3 kPa transmembrane pressure

Figure 2.4: Limiting current density (a,c), areal resistance per cell-pair of the membrane (b,d), and limiting polarization parameter (e,f)

2.3.2. Evaluation of current density and current efficiency

The average current density and the average current (or charge) efficiency for 60 minutes of the experimental period were observed for certain permutations of applied stack voltage per cell-pair of membranes, initial concentration of feed solution, and superficial velocity of feed solution for seven combinations of membranes (Figure 2.5). Note that the abscissa axis (voltage application) is categorical (not linear scale). An increasing trend of average current density was observed with increasing feed salinity for all of the membranes (Figure 2.5a, b, and c). The average current density for a given membrane and salinity combination increased with increasing stack voltage and increasing velocity. Generally, in Figure 2.5 parts (a) and (b), the current density for a given feed concentration and voltage application decreased in the following order (*i.e.*, from least to greatest electrical resistance): Fujifilm Type 1 AEM/CEM (purple), PCA PCSK/PCSA (green), AMX/SandiaCEM (blue), Neosepta AMX/CMX (red), SUEZ AR204/CR67 (orange), Ralex CMH-PES/AMH-PES (black), AMX/Polycarb (brown). The current density was generally negatively correlated with areal resistance (see Table 2).

The average current efficiency for most membranes was greater than 80% for feed salinity of 35 g/L or less, and a decreasing trend of average current efficiency was observed with increasing feed salinity for all of the membranes (Figure 2.5 d, e, and f). The average current efficiency for a given membrane and salinity combination increased slightly with increasing stack voltage and increasing velocity. Generally, in Figure 2.5 parts (d) and (e), the current efficiency for a given feed concentration and voltage application decreased (*i.e.*, from greatest efficiency to least efficiency) in the following order: Fujifilm Type 1 AEM/CEM (purple), PCA PCSK/PCSA (green), Neosepta AMX/CMX (red), SUEZ AR204/CR67 (orange), Ralex CMH-PES/AMH-PES (black), AMX/SandiaCEM (blue), AMX/Polycarb (brown). As with current density, the current efficiency was generally negatively correlated with areal resistance (see Table 2.2).

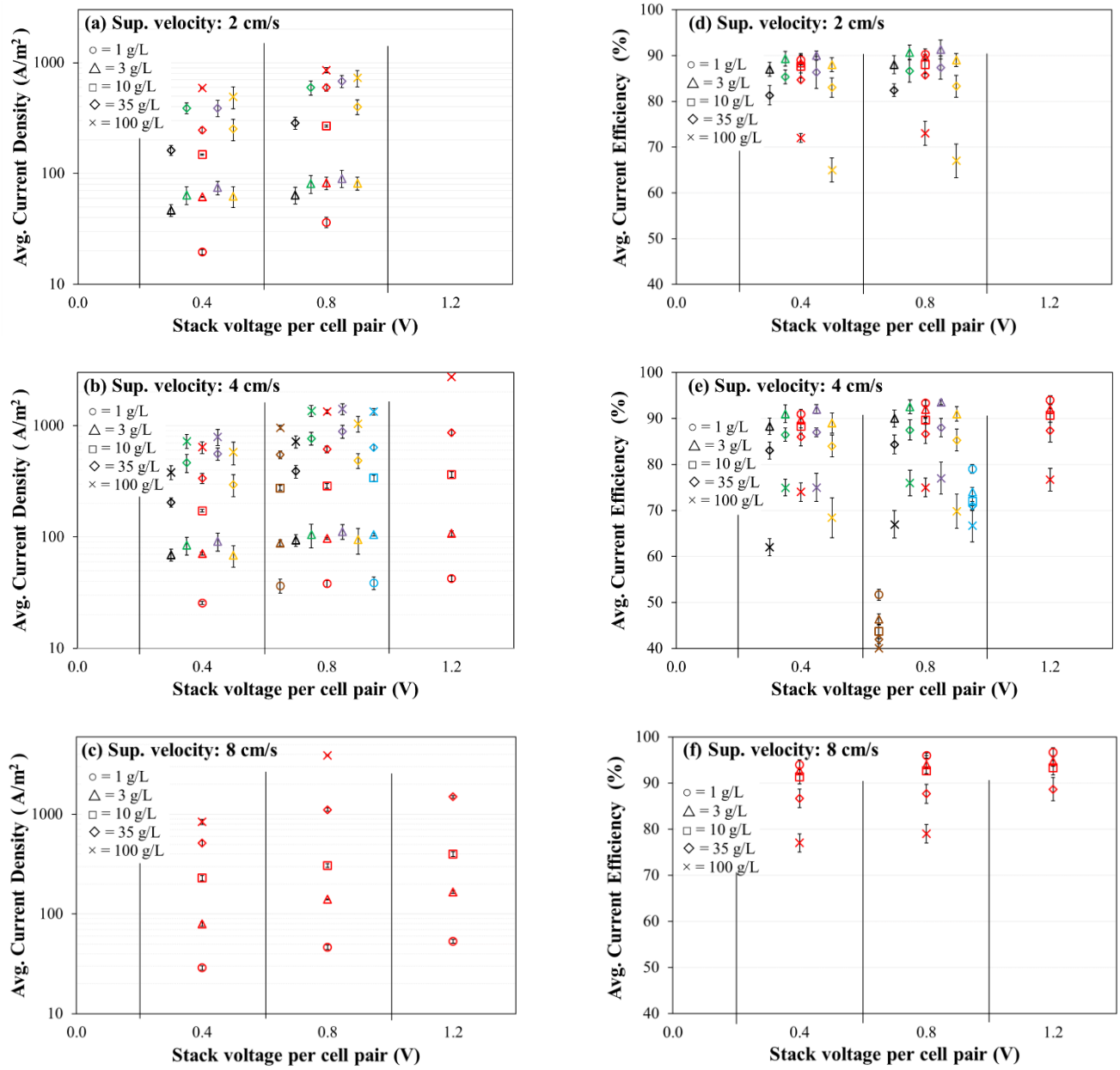

<u>Experimental conditions</u>: 5 Cell-pairs stack;1-100 g/L initial concentration of NaCl feed (diluate and concentrate) solutions (500 mL each); 2, 4, and 8 cm/s superficial velocity of feed solution; 0.4, 0.8, and 1.2 V/cell-pair constant applied stack voltage; 0.1 M (14.2 g/L) Na_2SO_4 electrode rinse solution; and 0.5 psi transmembrane pressure. <u>Representation of Membranes</u>, left to right: Brown: AMX/Polycarb, Black: Ralex CMH-PES/AMH-PES, Green: PCA PCSK/PCSA, Red: Neosepta AMX/CMX, Purple: Fujifilm Type 1 AEM/CEM, Orange: SUEZ AR204/CR67, Blue: AMX/SandiaCEM.

Figure 2.5: Average current density (a-c) and average charge efficiency (d-f) for 60 minutes of experiment against applied stack voltage per cell-pair of the membrane.

2.3.3. Evaluation of salinity reduction and normalized specific energy consumption

The salinity (NaCl concentration) reduction in the diluate stream after 60 minutes of operation was observed for certain permutations of applied stack voltage per cell-pair of membrane, initial concentration of feed solution, and superficial velocity of feed solution for seven combinations of membranes (Figure 2.6a, b, and c). Note that the abscissa axis (voltage application) is categorical (not linear scale). As expected, a decreasing trend of fractional salinity reduction was observed with increasing feed salinity for all of the membranes. The salinity reduction for a given membrane and salinity combination increased significantly with increasing stack voltage and increasing velocity. Generally, in Figure 2.5 parts (a) and (b), for feed concentrations of 3 g/L and 35 g/L, the salinity reduction for a given voltage application decreased in the following order: Fujifilm Type 1 AEM/CEM (purple), PCA PCSK/PCSA (green), Neosepta AMX/CMX (red), AMX/SandiaCEM (blue), SUEZ AR204/CR67 (orange), Ralex CMH-PES/AMH-PES (black), AMX/Polycarb (brown). As with current density and current efficiency, salinity removal was generally negatively correlated with areal resistance (see Table 2).

The normalized specific energy consumption (nSEC, energy intensity (kWh/m^3) per concentration (eq/L) removed) was determined with respect to applied stack voltage per cell-pair of membrane, initial concentration of feed solution, and superficial velocity of feed solution for seven combinations of membranes (Figure 2.5 part d, e, and f). Note that the abscissa axis (voltage application) is categorical (not linear scale). An increasing trend of nSEC was observed with increasing feed salinity for all of the membranes. The nSEC for a given membrane and salinity combination increased significantly with increasing stack voltage (as expected) and increased slightly with increasing velocity *(i.e.*, the increase in hydraulic pumping power with increasing velocity outweighs the decrease in resistances of the diffusion boundary layers). Generally, in Figure 2.6 parts (d) and (e), the nSEC for a given feed concentration (3 g/L and 35 g/L) and voltage application increased in the following order (*i.e.*, from least energy demand to greatest energy demand): Ralex CMH-PES/AMH-PES (black), SUEZ AR204/CR67 (orange), Neosepta

AMX/CMX (red), PCA PCSK/PCSA (green), Fujifilm Type 1 AEM/CEM (purple), AMX/SandiaCEM (blue), and AMX/Polycarb (brown). The nSEC increases with the increase in electrical resistance of IEMs.

For feed concentrations in the range of 3 g/L to 35 g/L, and a voltage application of 0.8 volts per cell pair, most of the membranes had very similar normalized energy consumption in the range of 23 to 27 kWh/m^3 per meq/L removed. The Ralex CMH-PES/AMH-PES (black) membranes were on the lower end of salinity reduction and normalized energy consumption in comparison with the other membranes. The AMX/SandiaCEM (blue) and AMX/Polycarb (brown) membranes were generally on the lower end of salinity reduction and higher end of normalized energy consumption, which shows opportunities for improving the permselectivity of the membranes.

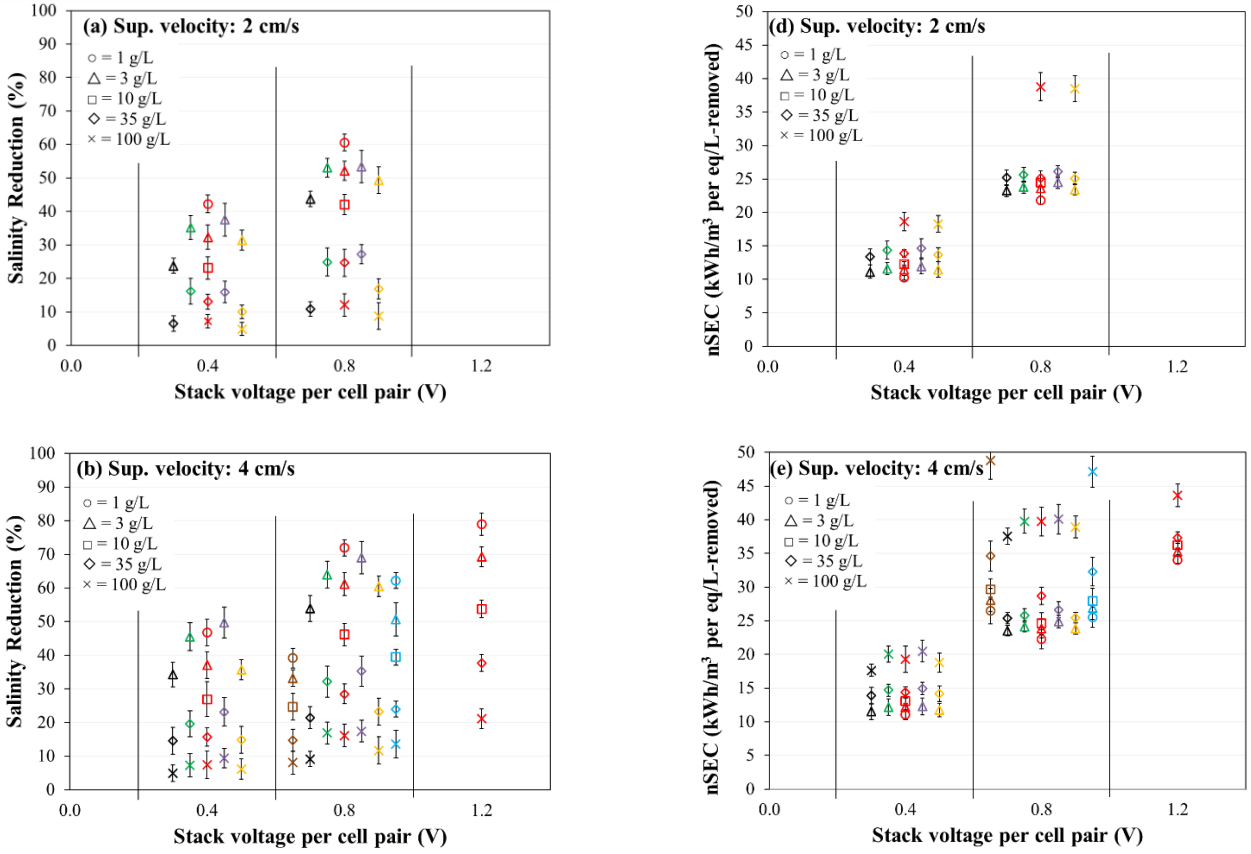

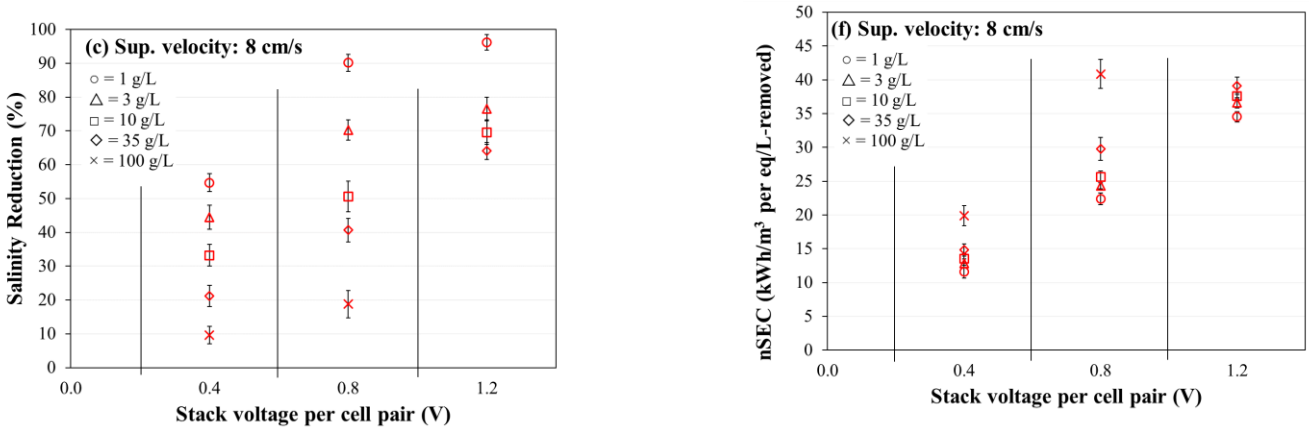

Experimental conditions: 5 Cell-pairs stack;1-100 g/L NaCl initial diluate and concentrate solutions (500 mL each); 2, 4, and 8 cm/s superficial velocity of feed solution; 0.4, 0.8, and 1.2 V/cell-pair constant applied stack voltage; 0.1 M (14.2 g/L) Na_2SO_4 electrode rinse solution; and 0.5 psi transmembrane pressure. Representation of Membranes, left to right: Brown: AMX/Polycarb, Black: Ralex CMH-PES/AMH-PES, Green: PCA PCSK/PCSA, Red: Neosepta AMX/CMX, Purple: Fujifilm Type 1 AEM/CEM, Orange: SUEZ AR204/CR67, Blue: AMX/SandiaCEM.

Figure 2.6: Salinity reduction (a-c) and normalized specific energy consumption (nSEC) (d-f) of diluate stream after 60 minutes of treatment.

2.3.4. Evaluation of water flux by osmosis

The water flux and permeance due to osmosis were measured with respect to the concentration differences and the osmotic pressure difference between concentrate and diluate streams for six combinations of membranes (Figure 2.7a and b). The osmotic water flux experiments were performed at the highest superficial velocity of feed solution of 8 cm/s without the application of any stack voltage. (Tests at 2 and 4 cm/s were omitted because greater osmotic water flux is achievable at the higher superficial velocity). The initial concentration differences between concentrate and diluate were 0.7 g/L (1 g/L vs. 0.3 g/L), 7 g/L (10 g/L vs. 3 g/L), and 65 g/L (100 g/L vs. 35 g/L), which corresponded to osmotic pressure differences of 0.58 bar, 5.42 bar, and 56.81 bar, respectively.

Generally, in Figure 2.7, the osmotic water flux increased in the following order (*i.e.*, from least water flux to greatest water flux): Ralex CMH-PES/AMH-PES (black), Fujifilm Type 1

AEM/CEM (purple), PCA PCSK/PCSA (green), Neosepta AMX/CMX (red), AMX/SandiaCEM (Blue), and SUEZ AR204/CR67 (orange) (Figure 2.7a and b). The Ralex (CMH-PES/AMH-PES) membrane pair exhibited a much lower osmotic water flux than the other four membranes, which was expected. As a heterogeneous membrane, Ralex (CMH-PES/AMH-PES) carries the non-uniform distribution of water content, crosslinking reagent, and charge density in its morphological structure; these properties consequently cause the higher resistance to permeation compared to the other four homogeneous commercial IEMs. Other than the Ralex membranes, osmotic permeance was not well correlated with membrane thickness, ion exchange capacity, or areal electrical resistance. For comparison, water permeance in ion exchange membranes is also reported in Kingsbury *et al*. [45].

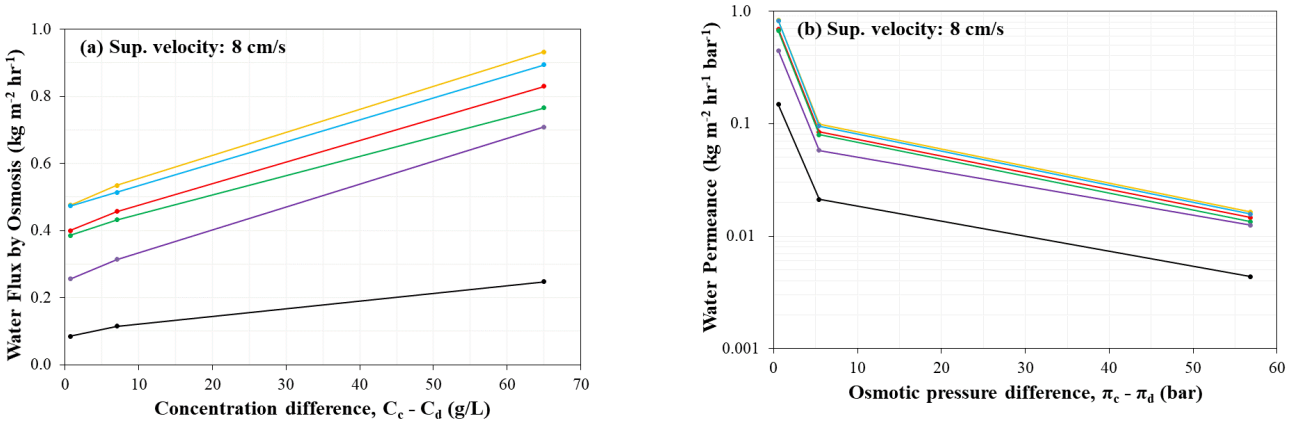

<u>Experimental conditions</u>: 5 Cell-pairs stack; 0.7, 7, and 65 g/L initial concentration differences between NaCl concentrate and diluate streams (500 mL each) corresponding to 0.6, 5.4, and 56.1 atm osmotic pressure differences between NaCl concentrate and diluate stream, respectively; 8 cm/s superficial velocity of feed solution; no applied stack voltage per cell-pair; 0.1 M (14.2 g/L) Na_2SO_4 electrode rinse solution; and 0.5 psi transmembrane pressure. <u>Representation of Membranes</u>, top to bottom: Orange: SUEZ AR204/CR67, Blue: AMX/SandiaCEM, Red: Neosepta AMX/CMX, Green: PCA PCSK/PCSA, Purple: Fujifilm Type 1 AEM/CEM, Black: Ralex CMH-PES/AMH-PES..

Figure 2.7: Water flux by osmosis versus concentration differences (a) and osmotic permeance versus osmotic pressure difference (b).

2.4. CONCLUSIONS AND RECOMMENDATIONS

The Laboratory-scale batch-recycle electrodialysis desalination experiments with aqueous sodium chloride solutions ranging from 1 g/L to 100 g/L was performed with permutations of voltage application (0.4 V, 0.8 V, and 1.2 V per cell pair) and superficial feed velocity (2 cm/s, 4 cm/s, and 8 cm/s) to compare five commercial ion exchange membrane sets with a novel bioinspired cation exchange membrane developed recently at Sandia National Labs [13,14]. The significant conclusions of the study are summarized below:

1. The limiting current density (LCD) of an ED stack with Neosepta AMX/CMX membranes, feed solution of 1 g/L to 10 g/L, and superficial velocity of 2 cm/s to 8 cm/s ranged from 50 to 600 A/m^2, increasing with salinity and increasing with superficial velocity. The voltage application required to achieve LCD ranged from 0.9 to 1.4 Volts per cell pair, and the corresponding areal resistance per cell pair at LCD ranged from 22 to 183 $\Omega\ cm^2$. The limiting polarization parameter ranged from 0.66 to 5.3 A/m^2 per meq/L.
2. Average current efficiency was observed to decrease with increasing feed salinity for all of the membranes. The average current efficiency for a given membrane and salinity combination increased slightly with increasing stack voltage and increasing velocity. Generally, for a given feed concentration and voltage application, the current efficiency decreased in the following order (i.e., from greatest efficiency to least efficiency): Fujifilm Type 1 AEM/CEM, PCA PCSK/PCSA, Neosepta AMX/CMX, SUEZ AR204/CR67, Ralex CMH-PES/AMH-PES, AMX/SandiaCEM, and AMX/Polycarb.
3. The fractional salinity reduction was observed to decrease with increasing feed salinity for all of the membranes, but for a given membrane and feed salinity, the salinity reduction increased significantly with increasing stack voltage and increasing velocity. Generally, the Ralex CMH-PES/AMH-PES, AMX/SandiaCEM, and AMX/Polycarb membranes were on the lower end of salinity reduction and Fujifilm Type 1 AEM/CEM showed the greatest salinity reduction for a given feed concentration (3 g/L and 35 g/L) and voltage

application. The rest of the membranes showed quite similar performance in salinity reduction, with slightly more differentiation at lower feed concentrations.

4. The normalized specific energy consumption (nSEC, kWh/m^3 per eq/L removed) was observed to increase with increasing feed salinity for all of the membranes. The nSEC for a given membrane and salinity combination increased significantly with increasing stack voltage and increased slightly with increasing velocity. Generally, the Ralex CMH-PES/AMH-PES membranes consumed the least energy, but AMX/SandiaCEM and AMX/Polycarb membranes were on the higher end of energy consumption compared to the other membranes for a given feed concentration (3 g/L and 35 g/L) and voltage application. The rest of the membranes showed quite similar performance from a nSEC perspective, with slightly more differentiation at higher feed concentration.
5. Water flux by osmosis was observed to increase with the increase of concentration difference (*i.e.,* osmotic pressure difference for a given IEM and superficial velocity. Generally, the osmotic water flux increased in the following order (*i.e.,* from least osmotic flux to greatest osmotic flux): Ralex CMH-PES/AMH-PES (black), Fujifilm Type 1 AEM/CEM (purple), PCA PCSK/PCSA (green), Neosepta AMX/CMX (red), AMX/SandiaCEM (Blue), and SUEZ AR204/CR67.
6. The ED desalination performance of the Sandia novel bioinspired cation exchange membrane (SandiaCEM) was observed to be competitive with the commercial cation exchange membranes.

Table 2.3: Membrane performance comparison.

Membrane	**Ralex CMH-PES/AMH-PES**	**PCA PCSK/PCSA**	**Neosepta AMX/CMX**	**Fujifilm Type 1 AEM/CEM**	**SUEZ AR204/CR67**	**AMX/ Sandia CEM**
Current Density*	min	> med	> med	**max**	< med	> med
Current Efficiency*	< med	> med	> med	**max**	< med	min
Salinity Reduction	min	> med	> med	**max**	< med	< med
Normalized SEC	**min**	> med	> med	> med	< med	max
Water Permeance	**min**	< med	> med	< med	max	> med

Notes: * for 0.8 V/cell-pair, 4 cm/s, and 3 to 35 g/L; "min" minimum of the six membranes; "< med" less than median; "> med" greater than median; "max" maximum; **boldface** indicates generally preferred attribute.

For the sake of simplicity, a membrane performance comparison is provided in Table 2.3. For most desalination applications in which the total life cycle costs are strongly influenced by energy costs, it is desirable to use membranes with a lower areal resistance and higher current efficiency; in high-salinity applications, it is very important to select low-resistance membranes, but there are some fresh/brackish applications in which the electrical resistance of the diluate cells greatly outweighs the membrane resistance. For desalination applications targeting a very high-water recovery, a low water permeance is a key membrane selection parameter.

Future work should investigate the long-term mechanical stability and durability of the novel bioinspired membrane.

2.5. REFERENCES

1. Banasiak, L. J., Kruttschnitt, T. W., & Schäfer, A. (2007). Desalination using electrodialysis as a function of voltage and salt concentration. Desalination, 205(1-3), 38-46, https://doi.org/10.1016/j.desal.2006.04.038.
2. Ortiz, J. M., Expósito, E., Gallud, F., García-García, V., Montiel, V., & Aldaz, A. (2008). Desalination of underground brackish waters using an electrodialysis system powered directly by photovoltaic energy. Solar Energy Materials and Solar Cells, 92(12), 1677-1688, https://doi.org/10.1016/j.solmat.2008.07.020.
3. Galama, A. H., Saakes, M., Bruning, H., Rijnaarts, H. H. M., & Post, J. W. (2014). Seawater predesalination with electrodialysis. Desalination, 342, 61-69, https://doi.org/10.1016/j.desal.2013.07.012.
4. Xu, P., Capito, M., & Cath, T. Y. (2013). Selective removal of arsenic and monovalent ions from brackish water reverse osmosis concentrate. Journal of hazardous materials, 260, 885-891, https://doi.org/10.1016/j.jhazmat.2013.06.038.
5. Dahm, K., & Chapman, M. (2014). Produced water treatment primer: case studies of treatment applications. [US Department of the Interior], Bureau of Reclamation, Technical Service Center.
6. Demircioğlu, M., Kabay, N. A. L. A. N., Ersöz, E., Kurucaovali, I., Şafak, Ç., & Gizli, N. İ. L. A. Y. (2001). Cost comparison and efficiency modeling in the electrodialysis of brine. Desalination, 136(1-3), 317-323, https://doi.org/10.1016/S0011-9164(01)00194-1.
7. El Midaoui, A., Elhannouni, F., Taky, M., Chay, L., Sahli, M. A. M., Echihabi, L., & Hafsi, M. (2002). Optimization of nitrate removal operation from ground water by electrodialysis. Separation and purification technology, 29(3), 235-244, https://doi.org/10.1016/S1383-5866(02)00092-8.
8. Campione, A., Gurreri, L., Ciofalo, M., Micale, G., Tamburini, A., & Cipollina, A. (2018). Electrodialysis for water desalination: A critical assessment of recent developments on

process fundamentals, models and applications. Desalination, 434, 121-160, https://doi.org/10.1016/j.desal.2017.12.044.

9. Van der Bruggen, B., Koninckx, A., & Vandecasteele, C. (2004). Separation of monovalent and divalent ions from aqueous solution by electrodialysis and nanofiltration. Water research, 38(5), 1347-1353, https://doi.org/10.1016/j.watres.2003.11.008
10. Walker, W. S., Kim, Y., & Lawler, D. F. (2014). Treatment of model inland brackish groundwater reverse osmosis concentrate with electrodialysis—Part I: sensitivity to superficial velocity. Desalination, 344, 152-162, https://doi.org/10.1016/j.desal.2014.03.035.
11. Walker, W. S., Kim, Y., & Lawler, D. F. (2014). Treatment of model inland brackish groundwater reverse osmosis concentrate with electrodialysis—Part II: sensitivity to voltage application and membranes. Desalination, 345, 128-135, http://dx.doi.org/10.1016/j.desal.2014.04.026.
12. Walker, W. S., Kim, Y., & Lawler, D. F. (2014). Treatment of model inland brackish groundwater reverse osmosis concentrate with electrodialysis—Part III: Sensitivity to composition and hydraulic recovery. Desalination, 347, 158-164, https://doi.org/10.1016/j.desal.2014.05.034.
13. Percival, S. J., Small, L. J., Spoerke, E. D., & Rempe, S. B. (2018). Polyelectrolyte layer-by-layer deposition on nanoporous supports for ion selective membranes. RSC advances, 8(57), 32992-32999, https://doi.org/10.1039/C8RA05580G.
14. Percival, S.J., Russo, S., Priest, C., Hill, R.C., Ohlhausen, J.A., Small, L.J., Rempe, S.B., and Spoerke. E.D. Bio-Inspired Incorporation of Phenylalanine Enhances Ionic Selectivity in Layer-by-Layer Deposited Polyelectrolyte Films. Journal of Physical Chemistry C, Submitted (2020).
15. Xu, T. (2005). Ion exchange membranes: state of their development and perspective. Journal of membrane science, 263(1-2), 1-29, https://doi.org/10.1016/j.memsci.2005.05.002.

16. Kemperman, A. J. (2000). Handbook bipolar membrane technology. Twente University Press (TUP).
17. Available at: http://www.astom-corp.jp/en/index.html, (accessed on 4 January 2020).
18. Available at: http://www.ameridia.com/html/mbt.html, (accessed on 10 January 2020).
19. Available at: http://www.pca-gmbh.com, (accessed on 23 January 2020).
20. Available at: http://www.ionics.com, (accessed on 6 February 2020).
21. Available at: http://www.fujifilmmembranes.com, (accessed on 6 February 2020).
22. Available at: https://www.sterlitech.com, (accessed on 8 February 2020).
23. Goh, P. S., Ismail, A. F., & Matsuura, T. (2018). Perspective and roadmap of energy-efficient desalination integrated with nanomaterials. Separation & Purification Reviews, 47(2), 124-141, https://doi.org/10.1080/15422119.2017.1335214.
24. Firdaous, L., Malériat, J. P., Schlumpf, J. P., & Quéméneur, F. (2007). Transfer of monovalent and divalent cations in salt solutions by electrodialysis. Separation Science and Technology, 42(5), 931-948, https://doi.org/10.1080/01496390701206413.
25. Strathmann, H. (2010). Electrodialysis, a mature technology with a multitude of new applications. Desalination, 264(3), 268-288, https://doi.org/10.1016/j.desal.2010.04.069.
26. Strathmann, H. (2004). Ion-exchange membrane separation processes, Membrane science and technology series, Elsevier, Boston.
27. He, Y., Hoi, H., Abraham, S., & Montemagno, C. D. (2018). Highly permeable bioinspired reverse osmosis membrane with amphiphilic peptide stabilized aquaporin as water filtering agent. Journal of Applied Polymer Science, 135(15), 46169, https://doi.org/10.1002/app.46169.
28. Kumar, M., Grzelakowski, M., Zilles, J., Clark, M., & Meier, W. (2007). Highly permeable polymeric membranes based on the incorporation of the functional water channel protein Aquaporin Z. Proceedings of the National Academy of Sciences, 104(52), 20719-20724, https://doi.org/10.1073/pnas.0708762104.

29. Agre, P., Bonhivers, M., & Borgnia, M. J. (1998). The aquaporins, blueprints for cellular plumbing systems. Journal of Biological Chemistry, 273(24), 14659-14662, https://doi.org/10.1074/jbc.273.24.14659.
30. P. Agre, Aquaporin water channels (Nobel Lecture), Angew. Chem. Int. Ed. 43 (2004) 4278–4290.
31. Borgnia, M. J., Kozono, D., Calamita, G., Maloney, P. C., & Agre, P. (1999). Functional reconstitution and characterization of AqpZ, the E. coli water channel protein. Journal of molecular biology, 291(5), 1169-1179, https://doi.org/10.1006/jmbi.1999.3032.
32. Sun, G., Chung, T. S., Jeyaseelan, K., & Armugam, A. (2013). A layer-by-layer self-assembly approach to developing an aquaporin-embedded mixed matrix membrane. Rsc Advances, 3(2), 473-481, https://doi.org/10.1039/C2RA21767H.
33. ASTOM Corporation, Product Catalogue, Ion exchange membranes, Electrodialyzers, Diffusion dialyzers, 2017, Available at: http://www.astom-corp.jp/en/catalog/pdf/Astom_Products_Catalogue.pdf, (accessed April 2020).
34. Nayar, K. G., Sundararaman, P., O'Connor, C. L., Schacherl, J. D., Heath, M. L., Gabriel, M. O., & Winter, A. G. (2017). Feasibility study of an electrodialysis system for in-home water desalination in urban India. Development Engineering, 2, 38-46, https://doi.org/10.1016/j.deveng.2016.12.001.
35. Sadrzadeh, M., & Mohammadi, T. (2008). Sea water desalination using electrodialysis. Desalination, 221(1-3), 440-447, https://doi.org/10.1016/j.desal.2007.01.103.
36. Sadrzadeh, M., & Mohammadi, T. (2009). Treatment of sea water using electrodialysis: Current efficiency evaluation. Desalination, 249(1), 279-285, https://doi.org/10.1016/j.desal.2008.10.029.
37. Luo, F., Wang, Y., Jiang, C., Wu, B., Feng, H., & Xu, T. (2017). A power free electrodialysis (PFED) for desalination. Desalination, 404, 138-146, https://doi.org/10.1016/j.desal.2016.11.011.

38. Krol, J. J., Wessling, M., & Strathmann, H. (1999). Concentration polarization with monopolar ion exchange membranes: current–voltage curves and water dissociation. Journal of Membrane Science, 162(1-2), 145-154, https://doi.org/10.1016/S0376-7388(99)00133-7.
39. Káňavová, N., Machuča, L., & Tvrzník, D. (2014). Determination of limiting current density for different electrodialysis modules. Chemical Papers, 68(3), 324-329, https://doi.org/10.2478/s11696-013-0456-z.
40. Lee, H. J., Strathmann, H., & Moon, S. H. (2006). Determination of the limiting current density in electrodialysis desalination as an empirical function of linear velocity. Desalination, 190(1-3), 43-50, https://doi.org/10.1016/j.desal.2005.08.004
41. Cappelle, M., Walker, W. S., & Davis, T. A. (2017). Improving desalination recovery using zero discharge desalination (ZDD): a process model for evaluating technical feasibility. Industrial & Engineering Chemistry Research, 56(37), 10448-10460, https://doi.org/10.1021/acs.iecr.7b02472.
42. Murray, P. (1995). Electrodialysis and Electrodialysis Reversal-Manual of Water Supply Practices, M38. American Water Works Association/Colorado.
43. Vanysek, P. (2012). CRC Handbook of Chemistry and Physics, 93rd Edition, 5–74.
44. Landolt-Börnstein: Numerical Values and Functions. 6th Edition, Volume II, Properties of Matter in their States of Aggregation. Part 7, Electrical Properties II (Electrochemical Systems). Springer Verlag, Berlin-Göttingen-Heidelberg 1960. 959 pages. Price: DM 478, -, Zeitschrift für Elektrochemie, reports of the Bunsen Society for Phys. Chemistry. 66 (1962) 74-74. https://doi.org/10.1002/BBPC.19620660118.
45. Kingsbury, R. S., Zhu, S., Flotron, S., & Coronell, O. (2018). Microstructure determines water and salt permeation in commercial ion-exchange membranes. ACS applied materials & interfaces, 10(46), 39745-39756. https://doi.org/10.1021/acsami.8b14494.

Chapter 3: Evaluation of electrodialysis desalination performance for five commercial ion exchange membrane sets with brackish water feed solutions

Abstract

Several studies have been performed to evaluate electrodialysis (ED) desalination performance of different commercial ion exchange membranes (IEMs), but most of these studies used their own sets of experimental parameters such as feed solution compositions and concentrations, superficial velocities of the process streams (diluate, concentrate, and electrode rinse), applied electrical voltages, and types of IEMs. Therefore, it is difficult to directly compare the ED desalination performance of different IEMs. The goal of this study was to evaluate the ED desalination performance differences between five commercial IEMs by determining (i) limiting current density, (ii) current density, (iii) current efficiency, (iv) diluate conductivity reduction, (v) specific energy consumption, (vi) ion separation rate (permselectivity), and (vii) relative transport between divalent and monovalent ions as a function of (a) compositions and concentrations of brackish ground water feed solutions, (b) superficial velocity of feed solution, and (c) applied stack voltage per cell-pair of membranes. A five cell-pairs laboratory-scale single stage batch-recycle electrodialysis experimental apparatus was assembled with an active cross-sectional area of 7.84 cm^2. In this study, five combinations of commercial IEMs were compared which include: (i) Neosepta AMX/CMX, (ii) PCA PCSA/PCSK, (iii) Fujifilm Type 1 AEM/CEM, (iv) SUEZ AR204SZRA/CR67HMR, (v) Ralex AMH-PES/CMH-PES. The PCA and Ralex membranes showed the greatest and the least ED performance, respectively, for current density, current efficiency, salinity reduction, and permselectivity; however, the rest of the membranes (Neosepta, Fujifilm, Suez) exhibited almost similar ED performances.

Keywords: Electrodialysis, desalination, ion-exchange membrane, brackish water.

3.1. INTRODUCTION

3.1.1. Background

Brackish groundwater (BW) is an important and abundant natural water resource [1,2], but its salinity exceeds acceptable limits for drinking water [1,2]. The principal salt ions in BW include sodium, calcium, magnesium, potassium, chloride, sulfate, bicarbonate, silica, fluoride, and nitrate [2,3,4] and their standard values for drinking water quality reported by the World Health Organization (WHO) [5] are listed in Table 3.1. Reduction of the salinity of BW resources is required prior to its use as a source for potable, irrigation, and industrial uses [6,7].

Reverse osmosis (RO) is the principal membrane desalination technology that has been used successfully for separating salt ions from BW [2,3]. However, the primary challenge of the RO process is the generation and disposal of concentrated brine [8]. As an alternative option, electrodialysis (ED) membrane desalination technology has been successfully utilized for desalinating BW to produce potable water [7,9,10,11,12,13]. ED desalination capacity is approximately 425,000 m^3/day for brackish water having salinity lower than 3,000 mg/L, and this accounts for 6% of the total brackish water desalination capacity, whereas RO has a capacity of 86% [12,13]. ED has recently received growing interest for brackish water desalination as it can achieve a higher recovery than RO, which mitigates disposal of concentrated brine [12,13]. Moreover, ED can tolerate silica, hardness, residual chlorine, and organic matter [6] in addition to controlling and modifying concentrations and compositions of salt ions in feed streams to meet a target water quality requirement through the regulation of the applied stack voltage, feed solution flow rate, IEM pairs, and by using several stages of ED [6].

Typically, an ED stack is built with a series of anion- and cation-exchange membranes in an alternating order, which allow some ions to pass through and block other ions depending on the

permselectivity of the ion exchange membranes (IEMs) and the composition of feed solutions containing multiple ions. Permselectivity of an IEM is the ratio of the mass flux of a specific counter ion to the total mass flux through the membrane and the transport of electric charges by the counter ions [14]. Permselectivity of IEMs is determined by the concentrations of counter ions and co-ions present in the internal structure of a membrane. The concentration of counter- and co-ions depends mainly on the ion-exchange capacity of the IEMs and the ion concentration in the outside solutions [11]. Permselectivity of an IEM for a specific ion can be controlled in different ways, including (i) transport of ions having the same charge can be regulated by their hydrated ion size; (ii) transport of certain ions can be regulated by adding a thin surface layer of the same charge on the IEM; and (iii) transport of ions can be regulated by functioning the interactions between the ion-exchange functional groups inside the membrane's structure and the mobile counter- and co-ions in solutions [15]. Physicochemical properties and morphology of IEMs also influence the permselectivity [16].

Conventional IEMs have different separation rates for the counter ions available in feed water solutions because the permselectivity of the IEMs is different for these counter ions. The separation rate of a specific counter ion is lower if the permselectivity of an IEM is lower for that counter ion. Therefore, the permselectivity of IEMs is important to know to find out the counter ions separation rate by the membranes. The permselectivity of IEMs can be identified by the relative transport number (RTN) of ions through the membranes. The RTN is also defined by the IEMs effectiveness at rejecting one ion while transporting another and is a function of the salt ions concentration in the depleting solution stream (diluate solution). For example, the RTNs have been reported between chloride and sulfate ions (*i.e.,* $\mathrm{RTN}_{\mathrm{SO_4}}^{\mathrm{Cl}} \approx 1.0$), and sodium and magnesium ions (*i.e.,* $\mathrm{RTN}_{\mathrm{Mg}}^{\mathrm{Na}} \approx 2.0\ to\ 5.0$), which represents that chloride and sulfate ions selectivity of a

membrane is similar, and sodium ion selectivity of a membrane is 2. to 5 times higher than magnesium ion [17].

Several existing studies evaluated the selective separation of monovalent ions (*e.g.,* Na^+, K^+, NH_4^+, Cl^-, and NO_3^-) versus multivalent ions (*e.g.,* Ca^{2+}, Mg^{2+}, SO_4^{2-}, PO_4^{3-}) from the multicomponent feed water solutions by using monovalent anion and cation permselective IEMs in ED [2,18,19,20]. Bruggen et. al. showed the preferential separation of monovalent cations using Neosepta CMS/ACS membranes and little cationic permselectivity using Selemion CMV/AMV membranes from a feed solution with mono- and di-valent ions [21]. Another study on selective removal of Na^+ over Ca^{2+} and Mg^{2+} from reclaimed water and groundwater was performed so that the ED treated reclaimed water and groundwater can be used in irrigation [22,23]. Some previous studies focused on the desalination of synthetic binary [19] and ternary salts in feed solutions with salinities between 1 and 10 g/L [19,20] while other studies desalinated real and synthetic brackish waters [24,25]. Kabay et. al. observed that potassium ions were removed more efficiently than sodium ions, and sulfate ion removal was the least efficient than other ions from a feed solution having binary salts [19].

General observations of the selected studies on ED desalination of multicomponent feed solutions are summarized here:

- Relative transport of ions depends on the physiochemical properties of IEMs [17].
- Ions transport rate depends on the applied voltage to the ED stack [26] as well as the compositions and concentrations of feed solutions [27].
- Selective separation of ions is governed by the physiochemical properties of IEMs [16], affinity of ions with IEMs, migration rate of ions through IEMs, and ion exchange capacity of IEMs [14].

In order to evaluate the permselectivity (or selective ion separation) performance of commercial and laboratory-scale IEMs, most studies mentioned in previous sections used their own independent sets of experimental parameters or conditions such as feed solution compositions and concentrations, superficial velocities of feed solution, applied electrical voltages, and IEMs combinations [2,3,7-15,18-21,24-27]. However, to our knowledge, there is no study that has systematically compared the ion transport of several commercially available membranes. Therefore, it is difficult to assess permselectivity as well as overall ED desalination performance of different commercially available and well-known IEMs and to recommend suitable IEMs for ED to achieve a desirable outcome (*i.e.,* high ion-selectivity, high salinity removal, high water recovery, low energy consumption, or low osmotic water flux).

3.1.2. Objectives

The goal of the study was to evaluate the permselectivity and overall desalination performances of five conventional IEM pairs using ED with a similar set of experimental parameters. The ED desalination performance of the IEMs was evaluated by determining (i) limiting current density, (ii) current density, (iii) current efficiency, (iv) conductivity (or salinity) reduction in diluate stream, (v) specific energy consumption, (vi) ion separation rate (permselectivity), and (vii) relative transport between divalent and monovalent ions as a function of (a) compositions and concentrations of brackish ground water feed solutions (diluate and concentrate streams), (b) superficial velocity of feed solution, and (c) applied stack voltage per cell-pair of membranes.

Table 3.1: Salt ions compositions and concentrations in brackish groundwaters

Parameters	Unit	KBH Desal Plant, Texas (BW)	BGNDRF Well 2, New Mexico (BW)	WHO drinking limit
TDS*	mg/L	2,787	5,258	1,000
EC*	mS/cm	4.72	6.21	-
pH	-	7.8	7.8	6.5-8.5
Na^+	mg/L	792	753	200
Ca^{2+}	mg/L	171	464	< 100
Mg^{2+}	mg/L	39	291	50
K^+	mg/L	16	29	12
Cl^-	mg/L	1319	565	250
SO_4^{2-}	mg/L	399	3154	500
NO_3^-	mg/L	-	51	50
F^-	mg/L	0.9	0.6	1.5
References		This study	This study	5

**TDS: total dissolved solids concentration, EC: electrical conductivity*

3.2. MATERIALS AND METHODS

3.2.1. Experimental plan, variables, system, and chemicals

A detailed description of the experimental plan, experimental design, experimental system and equipment, and experimental chemicals was reported in previous research performed by Hyder et al. [28] (see also in Chapter 2). For laboratory-scale batch-recycle electrodialysis experimental design, several experimental variables were considered, and their discrete values are shown in Table 3.2. In this study, real brackish water samples were used as the feed water solutions with initial concentrations of 2,787 mg/L and 5,258 mg/L TDS. The electrode rinse solution was prepared with a fixed concentration of 0.1 mol/L (14.2 g/L) sodium sulfate (Na_2SO_4). Laboratory-grade sodium sulfate (Na_2SO_4, ACS reagent grade) salt was purchased from Fisher Scientific

(USA) to prepare the electrode rinse solution. All reagent water was purified and deionized to a resistivity of 18.2 MΩ cm. The membranes used in this study were commercially available and well-known general desalination IEMs. The ED desalination performance of five membrane-pairs was compared through various experimental conditions (*e.g.*, superficial velocity of the feed solution, voltage application to ED stack, and concentrations and compositions of feed solutions) in terms of limiting current density, current density, current efficiency, conductivity reduction in diluate stream, specific energy consumption, individual monovalent and divalent ion separation rate, and relative transport rate of divalent ions over monovalent ions.

Table 3.2: Experimental variables, value ranges, and combinations

Variables	**Discrete Values/Combinations**
Brackish water feed solutions (concentration & electrical conductivity)	i. KBH: TDS* of 2,787 mg/L (corresponding conductivity of 4.72 mS/cm) ii. BGNDRF Well 2: TDS of 5,258 mg/L (corresponding conductivity of 6.21 mS/cm)
Superficial velocity of diluate stream	4 cm/s (corresponding flow: 30 mL/minute)
Stack voltage	0.4 & 0.8 Volts per cell-pair of membrane
Combination of membranes during stack assembly	i. Neosepta AMX & CMX ii. PCA PCSA & PCSK iii. Fujifilm Type 1 AEM & CEM iv. SUEZ AR204SZRA & CR67HMR v. Ralex AMH-PES & CMH-PES

*TDS: Total Dissolved Solids

3.2.2. Experimental feed water solutions

The real (natural) brackish water samples used in this study were collected from the Kay Bailey Hutchison (KBH) desalination plant located in El Paso, Texas, USA, and the Brackish Groundwater National Desalination Research Facility (BGNDRF) Well 2 located in Alamogordo, New Mexico, USA. The initial concentration of total dissolved solids (TDS) was measured as 2,787 mg/L in KBH brackish water and was found as 5,258 mg/L in BGNDRF Well 2 brackish water with the corresponding conductivity of 4.72 mS/cm and 6.21 mS/cm, respectively. Similar values were also reported by Cappelle et al. [29]. The major ion concentrations of the feed water solutions are summarized in Table 3.1.

3.2.3. Electrodialysis testing

A detailed description of the ED experimental testing, including experimental design, experimental system and equipment, ED stack and IEMs used, experimental procedure, and calculation methods of important ED parameters, was reported in previous research performed by Hyder et al. [28] (see also in chapter 2). This chapter focuses on the comparison of ED desalination performance differences between five well-known commercial IEMs. The standard physiochemical properties of IEMs used in this study are summarized in a previous study [28] (also in the second chapter). All of the membranes used in this study were soaked in 0.01 M NaCl solution for 24 hours prior to use and then trimmed to 6.4 cm x 4.4 cm size and punched with holes at precise locations.

The performance of the membranes for current density, current efficiency, salinity reduction, and energy consumption was tested using a laboratory-scale single stage electrodialysis stack (model: 08002-001, PCCell/PCA, GmbH, Germany) with an active cross-sectional area of membrane subjected to the applied electric field of 7.84 cm^2 (2.80 cm x 2.80 cm). The ED stack was assembled with five cell-pairs according to the schematic diagram of the ED process as shown

in an earlier study by Hyder et al. [28]. Polyester mesh spacer-gaskets of thickness 0.45 mm physically separated the AEMs and CEMs.

The diluate solution was circulated at a flow rate of 30 mL/minute (corresponding to a superficial velocity of 4 cm/s), and the pressure of the diluate cell for the relevant flow rate was recorded. The solution flow rate through the concentrate cells and electrode rinse compartments were adjusted to maintain the same pressure as diluate cells. A laboratory-scale Master Flex peristaltic cartridge pump (Cole-Parmer, USA, Model: 7519-00) was used to circulate the solutions through each of the process streams.

The electrical conductivity, pH, and temperature of the process stream reservoirs were determined using a pH/conductivity meter (Thermo Scientific, USA, model: Orion Star A325). The mass of the diluate reservoir was measured (Meller Toledo, USA, model: XS2002S) to quantify the net mass of water and salt transportation across the membranes. Analog pressure gauges (model: 18C774, Grainger, USA) were used at the inlet of the diluate, concentrate, and electrode rinse streams to observe the head loss through each stream and the average transmembrane pressures. A programmable DC Power Supply (B&K Precision, USA, Model: 9123A) was used for monitoring and controlling voltage and current through the electrodialysis stack.

Experimental data were recorded automatically at five-second intervals in spreadsheets in the computer by the LabVIEW 2017 supervisory control and data acquisition (SCADA) system. Finally, the acquired data from LabVIEW were analyzed to evaluate the ED desalination performance of the IEMs.

3.2.4. Calculation methods

The calculation methods of important ED parameters such as voltage loss at electrodes, specific energy consumption, limiting current density and polarization parameter, current

efficiency, and diluate conductivity reduction was reported in detail in the previous research performed by Walker et al. [26] and Hyder et al., [28].

3.2.4.1 Relative transport number (RTN) of salt ions

The relative transport number for an ion (X) relative to another ion (Y) can be calculated following the equation below [17]:

$$\mathrm{RTN}_{\mathrm{Y}}^{\mathrm{X}} = \frac{R_X}{R_Y} \tag{3.1}$$

where, R_X and R_Y indicate the percentage concentration reduction of X- and Y-ion, respectively in the diluate stream.

For example, the RTN for calcium ion relative to sodium ion can be calculated as below:

$$\mathrm{RTN}_{\mathrm{Na}}^{\mathrm{Ca}} = \frac{R_{Ca}}{R_{Na}} \tag{3.2}$$

where, R_{Ca} and R_{Na} indicate percentage concentration reduction of calcium and sodium ions, respectively, in the diluate stream.

The benefit of using this equation is that the RTN values can be calculated from analytical data, and the ratio of ion concentrations in the concentrate stream can be predicted from experimentally determined RTN values and experimentally measured concentrations in the diluate. Since, the RTN depends on the permselectivity of the IEMs, the composition of the concentrate solution can be predicted based on the membrane selected and the composition of the diluate solution.

3.3. RESULTS

3.3.1. Evaluation of limiting current density, areal resistance, and polarization parameter

As shown in Figure 3.1, the limiting current density (LCD) and the areal resistance per cell-pair of five cell-pairs of commercial membranes were determined with a superficial velocity

of 4 cm/s for feed solutions of KBH brackish water (4.72 mS/cm and 2,787 mg/L TDS) and BGNDRF Well 2 brackish water (6.21 mS/cm and 5,258 mg/L TDS). The LCD values were observed to be higher for the BGNDRF Well 2 brackish water feed solution than the KBH brackish water for all the given five membrane pairs (Figure 3.1a), due to the greater initial concentration of BGNDRF Well 2 brackish water, which is consistent with other studies [29-31]. The LCD ranged from 106 to 208 A/m^2, and the corresponding limiting polarization parameters ranged from 1.15 to 1.28 A/m^2 per meq/L (feed). The least LCD value of 106 A/m^2 was observed at a voltage application of 0.9 V/cell-pair for Ralex membranes with KBH brackish water, and the greatest LCD value of 208 A/m^2 was observed at 1.2 V/cell-pair for Neosepta membranes with BGNDRF Well 2 brackish water.

The stack voltage application required to achieve LCD ranged from 0.9 to 1.4 Volts per cell-pair, and the corresponding areal resistance per cell-pair at LCD ranged from 59 to 97 $\Omega\ cm^2$ (Figure 3.1b). Subsequent experiments were performed with the stack voltage application (*i.e.*, 0.4 and 0.8 V/cell-pair) less than the least LCD stack voltage (*i.e.*, 0.9 V/cell-pair).

In Figure 3.1a, the LCD for both given feed solutions (KBH and BGNDRF brackish water) decreased in the following order (*i.e.*, from greatest to least LCD): Neosepta AMX/CMX (red), Suez AR204/CR67 (orange), PCA PCSK/PCSA (green), Fujifilm Type 1 AEM/CEM (purple), and Ralex CMH-PES/AMH-PES (black). In Figure 3.1b, the areal resistance per cell-pair at LCD for both given feed solutions (KBH and BGNDRF brackish water) decreased in the following order (*i.e.*, from greatest to least areal resistance): Ralex CMH-PES/AMH-PES (black), Fujifilm Type 1 AEM/CEM (purple), PCA PCSK/PCSA (green), Suez AR204/CR67 (orange), and Neosepta AMX/CMX (red). Table 3.3 summarizes the trend in LCD and areal resistance for the five membrane sets.

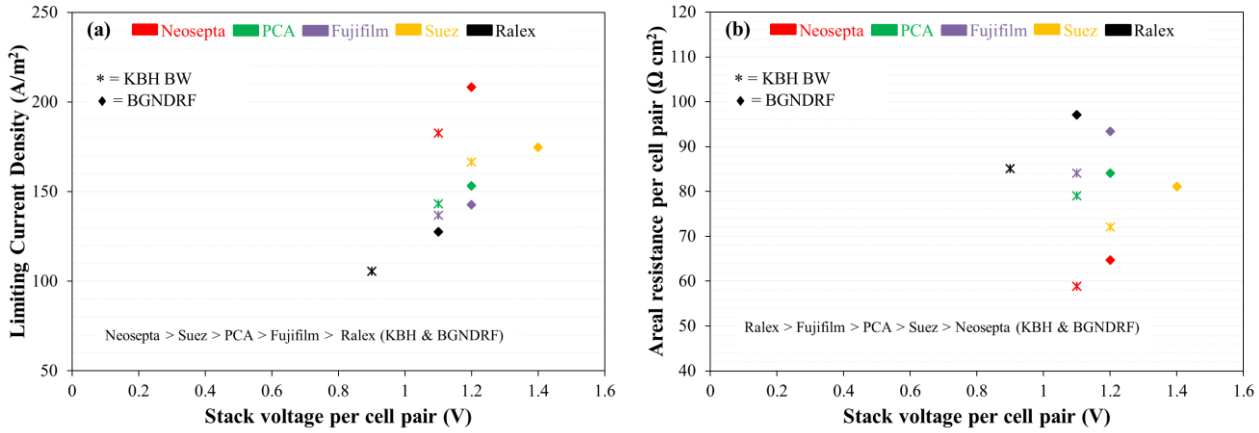

Experimental conditions: 5 cell-pair ED stack; 4 cm/s superficial velocity; constant stack voltage application; 1 L batch feed solution; 0.1 M (14.2 g/L) Na2SO4 electrode rinse solution; and <3 kPa transmembrane pressure

Figure 3.1: Limiting current density (a) and areal resistance per cell-pair of membranes at LCD (b) against ED stack voltage per cell-pair of membranes.

3.3.2. Evaluation of current density, and current efficiency

The current density and current efficiency of the five membrane sets were compared against the bulk conductivity reduction in diluate stream (or diluate tank or diluate cell-pair) for both applied stack voltages (*i.e.*, 0.4 and 0.8 Volts per cell-pair of membrane), both feed solutions (*i.e.*, KBH brackish water and BGNDRF Well 2 brackish water), and a superficial velocity of feed solution (*i.e.*, 4 cm/s) (Figure 3.2). As expected, current density decreased with greater conductivity reduction, increased with greater voltage application, and increased with greater feed salinity (Figure 3.2a and b); similar results are also reported in other studies [26, 28]. Similarly, the current efficiency (ranging from 63% to 95%) decreased with greater conductivity reduction and increased with greater voltage application; however, the current efficiency decreased with greater feed salinity (Figure 3.2c and d), which is consistent with other studies [26,28]. Trends in current density and current efficiency are listed in Table 3.

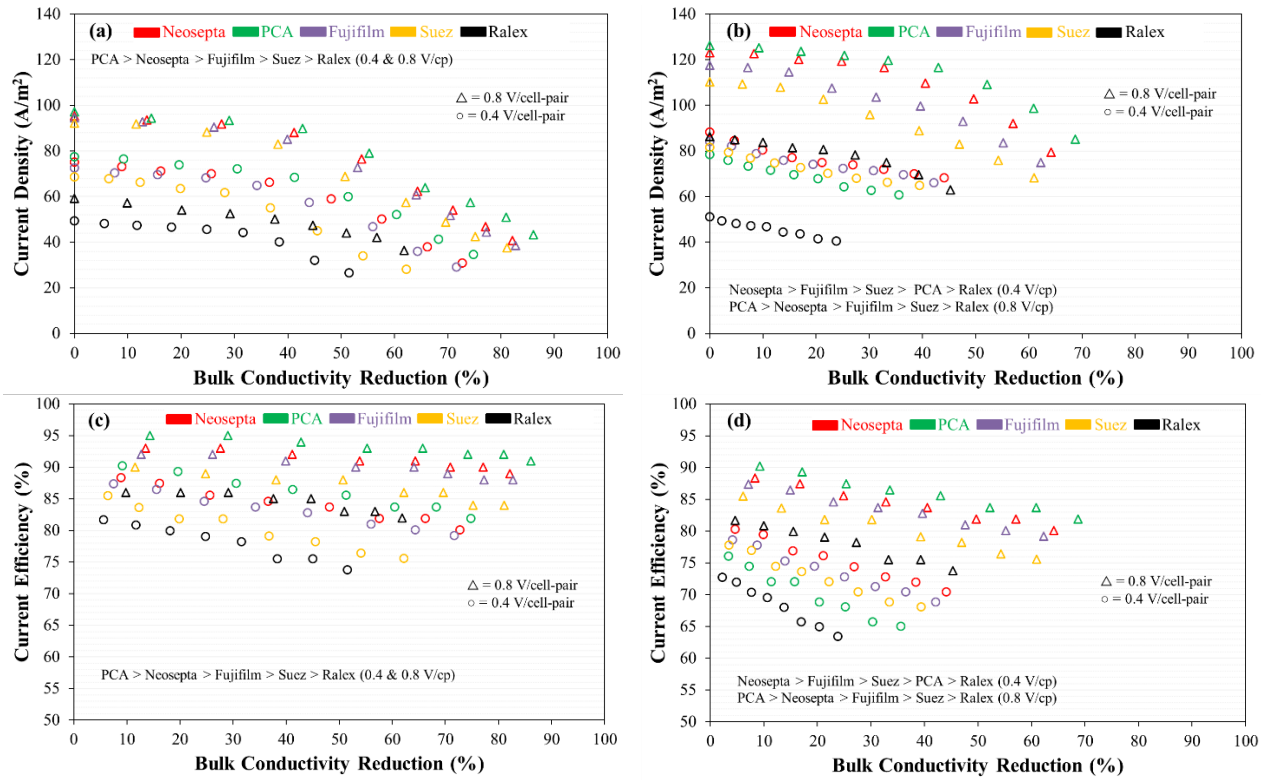

Experimental conditions: 5 cell-pair ED stack; 4.72 mS/cm initial conductivity of KBH brackish water and 6.21 mS/cm initial conductivity of BGNDRF Well 2 brackish water feed (diluate and concentrate) solutions (500 mL each); 4 cm/s superficial velocity of feed solution; 0.4 and 0.8 V/cell-pair constant applied stack voltage; 0.1 M (14.2 g/L) Na_2SO_4 electrode rinse solution; and 0.5 psi transmembrane pressure.

Figure 3.2: Effect of stack voltage and feed solution composition on current density (a,b) and current efficiency (c,d) for KBH (a,c) and BGNDRF (b,d) feed solutions.

3.3.3. Evaluation of conductivity reduction and specific energy consumption

Conductivity reduction was nearly proportional with time up to conductivity reductions of approximately 50%, and diminishing returns were observed for greater conductivity removal (Figure 3.3c and d). The rate of conductivity reduction increased with greater voltage application, as expected from Nernst-Planck theory [32], which is consistent with other studies [26,32,33,34].

The specific energy consumption (SEC) increased proportionally with conductivity reduction and voltage (Figure 3.3e and 3.3f), with an average of 0.274 kWh/m^3 per mS/cm reduction per V/cell-pair applied for the KBH feed, and an average of 0.438 kWh/m^3 per mS/cm reduction per V/cell-pair applied for the BGNDRF feed, which is in agreement with other studies

[26,32,34]. With respect to the treatment of these natural brackish waters with conductivity 4.72 and 6.21 mS/cm, the difference in the SEC due to the membranes was less than 10%. The specific energy reported in this study includes only the electrical energy applied to the stack, and it did not include the hydraulic energy invested in pumping the solution through the electrodialysis stack (a negligible portion).

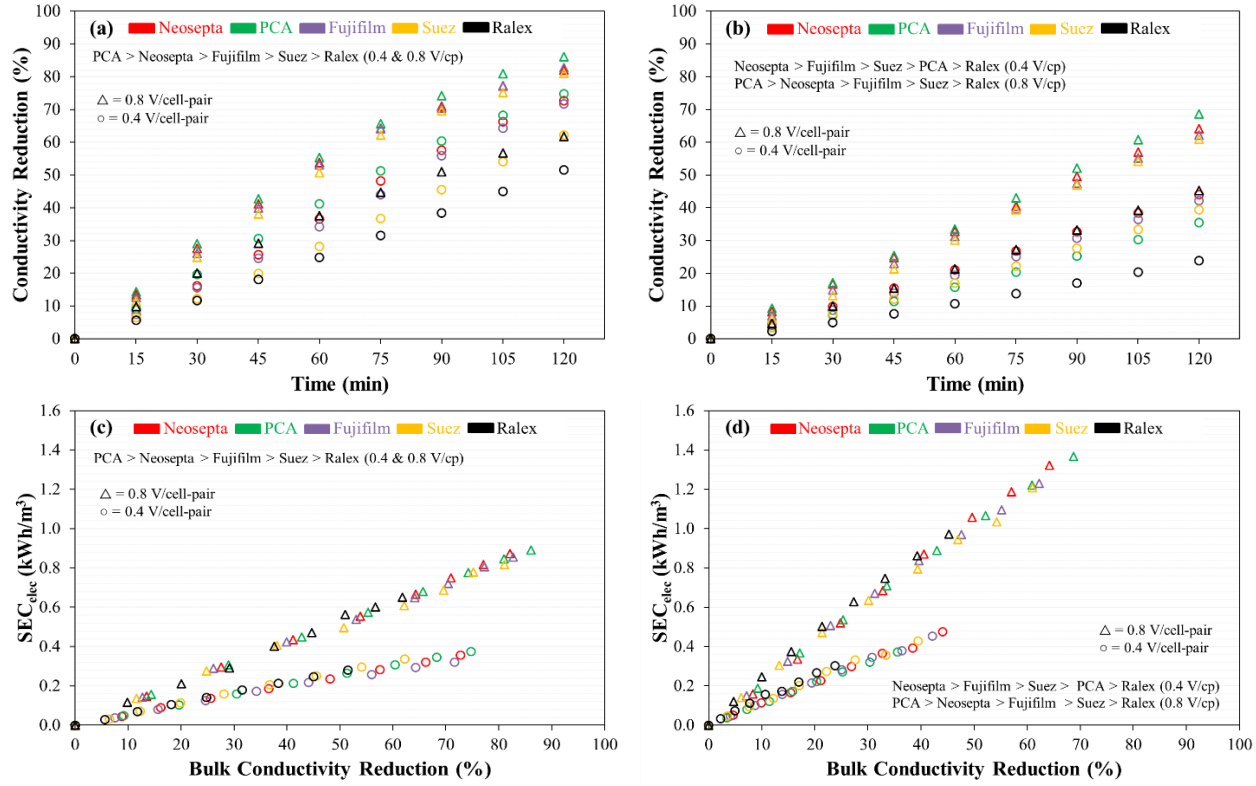

<u>Experimental conditions</u>: 5 cell-pairs ED stack; 4.72 mS/cm initial conductivity of KBH brackish water and 6.21 mS/cm initial conductivity of BGNDRF Well 2 brackish water feed (diluate and concentrate) solutions (500 mL each); 4 cm/s superficial velocity of feed solution; 0.4 and 0.8 V/cell-pair constant applied stack voltage; 0.1 M (14.2 g/L) Na_2SO_4 electrode rinse solution; and 0.5 psi transmembrane pressure.

Figure 3.3: Effect of stack voltage and feed solution composition on conductivity reduction (c,d), and specific energy consumption (SEC) (e,f) for two different brackish water feed solutions: KBH (a,c,e) and BGNDRF (b,d,f).

Table 3.3: Performance trends for five commercial membrane sets

Parameters	**Feed solution**	**Stack voltage (V/cell-pair)**	**Membranes* (Greatest to least order)**
LCD	KBH, BGNDRF	0.9-1.4	Neosepta > Suez > PCA > Fujifilm > Ralex
Areal resistance at LCD	KBH, BGNDRF	0.9-1.4	Ralex > Fujifilm > PCA > Suez > Neosepta
Current density	KBH	0.4, 0.8	PCA > Neosepta > Fujifilm > Suez > Ralex
Current density	BGNDRF	0.4	Neosepta > Fujifilm > Suez > PCA > Ralex
Current density	BGNDRF	0.8	PCA > Neosepta > Fujifilm > Suez > Ralex
Current efficiency	KBH	0.4, 0.8	PCA > Neosepta > Fujifilm > Suez > Ralex
Current efficiency	BGNDRF	0.4	Neosepta > Fujifilm > Suez > PCA > Ralex
Current efficiency	BGNDRF	0.8	PCA > Neosepta > Fujifilm > Suez > Ralex
Conductivity Reduction	KBH	0.4, 0.8	PCA > Neosepta > Fujifilm > Suez > Ralex
Conductivity Reduction	BGNDRF	0.4	Neosepta > Fujifilm > Suez > PCA > Ralex
Conductivity Reduction	BGNDRF	0.8	PCA > Neosepta > Fujifilm > Suez > Ralex
SEC	KBH	0.4, 0.8	PCA > Neosepta > Fujifilm > Suez > Ralex
SEC	BGNDRF	0.4	Neosepta > Fujifilm > Suez > PCA > Ralex
SEC	BGNDRF	0.8	PCA > Neosepta > Fujifilm > Suez > Ralex
Na^+ Removal	KBH, BGNDRF	0.4, 0.8	PCA > Fujifilm > Neosepta > Suez > Ralex
Ca^{2+} Removal	KBH, BGNDRF	0.4, 0.8	PCA > Neosepta > Fujifilm > Suez > Ralex
Cl^- Removal	KBH, BGNDRF	0.4, 0.8	Neosepta > Fujifilm > Suez > PCA > Ralex
SO_4^{2-} Removal	KBH, BGNDRF	0.4, 0.8	Fujifilm > Suez > PCA > Neosepta > Ralex

Note: *****Membranes: Neosepta AMX/CMX (red), PCA PCSK/PCSA (green), Fujifilm Type 1 AEM/CEM (purple), Suez AR204/CR67 (orange), and Ralex CMH-PES/AMH-PES (black).

3.3.4. Evaluation of concentration reduction of predominant monovalent and divalent ions

Typically, in brackish ground water, the predominant monovalent salt ions are comprised of sodium (Na^+) and chloride (Cl^-), while the divalent salt ions are calcium (Ca^{2+}) and sulfate (SO_4^{2-}), as shown in Table 3.1. That is why the concentration reduction performance of predominant salt ions was measured qualitatively against the diluate bulk conductivity reduction

as a function of voltages, feed salinities, and feed velocity for five combinations of membranes (Figure 3.4).

The concentrations of individual salt ions (Na^+, Cl^-, Ca^{2+}, and SO_4^{2-}) were reduced at approximately the same rate as the diluate bulk conductivity reduction ratio for all the given membrane pairs, applied stack voltages, and feed solutions (Figure 3.4a-h). It is considered that the solution conductivity is approximately proportional to the bulk concentration of salt ions [32], which is in agreement with the finding of this study. The higher reduction of individual salt ions concentration was found at the higher stack voltage of 0.8 V/cell-pair as compared to 0.4 V/cell-pair for both feed solutions and all the given membrane pairs. This is because higher voltage application to the ED stack results in a greater driving force for separating salt ions and consequently increases the removal rate of ions [26,28,32,33]. However, the lower reduction of individual salt ions was identified, relative to the bulk conductivity reduction, when their initial concentrations were higher in feed solutions. The higher concentration of individual salt ions in feed solutions results in slower electromigration when there is no rise in the applied stack voltage and superficial velocity of the feed solution [26,28,32].

A higher reduction of salt ions concentration (or separation rate of individual salt ions) was generally observed for the ion exchange membranes with lower areal resistance, higher ion exchange capacity, and higher ion selectivity (see Table 2.2). The performance of individual salt ion concentration reduction order (*i.e.*, from greatest to least) with respect to feed salinity and stack voltage application for all the given five membrane pairs is summarized in Table 3.3.

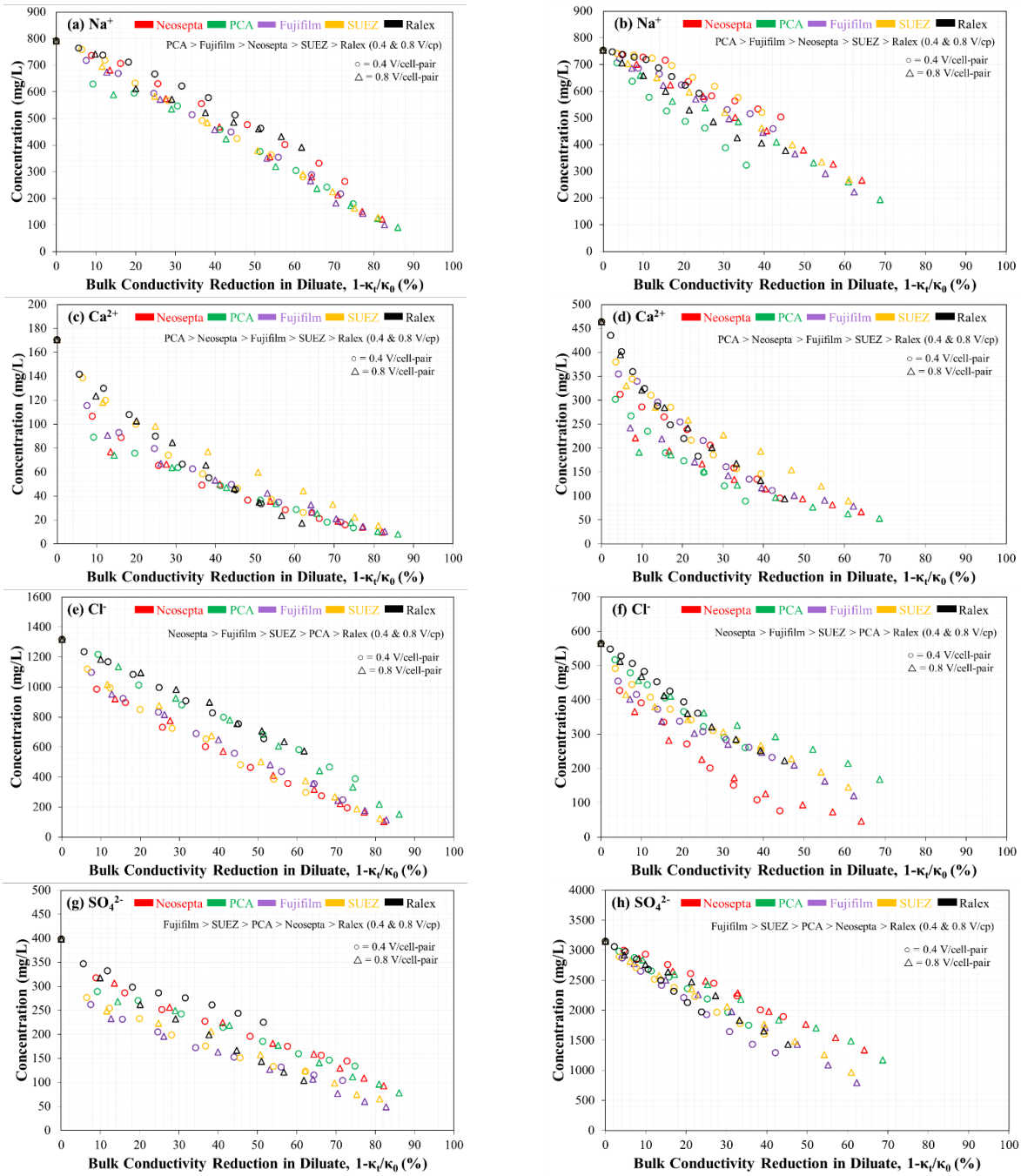

<u>Experimental conditions</u>: 5 Cell-pairs ED stack; 4.72 mS/cm initial conductivity of KBH brackish water and 6.21 mS/cm initial conductivity of BGNDRF Well 2 brackish water feed (diluate and concentrate) solutions (500 mL each); 4 cm^3/s superficial velocity of feed solution; 0.4 and 0.8 V/cell-pair constant applied stack voltage; 0.1 M (14.2 g/L) Na_2SO_4 electrode rinse solution; and 0.5 psi transmembrane pressure.

Figure 3.4: Effect of stack voltage and feed solution composition on removal performance of predominant monovalent and divalent ions from KBH (a,c,e,g) and BGNDRF (b,d,f,h) brackish water feed solutions.

3.3.5. Evaluation of relative transport ratio between divalent and monovalent ions

Based on a comparison of the relative removal of ions shown in Figure 3.4, the relative transport of divalent ions (Ca^{2+} and SO_4^{2-}) against monovalent ions (Na^+ and Cl^-) was analyzed (Figure 3.5). First, the relative transport of divalent ions against monovalent ions (Ca^{2+} vs Na^+ and SO_4^{2-} vs Cl^-) was generally similar for pair-wise comparisons of the two voltage applications.

Second, the relative transport of calcium to sodium (*i.e.*, the slope of Ca^{2+} removal vs. the slope of Na^+ removal) was observed to be greater than one for all tests and ranged from a factor of approximately 2 to 7 at low overall conductivity reduction to a factor less than 1.5 for conductivity reduction greater than 60% (Figure 3.5 a and b).

Third, for the KBH feed solution, the relative transport of SO_4^{2-}/Cl^- ranged from 0.8 to 2.1, with Neosepta at the lowest end of the range and Ralex at 0.8 V/cell-pair at the highest end of the range (Figure 3.5 c). For the BGNDRF feed solution, the relative transport of SO_4^{2-}/Cl^- ranged from 0.2 to 1.1, with Neosepta at the lowest end of the range and Ralex at 0.4 V/cell-pair at the highest end of the range (Figure 3.5 d).

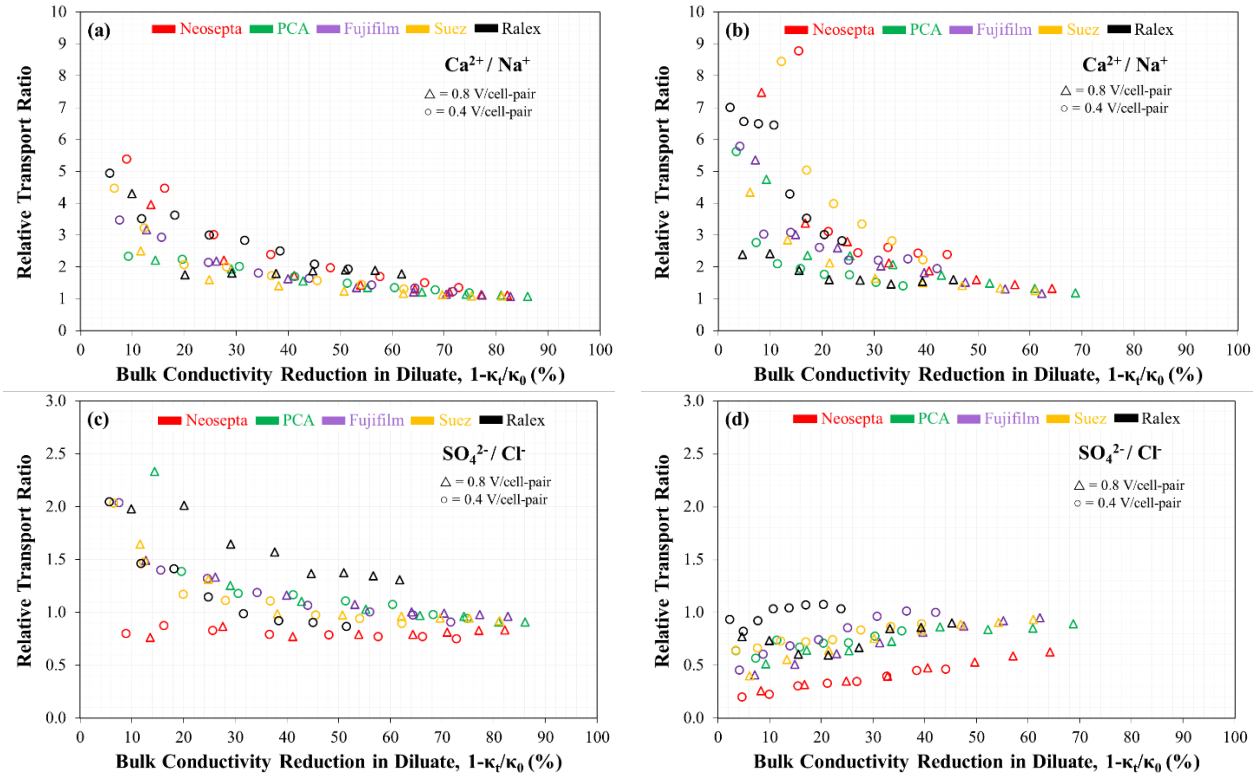

Experimental conditions: 5 Cell-pairs ED stack; 4.72 mS/cm initial conductivity of KBH brackish water and 6.21 mS/cm initial conductivity of BGNDRF Well 2 brackish water feed (diluate and concentrate) solutions (500 mL each); 4 cm/s superficial velocity of feed solution; 0.4 and 0.8 V/cell-pair constant applied stack voltage; 0.1 M (14.2 g/L) Na_2SO_4 electrode rinse solution; and 0.5 psi transmembrane pressure.

Figure 3.5: Effect of stack voltage and feed solution composition on relative transport of divalent ions against monovalent ions: Ca^{2+} vs Na^+ (a,b) and SO_4^{2-} vs Cl^- (c,d) from KBH (a,c) and BGNDRF (b,d) brackish water feed solutions.

3.4. CONCLUSIONS AND RECOMMENDATIONS

The electrodialysis desalination performances of five commercial ion exchange membrane sets were evaluated for brackish ground water feed solutions using stack voltage application of 0.4 and 0.8 V/cell-pair) and superficial feed velocity of 4 cm/s. The significant conclusions of the study are summarized below:

1. The limiting current density (LCD) increased with greater feed salinity for all the membranes used in the study. LCD ranged from 106 to 208 A/m^2 for Ralex and Neosepta membranes, respectively. The corresponding areal resistance per cell pair at LCD ranged

from 59 to 97 Ω $cm^{2,}$ and the corresponding limiting polarization parameter ranged from 1.15 to 1.28 A/m^2 per meq/L feed. The voltage application required to achieve these LCDs ranged from 0.9 to 1.4 Volts per cell pair of membranes.

2. Current density ranged from 25 to 95 A/$m^{2,}$ and current efficiency ranged from 63 to 95%, with the least values for Ralex and the greatest values for PCA membranes. Current density decreased with greater diluate conductivity reduction, however, it increased with greater voltage application and greater feed salinity. Similarly, current efficiency decreased with greater conductivity reduction and increased with greater voltage application; however, the current efficiency decreased with greater feed salinity.
3. The lower conductivity reduction in the diluate was observed with increasing feed salinity, but the conductivity reduction increased significantly with increasing stack voltage for a given membrane. For a given feed salinity and voltage application, the Ralex and PCA showed the least and the greatest diluate conductivity reduction, respectively.
4. The specific energy consumption (SEC) for a given membrane increased proportionally with conductivity reduction, increased significantly with increasing stack voltage, and increased slightly with increasing feed salinity. The average SEC of 0.274 and 0.438 kWh/m^3 per mS/cm conductivity reduction per V/cell-pair stack voltage application was determined by analyzing the slopes of each of the membranes for the KBH and the BGNDRF feed, respectively.
5. The concentrations of predominant monovalent and divalent salt ions (Na^+, Cl^-, Ca^{2+}, and SO_4^{2-}) were reduced linearly with the diluate bulk conductivity reduction ratio for all the given membrane pairs, applied stack voltages, and feed solutions.
6. The relative transport ratio between divalent and monovalent ions was generally similar for pair-wise comparisons of the two voltage applications. The relative transport of calcium vs. sodium was observed to be greater than one for all tests; however, the relative transport of sulfate vs. chloride ranged from 0.8 to 2.1 for the KBH feed and from 0.2 to 1.1 for the BGNDRF feed.

The key membrane performance parameters are summarized in Table 3.3. For most desalination applications, it is desirable to use membranes with a higher range of LCD, LPP, current density, current efficiency, salinity reduction, permselectivity, and water recovery; and a lower range of areal resistance and energy consumption. For brackish water applications, the electrical resistance of the diluate solution greatly outweighs the membrane resistance.

Future work should investigate the performances of the novel and commercial membranes with a wider range of ED operational parameters such as voltage application, feed velocity, and feed salinity, in addition to the scaling, fouling, and durability of the membranes.

Table 3.4: Key performance parameters comparison for membranes.

Membrane	**Ralex CMH-PES/AMH-PES**	**PCA PCSK/PCSA**	**Neosepta AMX/CMX**	**Fujifilm Type 1 AEM/CEM**	**SUEZ AR204/CR67**
LCD	min	> med	**max**	< med	> med
Current Density*	min	**max**	> med	> med	< med
Current Efficiency*	min	**max**	> med	> med	< med
Conductivity Reduction*	min	**max**	> med	> med	< med
SEC*	**min**	max	> med	> med	< med

*For 0.8 V/cell-pair, and KBH and BGNDRF feeds; “min” minimum of the five membranes; “< med” less than median; “> med” greater than median; “max” maximum; **boldface** indicates generally preferred attribute.

3.5. REFERENCES

1. U.S. Geological Survey, The World's Water. 2016. Available from: https://water.usgs.gov/edu/earthwherewater.html, Accessed on 2017 December 11.
2. Xu, P., Capito, M., & Cath, T. Y. (2013). Selective removal of arsenic and monovalent ions from brackish water reverse osmosis concentrate. Journal of hazardous materials, 260, 885-891.
3. Galama, A. H., Saakes, M., Bruning, H., Rijnaarts, H. H. M., & Post, J. W. (2014). Seawater predesalination with electrodialysis. *Desalination*, *342*, 61-69.
4. Cappelle, M., Walker, W. S., & Davis, T. A. (2017). Improving desalination recovery using zero discharge desalination (ZDD): A process model for evaluating technical feasibility. Industrial & Engineering Chemistry Research, 56(37), 10448-10460.
5. WHO/UNICEF, 2014. Progress on Drinking-water and Sanitation 2014 Update. World Health Organization, 1, 1.
6. Campione, A., Gurreri, L., Ciofalo, M., Micale, G., Tamburini, A., & Cipollina, A. (2018). Electrodialysis for water desalination: A critical assessment of recent developments on process fundamentals, models and applications. *Desalination*, *434*, 121-160.
7. Ortiz, J. M., Expósito, E., Gallud, F., García-García, V., Montiel, V., & Aldaz, A. (2008). Desalination of underground brackish waters using an electrodialysis system powered directly by photovoltaic energy. *Solar Energy Materials and Solar Cells*, *92*(12), 1677-1688.
8. Bonné, P. A. C., Hofman, J. A. M. H., and van der Hoek, J. P. (2000). "Scaling control of RO membranes and direct treatment of surface water." *Desalination*, 132(1-3), 109-119.
9. Banasiak, L. J., Kruttschnitt, T. W., & Schäfer, A. I. (2007). Desalination using electrodialysis as a function of voltage and salt concentration. *Desalination*, *205*(1-3), 38-46.

10. Chehayeb, K. M., Farhat, D. M., & Nayar, K. G. (2017). Optimal design and operation of electrodialysis for brackish-water desalination and for high-salinity brine concentration. *Desalination*, *420*, 167-182.
11. Y. Tanaka, R. Ehara, S. Itoi, T. Goto, Ion-exchange membrane electrodialytic salt production using brine discharged from a reverse osmosis seawater desalination plant, J. Membr. Sci. 222 (2003) 71 –86.
12. T.A. Davis, R.E. Lacey, Forced-Flow Electrodesalination, Report No. 710, United States Department of the Interior, Office of Saline Water, 1970.
13. Kabay, N., Kahveci, H., İpek, Ö., & Yüksel, M. (2006). Separation of monovalent and divalent ions from ternary mixtures by electrodialysis. *Desalination*, *198*(1-3), 74-83.
14. Tanaka, Y. (2007). *Ion exchange membranes: Fundamentals and applications*, Membrane science and technology series, Elsevier, Boston.
15. Saracco, G., Zanetti, M.C., and Onofrio, M. (1993) Novel application of monovalent-anion- permselective membranes to the recovery treatment of an industrial wastewater by electrodialysis. Ind. Eng. Chem. Res., 32: 657.
16. Strathmann, H. (2004). *Ion-exchange membrane separation processes*, Membrane science and technology series, Elsevier, Boston.
17. Yamane, R., Sata, T., Mizutani, Y., & Onoue, Y. (1969). Concentration polarization phenomena in ion-exchange membrane electrodialysis. II. The effect of the condition of the diffusion-boundary layer on the limiting-current density and on the relative transport numbers of ions. *Bulletin of the Chemical Society of Japan*, *42*(10), 2741-2748.
18. T. Sata, T. Sata, W. Yang, Studies on cation-exchange membranes having permselectivity between cations in electrodialysis, J. Membr. Sci. 206 (2002) 31 –60.
19. Kabay, N., İpek, Ö., Kahveci, H., & Yüksel, M. (2006). Effect of salt combination on separation of monovalent and divalent salts by electrodialysis. *Desalination*, *198*(1-3), 84-91.

20. Kabay, N., Kahveci, H., İpek, Ö., & Yüksel, M. (2006). Separation of monovalent and divalent ions from ternary mixtures by electrodialysis. *Desalination*, *198*(1-3), 74-83.
21. B. Van der Bruggen, A. Koninckx, C. Vandecasteele, Separation of monovalent and divalent ions from aqueous solution by electrodialysis and nanofiltration, Water Res. 38 (2004) 1347.
22. S. Zektser, H.A. Loáiciga, J. Wolf, Environmental impacts of groundwater overdraft: selected case studies in the southwestern United States, Environ. Geol. 47 (2005) 396 – 404.
23. S. Miyamoto, J. Henggeler, J.B. Storey, Water management in irrigated pecan orchards in the southwestern United States, HortTechnology 5 (1995) 214 –218
24. M. Chandramowleeswaran, K. Palanivelu, Treatability studies on textile effluent for total dissolved solids reduction using electrodialysis, Desalination 201 (2006) 164–174.
25. J.F. Koprivnjak, E.M. Perdue, P.H. Pfromm, Coupling reverse osmosis with electrodialysis to isolate natural organic matter from fresh waters, Water Res. 40 (2006) 3385–3392.
26. W. Shane, Younggy Kim, and Desmond F. Lawler. "Treatment of model inland brackish groundwater reverse osmosis concentrate with electrodialysis—Part I: sensitivity to superficial velocity." Desalination 344 (2014): 152-162, https://doi.org/10.1016/j.desal.2014.03.035.
27. Y. Zhang, B. Van der Bruggen, L. Pinoy, B. Meesschaert, Separation of nutrient ions and organic compounds from salts in RO concentrates by standard and monovalent selective ion-exchange membranes used in electrodialysis, J. Membr. Sci. 332 (2009) 104–112.
28. Hyder, A. H. M., Brian A. Morales, Malynda A. Cappelle, Stephen J. Percival, Leo J. Small, Erik D. Spoerke, Susan B. Rempe, and W. Shane Walker. "Evaluation of Electrodialysis Desalination Performance of Novel Bioinspired and Conventional Ion Exchange Membranes with Sodium Chloride Feed Solutions." Membranes 11, no. 3 (2021): 217.

29. Cappelle, M., Walker, W. S., & Davis, T. A. (2017). Improving desalination recovery using zero discharge desalination (ZDD): a process model for evaluating technical feasibility. *Industrial & Engineering Chemistry Research*, *56*(37), 10448-10460, https://doi.org/10.1021/acs.iecr.7b02472.
30. Káňavová, N., Machuča, L., & Tvrzník, D. (2014). Determination of limiting current density for different electrodialysis modules. *Chemical Papers*, *68*(3), 324-329, https://doi.org/10.2478/s11696-013-0456-z.
31. Lee, H. J., Strathmann, H., & Moon, S. H. (2006). Determination of the limiting current density in electrodialysis desalination as an empirical function of linear velocity. *Desalination*, *190*(1-3), 43-50, https://doi.org/10.1016/j.desal.2005.08.004
32. Walker, W. Shane, Younggy Kim, and Desmond F. Lawler. "Treatment of model inland brackish groundwater reverse osmosis concentrate with electrodialysis—Part II: Sensitivity to voltage application and membranes." Desalination 345 (2014): 128-135.
33. Walker, W. Shane, Younggy Kim, and Desmond F. Lawler. "Treatment of model inland brackish groundwater reverse osmosis concentrate with electrodialysis—Part III: Sensitivity to composition and hydraulic recovery." Desalination 347 (2014): 158-164.
34. Kabay, N. A. L. A. N., M. Demircioglu, E. Ersöz, and I. Kurucaovali. "Removal of calcium and magnesium hardness by electrodialysis." Desalination 149, no. 1-3 (2002): 343-349.

Chapter 4: Preliminary development of polyethersulfone cation exchange membranes for electrodialysis desalination

Abstract

Due to the lack of fresh water, one of the most significant industrial applications of ion exchange membranes (IEMs) is recovering fresh water from brackish groundwater using electrodialysis (ED) desalination. Therefore, the advancement and development of cost-effective IEMs with good electrochemical properties and physicochemical stability for water desalination is highly desired. This study focuses on the preliminary development of polyethersulfone (PES) cation exchange membranes (CEMs) using phase inversion and solvent evaporation methods for ED desalination. Initially, PES was dissolved in solvent (e.g., chloroform: $CHCl_3$ and dichloromethane: CH_2Cl_2) and then sulfonated using chlorosulfonic acid (CSA: HSO_3Cl). The sulfonated PES (sPES) was dissolved in N-Methyl-2-Pyrrolidone (NMP, C_5H_9NO) to prepare a dope solution, and then polyvinylpyrrolidone (PVP) crosslinker and graphene oxide (GO) nanomaterial were added to the dope solution to fabricate membranes. The influence of using two different solvents, such as chloroform and dichloromethane, was identified during the sulfonation of PES with CSA. In addition, the role of adding PVP crosslinking agent and GO nanofiller in the main chain of sulfonated polyethersulfone (sPES) polymer was studied. The findings highlight the potential for PES materials fabricated using phase inversion methods and warrants further investigation of IEM microstructure (*e.g.*, fabrication method, nanofillers, and crosslinking agents) as an important strategy for advancing the development of cost-effective IEMs for commercial use. Results show that sPES with crosslinkers (PVP) and nanofillers (GO nanoparticles) had the highest overall limiting current density, current (charge) efficiency, and salinity reduction despite having lower ion exchange capacity (IEC) and sulfonation than sPES and demonstrates the utility of adding crosslinkers and nanofillers to improve the performance of IEMs.

Keywords: Electrodialysis, polyethersulfone, cation exchange membrane, PVP crosslinker, GO nanofiller, NaCl feed.

4.1. INTRODUCTION

4.1.1 Background

Ion-exchange membranes (IEMs) are essential to the field of fuel cells, as well as electro-driven desalination techniques such as electrodialysis (ED), capacitive deionization (CDI), and electro deionization (EDI) [1,2]. ED is an electrical potential driven membrane desalination technique that can be used for the demineralization and purification of industrial wastewater brines recovered from industries related to chemical processing, food production, and pharmaceutical production [3,4]. However, due to lack of fresh water, advancing IEMs for recovering fresh water from brackish ground water is one of the most significant industrial applications of IEMs using ED [5]. Therefore, the development of cost-effective ion-exchange membranes with good electrochemical properties and physicochemical stability for water desalination is highly desired [6].

Commercial cation exchange membranes are typically made from copolymers styrene and divinylbenzene (DVB), followed by sulfonation. The commercial Neosepta AMX (anion exchange) and CMX (cation exchange) membranes were used in this study as control membranes for comparison purposes. The sulfonation of the styrene/divinylbenzene polymer is typically achieved by chlorosulfonic acid and/or concentrated sulfuric acid in dichloroethane using silver sulfate as catalyst [7,1].

Sulfonated arylene main chain polymers such as sulfonated polyethersulfone (sPES) are considered as an attractive material for CEM due to lower cost, ease of processability in low-cost solvents, as well as its chemical and thermal stability [8,9]. The sulfonation of PES is difficult due to the sulfone linkages, which have an electron withdrawing effect that deactivate adjacent aromatic rings for an electrophilic substitution [10].

A high degree of sulfonation is required to attain good conductivity, ion exchange capacity (IEC), and permselectivity of IEMs. However, there is a trade-off as the high degree of sulfonation causes membrane mechanical instability; thus, fine-tuning the degree of sulfonation without

compromising the structure of the polymer is essential for developing potential CEM forming material. The polymer main chains maintain CEM mechanical stability, and the functional groups endow CEMs with good permselectivity [11,12,13]. Thus, the preservation of the polymer main chains is of importance to the membrane mechanical stability when sulfonating the aromatic rings in polyethersulfone structures. In this study, sulfonation of PES was performed without H_2SO_4 as a solvent or sulfonating agent to decrease the possibility of damaging the main chain structure while retaining good degrees of sulfonation.

The energy losses of IEMs can be reduced by minimizing the permeability of IEMs to water and salt. Therefore, it is necessary to consider the limited transport of salt and non-deal water (salt diffusion and osmosis) through IEMs when developing an advanced IEM to improve ED processes [5]. There are indications that microstructural differences among the IEMs may significantly affect permeability [5]. Therefore, further study of IEM microstructure, *e.g.,* fabrication method, nanofillers, and crosslinkers, is an important strategy for advancing the development of commercial IEMs.

Due to its high surface area, graphene oxide (GO) is an excellent material to be used as an organic filler for membranes to improve thermal and mechanical stability but also provide higher ionic conductivity. GO and functionalized GO have been used previously as nanofiller for IEMs in ED desalination [14,15,16] and, in general, have been shown to perform well in ED experiments to achieve substantial salt removal rates due to the formation of ion conducting channels for ionic transport facilitation [17,18,19]. Recently, polyvinylpyrrolidone (PVP) has been used as a hydrophilic additive for sPES membranes used in desalination experiments to improve the distances between the main chain polymer functional groups and provide extra stability [20].

In order to develop laboratory-scale CEMs for improving ED performance, several studies had been performed as mentioned in previous sections, but they designed the experiment with their own independent sets of experimental parameters such as either solvent evaporation [21] or phase inversion [6,22] fabrication methods, either chloroform or dichloroethane as solvent [1,7], either sulfuric acid [23] or chlorosulfonic acid for sulfonation of PES [1,7,10], PVP as a hydrophilic

additive for sPES [20], and GO as nanofiller for controlled porosity and permselectivity [14,15,16]. However, to our knowledge, there is no study that has systematically compared the influence of these microstructural properties of CEMs on the ED desalination performances with varying concentrations and compositions of feed water solutions.

4.1.2. Objective

The overall aim of this study is the preliminary development of polyethersulfone (PES) cation exchange membranes (CEMs) for ED desalination. The specific objectives are:

i. To evaluate the ED performance differences between CEMs fabricated by phase inversion and solvent evaporation methods.
ii. To evaluate the influence of using two different solvents such as chloroform and dichloromethane (DCM) during the sulfonation of PES with chlorosulfonic acid.
iii. To evaluate the role of adding polyvinylpyrrolidone (PVP) crosslinker and graphene oxide (GO) nanofiller in the main chain of sulfonated polyethersulfone (sPES) polymer.

4.2 Materials and Methods

4.2.1. Chemicals

PES was purchased from Goodfellow (SU30631114, USA). Chloroform ($CHCl_3$) (HPLC grade, JC Baker, USA) and Dichloromethane (DCM, CH_2Cl_2) (ACS grade, BDH, USA) were used as the solvent for PES during sulfonation reactions. Chlorosulfonic acid (CSA, HSO_3Cl) (> 98.0%, Fluka, USA) was used as the sulfonating agent and N-Methyl-2-Pyrrolidone (NMP, C_5H_9NO) (ACS grade, Fisher Scientific, USA) was used for the solvent in membrane fabrication. Polyvinylpyrrolidone (PVP, $(C_6H_9NO)_n$,~29,000 mw) was purchased from Sigma Aldrich (USA), and Graphene Oxide (GO) nanoparticles were received from GrapheneAll (South Korea).

Laboratory-grade (ACS reagent grade) sodium chloride (NaCl) and sodium sulfate (Na_2SO_4) salts were purchased from Fisher Scientific (USA) to prepare the feed solutions and the

electrode rinse solution, respectively. All reagent water was purified and deionized to a resistivity of 18.2 MΩ cm. All the ED tests were performed in triplicate for statistical characterization.

4.2.2. Sulfonated polyethersulfone (sPES) preparation

Blank PES (used for Membrane-A) was sulfonated using two methods to be compared for cationic exchange membranes (CEMs) used in ED.

In the first method of sulfonation, briefly, PES was dissolved in chloroform ($CHCl_3$) (10% wt/v), and the solution was cooled to 0 °C in an ice bath. Chlorosulfonic acid (CSA) (10% v/v) was added drop-wise to the PES/$CHCl_3$ solution. After 60 min stirring, the reaction was terminated by the addition of a fivefold volume of methanol to the reaction mixture. The precipitate was collected, washed thoroughly with methanol, and dried at 50 °C, which resulted in the sPES (sPES material A used for Membrane-B and -E) [21].

In the second sulfonating method, PES was dissolved in dichloromethane (DCM) (10% wt/v), CSA (10% v/v) was added to the PES/DCM solution and stirred for 60 min on ice before quenching the reaction following the same procedure as above to produce sPES (sPES material B used for Membrane-C and D). The sPES samples were washed in 500 mL of hot water until the pH was neutralized and then dried in a vacuum oven at 60 °C for 24 hr [22]. Figure 4.1 illustrates the sulfonation reactions and the chemical components of the prepared sPES CEMs.

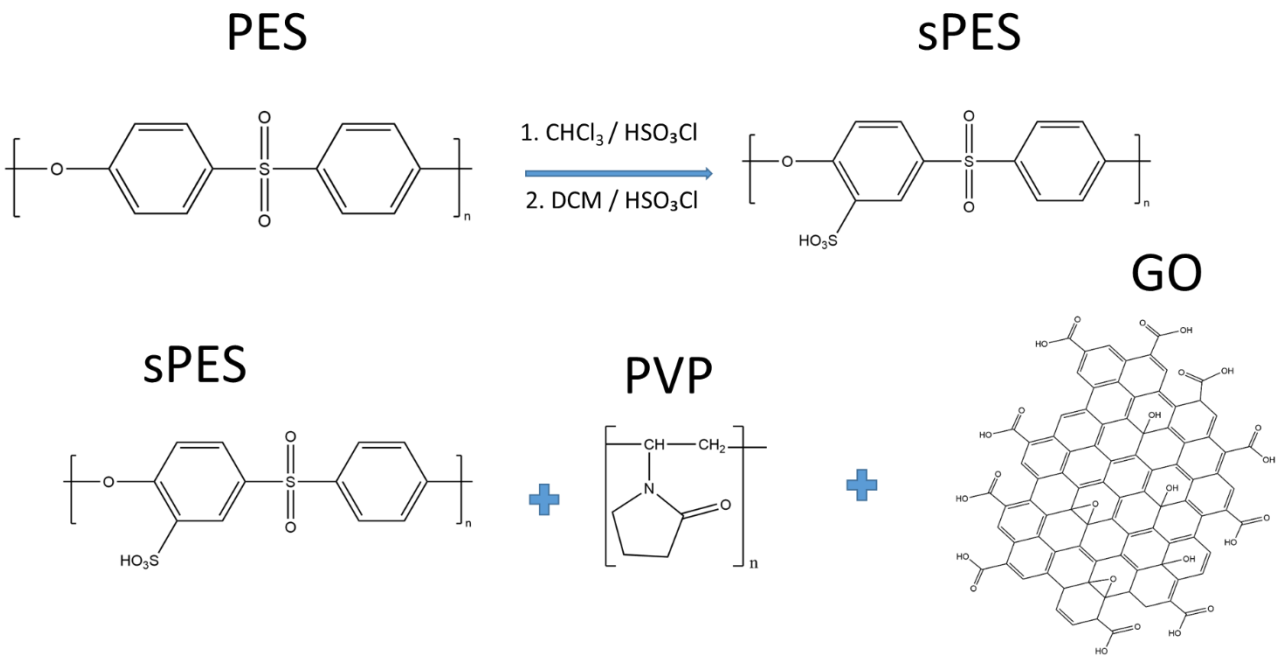

Figure 4.1: Chemical structure of PES, sPES, PVP, GO and diagram of sulfonation methods.

4.2.3. Membrane fabrication

First, dope solutions were prepared by dissolving blank PES (15% w/w) in NMP for Membrane-A and sPES (15% w/w) in NMP for Membrane-B, C, D, & E, and stirring at 60 °C in a closed flask for 12 hr after a clear solution was obtained.

For Membrane-D, GO nanoparticles (1 mg/mL) were first dissolved in NMP, and then dissolved GO (0.5% wt. GO/sPES) and PVP (30% wt. PVP/sPES) solution were added to the sPES/NMP dope solution.

All the above-mentioned dope solutions were stirred for 12 hr to achieve a homogenous solution, then degassed for 15 minutes, then applied to a glass substrate to place in a spin coater, and finally cast membrane using phase inversion in DI water [22].

Membrane-E was prepared via the solvent evaporation method by dissolving sPES (material A) (15% w/w) in NMP, and then PVP (1% wt. PVP/sPES) was mixed with sPES/NMP dope solution. Finally, the dope solution was added to petri dish plates and dried at 65 °C for 24

hr and then detached the membranes from plates by submerging in DI water [21]. The sPES material A was used for fabricating Membrane-B and E, and sPES material B was used for fabricating Membrane-C and D.

The prepared membranes were treated in 1 M HCl for 24 hr, then rinsed with DI water and kept in 1 M NaCl solution. All membranes were equilibrated in working solution for at least 6 hr before use.

4.2.4. Membrane characterization

4.2.4.1.Degree of sulfonation (DS) measurement

The degree of sulfonation (DS) is the fraction of the sulfonated monomer units after the reaction. It is determined as follows: First, 0.3 g of sPES was stirred in 30 mL of 2 M NaCl solution for 24 hr to release the H^+ ions. Then the mixture was titrated with standardized 0.1 M NaOH solution using phenolphthalein as an indicator. DS is calculated according to the following equation [10,21,24]:

$$DS = \frac{244_{g/mol}\,(C_{NaOH} \cdot V_{NaOH})}{W - 81_{g/mol}\,(C_{NaOH} \cdot V_{NaOH})} \tag{4.1}$$

where C_{NaOH}, V_{NaOH}, and W are the concentration (mol/L) of standard NaOH solution, volume (mL) of NaOH solution, and weight (g) of dry sPES, respectively. The molecular weight of PES repeat unit is 244 g/mol, and 81 g/mol is the molar mass of the sulfonate SO_3H group.

4.2.4.2.Water content measurement

Membrane water content was determined by the weight of the membrane in wet and dry conditions. The water content was calculated using the following equation [25]:

$$Water\ content\ = \frac{W_w - W_d}{W_d} \tag{4.2}$$

where W_w and W_d are the weight of the wet and dry membranes, respectively.

4.2.4.3. Ion-exchange capacity (IEC) measurement

The membranes were soaked for 24 hr in 1 M HCl, followed by rinsing with deionized water to remove the acid from the surface, and then immersing the membrane in 2 M NaCl for 24 hr. Then the solution was titrated with NaOH using phenolphthalein as an indicator. The IEC (meq/g) value was obtained using Equation 4.3 [24,25]:

$$IEC = \frac{C_{NaOH} \cdot V_{NaOH}}{W_{dry}} \quad (4.3)$$

where C_{NaOH} is the concentration (mol/L) of NaOH solution, V_{NaOH} is the volume (mL) of NaOH solution required for neutralization, and W_{dry} is the weight (g) of the dry membrane.

4.2.5. Electrodialysis testing

A detailed description of the ED experimental testing, including experimental design, experimental system and equipment, experimental procedure, and calculation methods of important ED parameters, was reported in previous research performed by Hyder et al. [26]. This paper focuses on the fabrication of novel cation exchange membranes and a comparison of ED performance differences between newly developed and commercial IEMs. For laboratory-scale batch-recycle electrodialysis experimental design, several experimental variables were considered, and their discrete values are shown in Table 4.1.

Table 4.1: Experimental variables, value ranges, and combinations

Variables	**Discrete Values/Combinations**
Feed water	3 and 35 g/L NaCl* (corresponding conductivity of 5.62 and 54.88 mS/cm)
Electrode rinse solution	a fixed concentration of 0.1 mol/L (14.2 g/L) sodium sulfate (Na_2SO_4)
Superficial velocity of diluate stream	4 cm/s (corresponding flow: 30 mL/minute)
Stack voltage	0.8 Volts per cell-pair of membrane
Combination of membranes during stack assembly	i. Neosepta AMX & CMX ii. Neosepta AMX & Membrane A iii. Neosepta AMX & Membrane B iv. Neosepta AMX & Membrane C v. Neosepta AMX & Membrane D vi. Neosepta AMX & Membrane E

*Note: 3 and 35 g/L sodium chloride (NaCl) represent the typical concentrations of brackish groundwater and seawater, respectively.

In this study, novel cation exchange membranes were prepared (see detail in Table 4.3) and compared to a commercial membrane (Neosepta CMX). The physicochemical property of Neosepta AMX/CMX membranes is summarized in a previous study [26]. All the membranes used in this study were soaked in 0.01 M NaCl solution for 24 hours prior to use and then trimmed to 6.4 cm x 4.4 cm size and punched holes at precise locations.

The performance of the prepared membranes for current density, current efficiency, salinity reduction, and energy consumption was tested using a laboratory-scale single stage electrodialysis stack (model: 08002-001, PCCell/PCA, GmbH, Germany) with an active cross-sectional area of membrane subjected to the applied electric field of 7.84 cm^2 (2.80 cm x 2.80 cm). The ED stack was assembled with five cell-pairs according to the schematic diagram of the ED process as shown in an earlier study by Hyder et al. [26]. Polyester mesh spacer-gaskets of thickness 0.45 mm physically separated the AEMs and CEMs.

The diluate solution was circulated at a flow rate of 30 mL/minute (corresponding to a superficial velocity of 4 cm/s), and the pressure of the diluate cell for the relevant flow rate was recorded. The solution flow rate through the concentrate cells and electrode rinse compartments

were adjusted to maintain the same pressure as diluate cells. A laboratory-scale Master Flex peristaltic-cartridge pump (Cole-Parmer, USA, Model: 7519-00) was used to circulate the solutions through each of the process streams.

The electrical conductivity, pH, and temperature of the process stream reservoirs were determined using a pH/conductivity meter (Thermo Scientific, USA, model: Orion Star A325). The mass of the diluate reservoir was measured (Meller Toledo, USA, model: XS2002S) to quantify the net mass of water and salt transportation across the membranes. Analog pressure gauges (model: 18C774, Grainger, USA) were used at the inlet of the diluate, concentrate, and electrode rinse streams to observe the head loss through each stream and the average transmembrane pressures. A programmable DC Power Supply (B&K Precision, USA, Model: 9123A) was used for monitoring and controlling voltage and current through the electrodialysis stack.

Experimental data were recorded automatically at five-second intervals in spreadsheets in the computer by the LabVIEW 2017 supervisory control and data acquisition (SCADA) system. Finally, the acquired data from LabVIEW were analyzed to evaluate ED desalination performance of the IEMs.

The calculation methods of important ED parameters such as voltage loss at electrodes, normalized specific energy consumption, limiting current density, current efficiency, and diluate salinity reduction were reported in detail in the previous research performed by Hyder et al. [26] and Walker et al. [27].

4.3 RESULTS

4.3.1. Evaluation of limiting current density, areal resistance, and polarization parameter

The limiting current density (LCD), limiting areal resistance p, and limiting polarization parameter (LPP) were determined for five arrangements of a five cell-pair ED stack. In all five arrangements, the stack was assembled with Neosepta AMX anion exchange membranes, and each

of the five arrangements used a different cation exchange membrane: the commercial Neosepta CMX (control), and four novel cation exchange membranes developed in this study (compared with the CMX). Experiments were performed with a superficial velocity of 4 cm/s using a sodium chloride (NaCl) feed solution concentration of 3 g/L (corresponding conductivity of 5.62 mS/cm) as shown in Figure 4.2. The LCD, aerial resistance, and LPP results were not achieved for a NaCl feed solution concentration of 35 g/L because the maximum working capacity of the power supply (30 V, 5 A) was reached before observing LCD.

The LCD ranged from 147 to 234 A/m^2 (Figure 4.2a), and the corresponding areal resistance per cell-pair at these LCDs ranged from 78 to 42 $\Omega\ cm^2$, respectively (Figure 4.2b). The least LCD value of 147 A/m^2 was observed at a voltage application of 0.9 V/cell-pair for AMX-A membrane pair (blue), and the greatest LCD value of 234 A/m^2 was observed at 1.0 V/cell-pair for AMX-D (purple). The LPP ranged from 2.9 to 4.6 A/m^2 per meq/L (feed) for LCD values of 147 to 234 A/m^2, respectively (Figure 4.2c). Subsequent experiments were performed with stack voltage application (*i.e.*, 0.8 V/cell-pair) less than the least LCD stack voltage (*i.e.*, 0.9 V/cell-pair). Table 4.2 summarizes the trend in LCD, areal resistance, and LPP for the five membrane sets.

Increasing the degree of sulfonation within the sPES/GO cation exchange membranes (CEMs) from A to D increased the LCD and LPP values (*i.e.*, the greatest LCD and LPP were achieved for AMX-D membrane pair), and the opposite trend was found for the CEMs in terms of areal resistance, which is consistent with other studies [14].

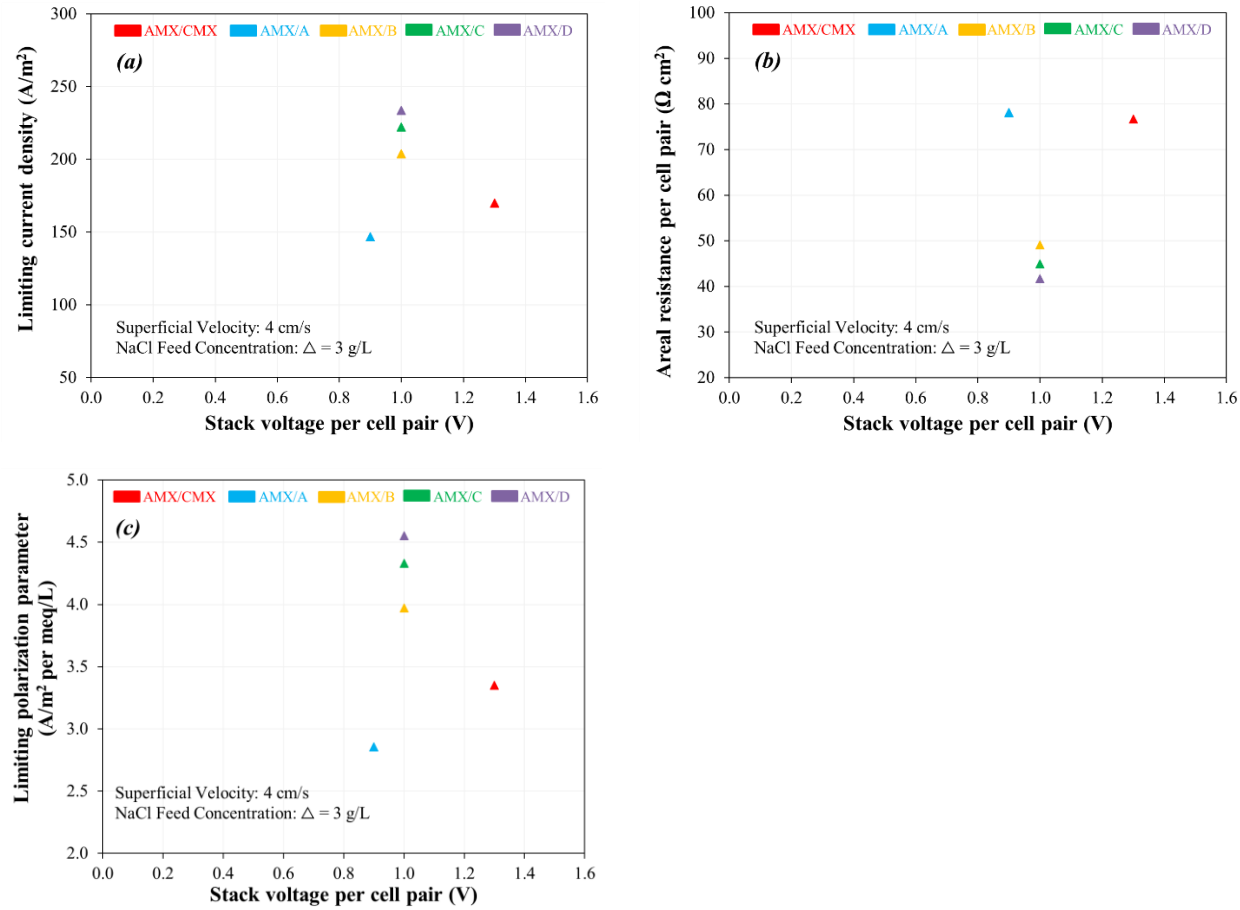

Experimental conditions: 5 cell-pair ED stack; 4 cm/s superficial velocity; constant stack voltage application; 1 L batch feed solution; 0.1 M (14.2 g/L) Na_2SO_4 electrode rinse solution; and <3 kPa transmembrane pressure

Figure 4.2: (a) Limiting current density, (b) areal resistance per cell-pair of membranes at LCD, and (c) limiting polarization parameter versus ED stack voltage per cell-pair.

Table 4.2: Performance trends for five membrane sets (each with AMX anion membranes)

Parameters	**Membranes* (Greatest to least order)**
LCD & LPP	D > C > B > CMX > A
Areal resistance at LCD	A > CMX > B > C > D
Current density	D > C > B > A > CMX
Current efficiency	CMX > D > C > B > A
Diluate Salinity Reduction	CMX > D > C > B > A
nSEC	D > C > B > A > CMX

Experimental conditions: 3 and 35 g/L NaCl feed solutions, 4 V/cell-pair stack voltage, and 4 cm/s (30 mL/min) superficial velocity of feed solution.

4.3.2. Evaluation of current density and current efficiency

The average current density (CD) and average current efficiency (CE) of the five membrane sets were compared during ED experiments using NaCl feed solutions (*i.e.*, 3 and 35 g/L) and an applied stack voltage of 0.8 Volts per cell-pair at 4 cm/s superficial velocity of feed solution (Figure 4.3). As expected, the current density increased with greater feed salinity (Figure 4.3a), and the current efficiency decreased with greater feed salinity (Figure 4.3b). Similar trends of current density and current efficiency are also reported in other studies [26, 28]. The current density and current efficiency trends of the commercial and developed membranes are listed in Table 4.2.

The current density of the membrane stacks with the developed sPES membranes ranged from 135 to 1163 A/m^2 which were approximately 40% to 85% greater than the Neosepta AMX/CMX membrane stack (97 to 613 A/m^2). However, the current efficiency of the stacks with the newly developed membranes ranged from 40% to 50%, which was approximately half that of the Neosepta AMX/CMX membrane stack (87% to 92%). The sPES membranes had a greater water uptake and ion exchange capacity (Table 4.3), leading to higher counter-ion transport and lower current efficiency. The higher current density and the lower current efficiency in the developed membranes compared to the Neosepta AMX/CMX membranes indicate that the permselectivity (or counter ions transport capability) of the developed membranes are very low, and both counter ions and co-ions are transported through the newly developed cation exchange membranes. It is hypothesized that a greater degree of sulfonation in the sPES membranes might improve the permselectivity.

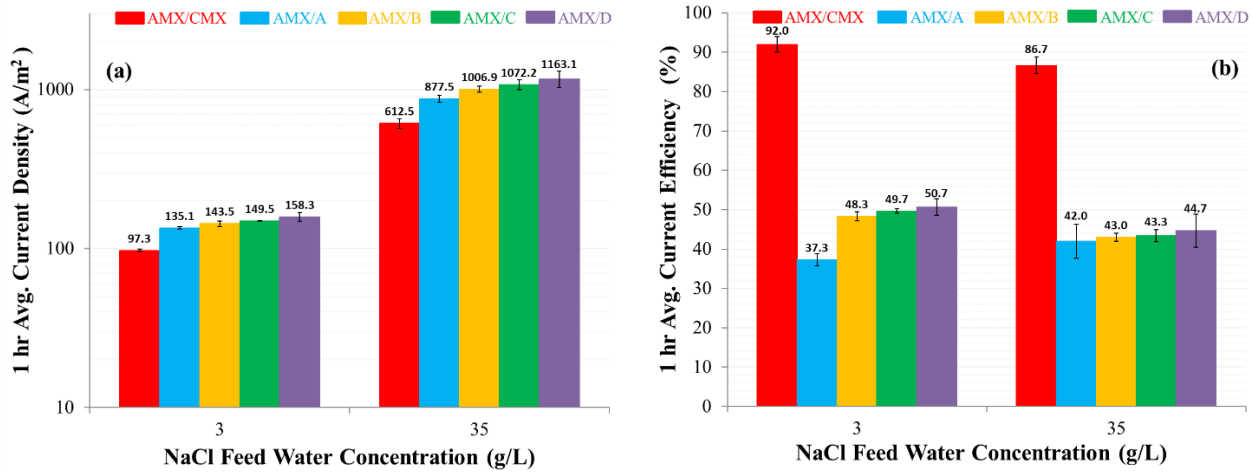

Experimental conditions: 5 cell-pair ED stack; 3 and 35 g/L initial concentrations of NaCl feed (diluate and concentrate) solutions (500 mL each); 4 cm/s superficial velocity of feed solution; 0.8 V/cell-pair constant applied stack voltage; 0.1 M (14.2 g/L) Na_2SO_4 electrode rinse solution; and 3.4 kPa transmembrane pressure.

Figure 4.3: Effect of membranes and feed solution concentrations on (a) current density and (b) current efficiency for five membrane sets.

4.3.3. Evaluation of diluate salinity reduction and specific energy consumption

The salinity reduction (SR) and normalized specific energy consumption (nSEC) of the five membrane sets after 60 minutes of ED testing using NaCl feed solutions were compared with concentrations of 3 and 35 g/L and an applied stack voltage of 0.8 Volts per cell-pair at 4 cm/s superficial velocity of feed solution (Figure 4.4).

The salinity reduction in diluate stream decreased with greater feed salinity, as expected (Figure 4.4a), which is consistent with other studies [26,27]. The salinity reduction of sPES membranes (31% to 43%) was half to three-fourths that of the Neosepta AMX/CMX membranes (61%) for 3 g/L feed, and was around three-fifths to four-fifths (18% to 24%) that of the Neosepta AMX/CMX membranes (29%) for 35 g/L feed.

The normalized specific energy consumption (nSEC) increased with the increase in feed salinity (Figure 4.4b), which is in agreement with other studies [10]. The nSEC of newly developed membranes ranged from 44 to 54 kWh/m^3 per eq/L-removed, which were almost double those of

the Neosepta AMX/CMX membranes (23.9 and 28.7 kWh/m^3 per eq/L-removed). The difference in the SEC among the experiments with sPEC membranes was less than 10%. The specific energy reported in this study includes only the electrical energy applied to the stack; it did not include the hydraulic energy invested to pump the solution through the electrodialysis stack.

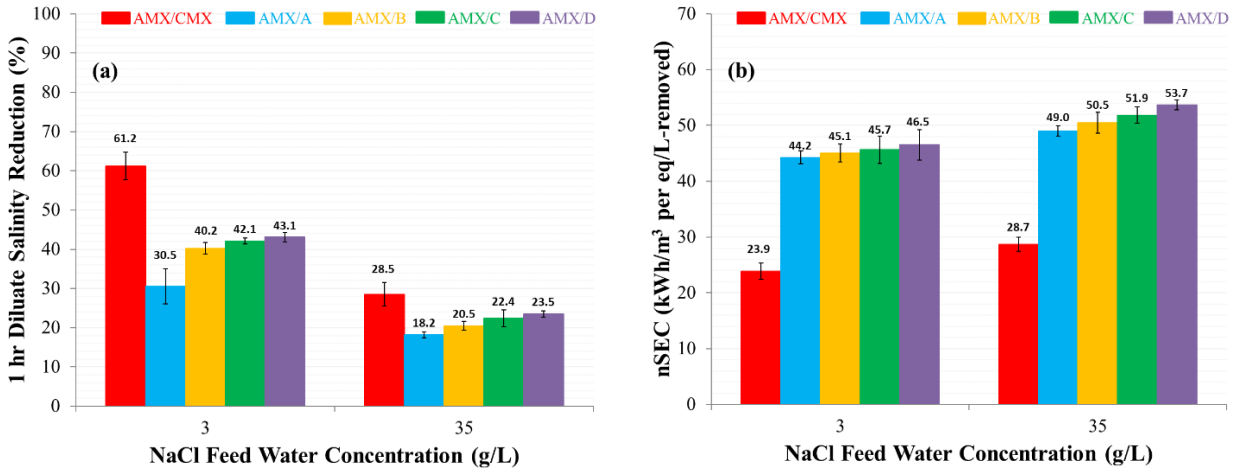

Experimental conditions: 5 cell-pairs ED stack; 3 and 35 g/L initial concentrations of NaCl feed (diluate and concentrate) solutions (500 mL each); 4 cm/s superficial velocity of feed solution; 0.8 V/cell-pair constant applied stack voltage; 0.1 M (14.2 g/L) Na_2SO_4 electrode rinse solution; and 3.4 kPa transmembrane pressure.

Figure 4.4: Effect of membranes and feed solution concentrations on (a) salinity reduction, and (b) normalized specific energy consumption (nSEC) for five membrane sets.

4.3.4. Evaluation of membrane structure-property relationships

The different degrees of PES sulfonation have been previously evaluated in IEMs for fuel cells [1] and desalination applications [2]; however, these studies involve the use of concentrated sulfuric acid. We attempted in this study to compare chlorosulfonic acid (CSA) sulfonating agent to PES sulfonated using hydrosulfuric acid, but the mechanical strength was too limited to complete the ED experiments as it dissolved. We continued using only CSA for the remainder of our efforts to avoid the adverse effects of sulfuric acid. As discussed in the introduction, a high degree of sulfonation is necessary to achieve a good IEC and, therefore permselectivity, but fine-

tuning the sulfonation is necessary to avoid compromising the main chain backbone structure of the polymer. Figure 4.5 shows the SEM images (top) and the constituents of the fabricated membranes.

The two competing sulfonation methods used in our study involve just changing the solvent for the PES. All membranes were fabricated from the same solvent (NMP), but the two sulfonation methods (Membrane-B vs Membrane-C) compared used chloroform and dichloromethane during the sulfonation, respectively. We can see from Table 4.3 that the degree of sulfonation in Membrane-C is 77% while Membrane-B is 47%. Conversely, Membrane-B has a higher water uptake than Membrane-C, which is counterintuitive. IEC and % sulfonation can be well correlated as both measurements depend on functional groups present, but water uptake is slightly more complicated [3,5]. These findings would indicate that although Membrane-C has a higher degree of sulfonation than Membrane-B, the main chain polymer is possibly more intact, contributing to higher regions of the hydrophobic polymer where water is not uptaken. While the difference in percent sulfonation is very pronounced between these two membranes (B and C), it did not translate into dramatic improvements in current efficiency (CE) or salinity reduction (SR). Due to the higher sulfonation percentage and the lack of crosslinkers or fillers, Membrane-C had the highest overall IEC next to Membrane-B. It would seem to follow that these two membranes would perform the best during the ED experiment, but Membrane-D had the best current efficiency and salinity reduction, revealing that microstructure effects (adding crosslinkers and/or nanofillers) had a higher influence on these two conditions (CE, SR) than just IEC or percent sulfonation.

Table 4.3: Physiochemical properties and ED performances of fabricated membranes

Sample	Description	Fabrication	IEC (meq/g)	H_2O (%)	SO_3 (%)	CE (%) @3g/L	SR (%) @3g/L
A: Mem-A	PES	Phase Inversion	0.5	47	14	37	31
B: Mem-B	sPES / CSA / $CHCl_3$	Phase Inversion	1.9	58	47	48	40
C: Mem-C	sPES / CSA / DCM	Phase Inversion	2.5	57	77	50	42
D: Mem-D	(sPES / CSA / DCM) / PVP (30%) / GO (5%)	Phase Inversion	1.3	76	35	51	43
E: Mem-E	(sPES / CSA / $CHCl_3$) / PVP (1%)	Solvent Evaporation	0.8	16	21	38	1

Membrane-E was fabricated using solvent evaporation to control for limiting non-ideal water and salt transport (osmosis and salt diffusion) as compared with membranes fabricated using phase inversion. Even with sPES (sPES material B) polymer and 1% of hydrophilic crosslinking co-polymer PVP, Membrane-E showed very poor results in IEC (0.8 meq/g) and SR (0.8%). These findings illustrate the relative significance of permeability as Membrane-E had the lowest water uptake (16%) out of all the membranes. Reducing the overall permeability of Membrane-E reduced the water transport and, therefore, ion transport. As a result, limiting these factors makes a poor membrane.

Blank PES (Membrane A) does not have any sulfonation functionalization; however, there is an inherent sulfone group in the polymer backbone contributing to sulfonation (14%) and a low IEC (0.5 meq/g), but a relatively high-water uptake (47%) due to the microstructure created from phase inversion.

The same sPES material B was used to prepare Membrane-B and -E, but their fabrication methods were different *i.e.*, phase inversion and solvent evaporation, respectively. Thus, Membrane-B, as compared to Membrane-E, has much larger pores and an asymmetric structure (Figure 4.5), which are common in membranes fabricated from phase inversion. Membrane-B had

almost 40 times the SR than Membrane-E, as well as more than double the IEC (1.9 vs 0.8 meq/g) and degree of sulfonation (47 vs. 21%) compared to Membrane-E. These results illustrated the importance of fabrication methods (phase inversion versus solvent evaporation) on pore size and showed the relative significance of the IEC and degree of sulfonation in IEM performance with respect to SR.

To understand the role of a hydrophilic crosslinker and nanofiller on the CE and SR of sulfonated PES, a sPES polymer using PVP and GO was fabricated in an attempt to decrease porosity for tuning the ion transport mechanism in matrix materials for ion exchange membranes. Results show that the ED stack with Membrane-D had the highest overall CE and SR, despite having lower IEC and percent sulfonation than the stacks with Membrane-B and Membrane-C, demonstrating the utility of adding crosslinking and nanofillers to improve the CEM. The higher CE and SR correlated with a higher overall SEC (Membrane-D showed the highest nSEC, Figure 4.4) as more ions are passing through the membrane and energy is being used to remove them from the solution, as was found by previous authors [4,5,6].

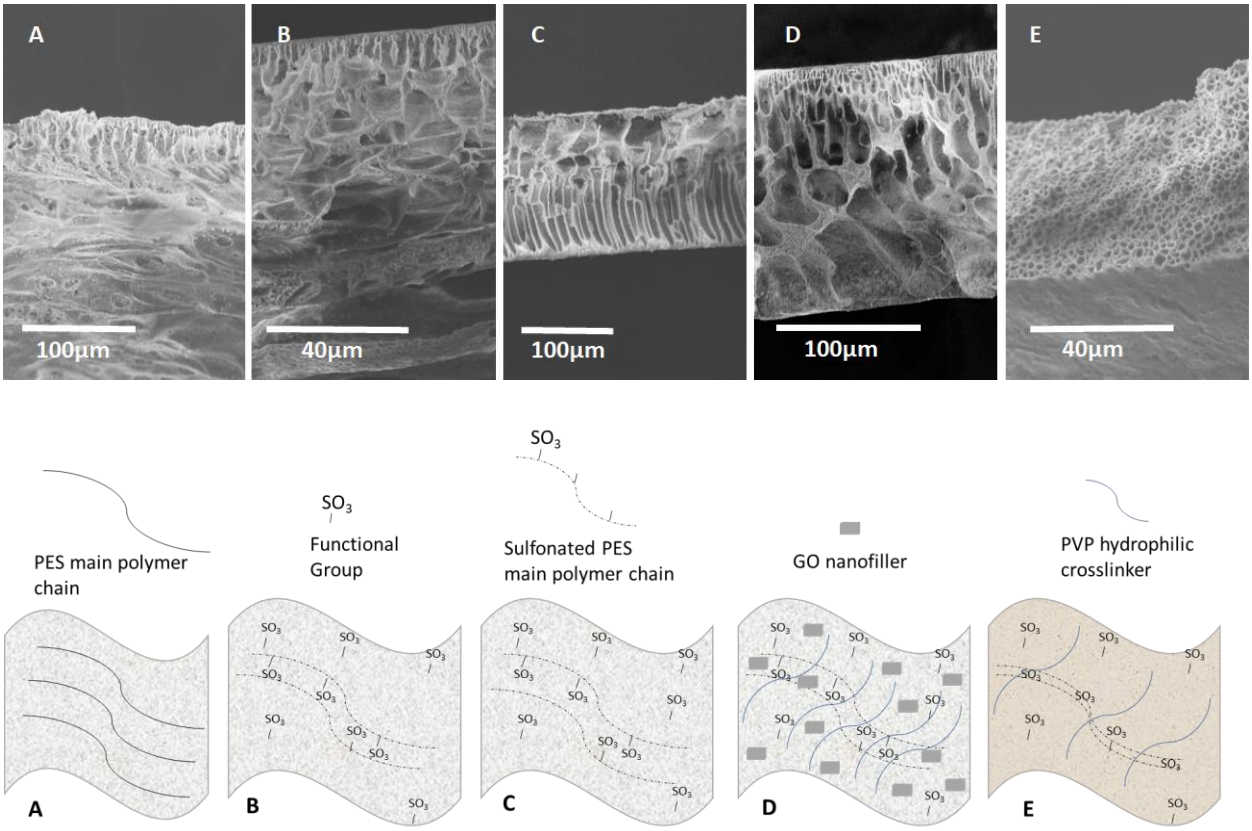

Membrane samples shown here are labeled the same in Table 4.3

Figure 4.5. Scanning Electron Micrographs (SEM) of fabricated membranes (top) and diagram showing constituents in membranes (bottom).

4.4 Conclusions and Future Work

These results highlight the potential of PES materials for CEMs and illustrate how water permeability and water transport strongly influence the salt removal performance of a CEM. The findings reinforce the need for further study of CEM microstructure (which is a function of the fabrication method, nanofillers, and crosslinking) to advance the development of cost-effective CEMs for commercial use. Future work should investigate the synthesis of membranes that are non-porous but maintain high moisture content and low electrical resistivity.

Future work should also consider the exact role of the nanofiller and the crosslinkers used in this study independently of each other, and further elucidate the influence of the weight

percentage of these constituents within the membrane and its impact on the performance in IEMs for ED desalination in terms of salinity reduction, current efficiency, energy consumption, and water permeability. In addition, further study can be performed to functionalize these constituents and determine if this improves IEM performance.

4.5 REFERENCES

1. Strathman, Heiner, W.S.W. Ho, K.K. Sirkar, Membrane Handbook, Van Nostrand Reinhold, New York, 1992, pp. 219–262.
2. E. Korngold, Electrodialysis" membranes and mass transfer, in: G. Belfort (Ed.), Synthetic Membrane Processes, Academic Press, New York, 1984, pp. 192–219.
3. Strathmann, Heiner. "Electrodialysis, a mature technology with a multitude of new applications." Desalination 264, no. 3 (2010): 268-288, https://doi.org/10.1016/j.desal.2010.04.069.
4. Sato, Kazuhisa, Tetsuya Sakairi, Toshikuni Yonemoto, and Teiriki Tadaki. "The desalination of a mixed solution of an amino acid and an inorganic salt by means of electrodialysis with charge-mosaic membranes." Journal of membrane science 100, no. 3 (1995): 209-216, https://doi.org/10.1016/0376-7388(94)00236-R.
5. Kingsbury, R. S., K. Bruning, S. Zhu, S. Flotron, C. T. Miller, and O. Coronell. "Influence of water uptake, charge, manning parameter, and contact angle on water and salt transport in commercial ion exchange membranes." Industrial & Engineering Chemistry Research 58, no. 40 (2019): 18663-18674, https://doi.org/10.1021/acs.iecr.9b04113.
6. Nagarale, R. K., G. S. Gohil, and Vinod K. Shahi. "Recent developments on ion-exchange membranes and electro-membrane processes." Advances in colloid and interface science 119, no. 2-3 (2006): 97-130, https://doi.org/10.1016/j.cis.2005.09.005.
7. Chakrabarty, Tina, A. Michael Rajesh, Amaranadh Jasti, Amit K. Thakur, Ajay K. Singh, S. Prakash, Vaibhav Kulshrestha, and Vinod K. Shahi. "Stable ion-exchange membranes for water desalination by electrodialysis." Desalination 282 (2011): 2-8.
8. Zhao, Jinli, Lin Guo, and Jianyou Wang. "Synthesis of cation exchange membranes based on sulfonated polyether sulfone with different sulfonation degrees." Journal of Membrane Science 563 (2018): 957-968.

9. Harada, Miyuki, Mio Hirotani, and Mitsukazu Ochi. "Synthesis and improved mechanical properties of twin-mesogenic epoxy thermosets using siloxane spacers with different lengths." Journal of Applied Polymer Science 136, no. 34 (2019): 47891.
10. Guan, Rong, Hua Zou, Deping Lu, Chunli Gong, and Yanfang Liu. "Polyethersulfone sulfonated by chlorosulfonic acid and its membrane characteristics." European Polymer Journal 41, no. 7 (2005): 1554-1560. https://doi.org/10.1016/j.eurpolymj.2005.01.018
11. Thakur, Amit K., Murli Manohar, and Vinod K. Shahi. "Controlled metal loading on poly (2-acrylamido-2-methyl-propane-sulfonic acid) membranes by an ion-exchange process to improve electrodialytic separation performance for mono-/bi-valent ions." Journal of Materials Chemistry A 3, no. 35 (2015): 18279-18288.
12. Kamcev, Jovan, Donald R. Paul, and Benny D. Freeman. "Effect of fixed charge group concentration on equilibrium ion sorption in ion exchange membranes." Journal of Materials Chemistry A 5, no. 9 (2017): 4638-4650.
13. Li, Zhen, Yu Han, Junhua Wei, Wenqiang Wang, Tiantian Cao, Shengming Xu, and Zhenghe Xu. "Suppressing Shuttle Effect Using Janus Cation Exchange Membrane for High-Performance Lithium–Sulfur Battery Separator." ACS applied materials & interfaces 9, no. 51 (2017): 44776-44781.
14. Gahlot, Swati, Prem P. Sharma, and Vaibhav Kulshrestha. "Dramatic improvement in ionic conductivity and water desalination efficiency of SGO composite membranes." Separation Science and Technology 50, no. 3 (2015): 446-453. https://doi.org/10.1080/01496395.2014.973525
15. Gerani, Kobra, Hamid Reza Mortaheb, and Babak Mokhtarani. "Enhancement in performance of sulfonated PES cation-exchange membrane by introducing pristine and sulfonated graphene oxide nanosheets synthesized through hummers and staudenmaier methods." Polymer-Plastics Technology and Engineering 56, no. 5 (2017): 543-555., https://doi.org/10.1080/03602559.2016.1233260.

16. Alabi, Adetunji, Levente Cseri, Ahmed Al Hajaj, Gyorgy Szekely, Peter Budd, and Linda Zou. "Graphene-PSS/L-DOPA nanocomposite cation exchange membranes for electrodialysis desalination." Environmental Science: Nano 7, no. 10 (2020): 3108-3123, https://doi.org/10.1039/D0EN00496K.
17. Alabi, Adetunji, Levente Cseri, Ahmed Al Hajaj, Gyorgy Szekely, Peter Budd, and Linda Zou. "Electrostatically-coupled graphene oxide nanocomposite cation exchange membrane." Journal of Membrane Science 594 (2020): 117457, https://doi.org/10.1016/j.memsci.2019.117457.
18. Alabi, Adetunji, Ahmed AlHajaj, Levente Cseri, Gyorgy Szekely, Peter Budd, and Linda Zou. "Review of nanomaterials-assisted ion exchange membranes for electromembrane desalination." npj Clean Water 1, no. 1 (2018): 1-22.
19. Choi, Bong Gill, Jinkee Hong, Young Chul Park, Doo Hwan Jung, Won Hi Hong, Paula T. Hammond, and HoSeok Park. "Innovative polymer nanocomposite electrolytes: nanoscale manipulation of ion channels by functionalized graphenes." ACS nano 5, no. 6 (2011): 5167-5174, https://doi.org/10.1021/nn2013113.
20. Jinli Zhao, Luyao Ren, Qing-bai Chen, Pengfei Li, Jianyou Wang, Fabrication of cation exchange membrane with excellent stabilities for electrodialysis: A study of effective sulfonation degree in ion transport mechanism, Journal of Membrane Science, Volume 615, 2020, 118539, ISSN 0376-7388, https://doi.org/10.1016/j.memsci.2020.118539.
21. Klaysom, Chalida, Bradley P. Ladewig, GQ Max Lu, and Lianzhou Wang. "Preparation and characterization of sulfonated polyethersulfone for cation-exchange membranes." Journal of Membrane Science 368, no. 1-2 (2011): 48-53, https://doi.org/10.1016/j.memsci.2010.11.006.
22. Shahi, Vinod K. "Highly charged proton-exchange membrane: sulfonated poly (ether sulfone)-silica polyelectrolyte composite membranes for fuel cells." Solid State Ionics 177, no. 39-40 (2007): 3395-3404. https://doi.org/10.1016/j.ssi.2006.10.023.

23. Zhao, Jinli, Luyao Ren, Qing-bai Chen, Pengfei Li, and Jianyou Wang. "Fabrication of cation exchange membrane with excellent stabilities for electrodialysis: A study of effective sulfonation degree in ion transport mechanism." Journal of Membrane Science 615 (2020): 118539, https://doi.org/10.1016/j.memsci.2020.118539.
24. Li, Zhixue, Zhun Ma, Yuting Xu, Xiaomeng Wang, Yongchao Sun, Rong Wang, Jian Wang, Xueli Gao, and Jun Gao. "Developing homogeneous ion exchange membranes derived from sulfonated polyethersulfone/N-phthaloyl-chitosan for improved hydrophilic and controllable porosity." Korean Journal of Chemical Engineering 35, no. 8 (2018): 1716-1725, https://doi.org/10.1007/s11814-018-0064-2.
25. Klaysom, Chalida, Seung-Hyeon Moon, Bradley P. Ladewig, GQ Max Lu, and Lianzhou Wang. "Preparation of porous ion-exchange membranes (IEMs) and their characterizations." Journal of membrane science 371, no. 1-2 (2011): 37-44. https://doi.org/10.1016/j.memsci.2011.01.008.
26. Hyder, A. H. M., Brian A. Morales, Malynda A. Cappelle, Stephen J. Percival, Leo J. Small, Erik D. Spoerke, Susan B. Rempe, and W. Shane Walker. "Evaluation of Electrodialysis Desalination Performance of Novel Bioinspired and Conventional Ion Exchange Membranes with Sodium Chloride Feed Solutions." Membranes 11, no. 3 (2021): 217, https://doi.org/10.3390/membranes11030217.
27. W. Shane, Younggy Kim, and Desmond F. Lawler. "Treatment of model inland brackish groundwater reverse osmosis concentrate with electrodialysis—Part I: sensitivity to superficial velocity." Desalination 344 (2014): 152-162, https://doi.org/10.1016/j.desal.2014.03.035.

Chapter 5: General Conclusions

After reviewing relevant current literature, it was revealed that the ED desalination performances of commercial and laboratory-made IEMs had been performed previously, but not in a systematic way so that the planners, designers, and engineers can evaluate a trade-off in selecting the suitable IEMs and optimum ED experimental conditions for their desired outcomes such as high ion-selectivity, high salinity removal, high water recovery, low energy consumption, or low water transport. In addition to this knowledge gap, the existing conventional and laboratory-made IEMs reported previously showed various technical and economic limitations with respect to permeability, permselectivity, ion-selectivity, electrical resistance, stability (mechanical, chemical, and thermal), and production costs.

Thus, this research work addressed knowledge gaps identified in the published literature. The main focus of this research was the systematic comparison of ED desalination performances of well-known conventional IEMs and newly developed IEMs under a set of well-controlled experimental conditions. To achieve the overall goal, the entire research work was divided into three projects.

The aim of the first project was to evaluate the ED desalination performance of five well-known and commonly used commercial ion exchange membranes (IEMs) and compare their performances with a novel bioinspired cation exchange membrane (CEM) developed recently at Sandia National Laboratory for synthetic sodium chloride (NaCl) feed water solutions. In this project, laboratory-scale batch-recycle ED desalination experiments were performed with sodium chloride feed solution concentrations of 1, 3, 10, 35, and 100 g/L, voltage application to ED stack of 0.4, 0.8, and 1.2 volts per cell pair of membranes, and superficial velocity of feed solution of 2, 4, and 8 cm/s to compare commercial IEMs with Sandia CEM. The desalination performance of IEMs was evaluated by determining the significant ED experimental parameters such as the limiting current density (LCD), current efficiency (CE), salinity reduction (SR), normalized specific energy consumption (nSEC), and osmotic water flux (oWF). Sandia's bioinspired CEM

performed relatively well compared to the commercial membranes. Future work should investigate the long-term mechanical stability and durability of the Sandia novel bioinspired CEM.

The second project investigated the effects of key ED operational parameters on the desalination performance of commercial IEMs. In this effort, the ED desalination performance of the same five commercial IEMs used in the first project was evaluated by determining the limiting current density (LCD), current efficiency (CE), electrical conductivity reduction (CR), specific energy consumption (SEC), the separation rate of specific ions (or permselectivity), and relative ion transport number with respect to real brackish groundwater feed solutions (4.72 and 6.21 g/L TDS), 0.4 and 0.8 volts per cell pair stack voltage application, and 4 cm/s superficial velocity of feed solution. The membranes were ranked according to performance with respect to several figures of merit. The results of this work will be helpful for ED process optimization and performance analysis for the specific application and expected outcomes. In the future, the ED desalination performance should be investigated for not only well-known convention IEMs but also novel IEMs with respect to a wider range of experimental parameters such as compositions and concentrations of the feed solution, voltage application, and velocity of feed solution.

In the third project, we attempted to develop a set of novel polymeric CEMs from a highly durable and relatively inexpensive material (PES), and to evaluate the ED desalination performance of the developed CEMs. This study identified the influence of IEM's microstructure, fabrication method, physiochemical properties of polymeric substances, nanofillers, and crosslinkers on ED desalination performance. The results showed the potential of using sulfonated PES with GO nanofillers and PVP crosslinkers for fabricating CEMs using phase inversion methods. Future work should investigate synthesis methods that produce nonporous membranes with low electrical resistivity.

This research contributes to the field of ED by the systematic evaluation methodology, by illustrating the importance of evaluation with real feed water, and by investigating the influence of IEM microstructural and physicochemical properties on ED desalination performance.

Vita

AHM Golam Hyder was born and raised in a small town called "Rajbari" at Dhaka Division in Bangladesh, where he studied from elementary to high school. He completed his Bachelor's degree in Civil Engineering from Rajshahi University of Engineering and Technology in Bangladesh in Fall 2006. Just after graduation, he started his professional career in a multinational consulting company in Bangladesh as a Junior Design Engineer.

In the Fall of 2010, Hyder began graduate studies in the Environmental Engineering and Sustainable Infrastructure program at the Royal Institute of Technology in Stockholm, Sweden. He got an opportunity to conduct his Master's thesis research work at Tuskegee University, Alabama, USA in Spring 2012 as a Visiting Research Scholar. He received an M.S.E. degree in the Spring of 2013. After completing his Master's degree, he started working again in a consulting company as an Environmental Specialist, and in a university as a Lecturer in Bangladesh.

In the Fall of 2016, Hyder began working toward the doctoral degree in the Environmental Science and Engineering program at The University of Texas at El Paso under the direct supervision of Dr. W. Shane Walker, Associate Prof, Civil Engineering Department, UTEP.

He was blessed to receive numerous fellowships and scholarships from prestigious organizations such as the American Society of Civil Engineers and the American Water Works Association. To date, Hyder published more than 10 articles with over 170 citations and an h-index of 5. He gained more than 6 years of research and industrial experience and more than 5 years of active teaching experience in Civil and Environmental Engineering in academia.

Hyder was pleased to accept a Post-Doctoral researcher position starting from Fall 2021 in the Advanced Materials Division at Argonne National Laboratory, Illinois, USA.

Permanent Contact Information: ahm.g.hyder@gmail.com